COMPUTATIONAL INVESTIGATION INTO CATALYTIC MECHANISMS OF DISEASE-CAUSING ENZYMES AND BIOCATALYSTS

by

Corey Andrew MacDonald

Submitted in partial fulfilment of the requirements
for the degree of Doctor of Philosophy

at

Dalhousie University
Halifax, Nova Scotia
July 2015

© Copyright by Corey Andrew MacDonald, 2015

To my wife, who always believed in me more than I ever have.

TABLE OF CONTENTS

LIST OF TABLES

LIST OF FIGURES

ABSTRACT

Computational chemistry, namely the ONIOM method, is used to investigate areas of interest to drug design, including malaria and inflammation, as well as biocatalysts for the hydration of nitrile substrates.

With the risk of malarial resistance reaching catastrophic levels, novel methods into the inhibition of this disease need to be prioritized. The current work uses high performance docking methods to model different substrates binding into the active sites of varying *Homo sapiens* and *Plasmodium* peptidyl-prolyl *cis*/*trans* isomerase enzymes and compares their subsequent docking scores. This approach has shown that the substrates ILS-920 and WYE-592 will bind less-favourably with *h*FKBP12 and *Pf*FKBP35 compared to a competing substrate rapamycin; however, the binding appears to be more favourable in *Pv*FKBP35. This could suggest a possible target for inhibition of the *Plasmodium vivax* parasite. Alternatively, the exploitation of active site differences between parasitic and human peptidyl-prolyl *cis*/*trans* isomerases can be used for suicide inhibition of malaria, effectively poisoning the parasite without affecting the patient. This method of inhibition was explored using *Plasmodium falciparum* and *Homo sapiens* Fk506-binding proteins as templates for quantum mechanics/molecular mechanics calculations. Modification of the natural substrate has shown suicide inhibition is a valid approach for novel anti-malarials with little risk for parasitic resistance.

Leukotrienes are a family of drug-like molecules involved in the pathobiology of bronchial asthma and are responsible for smooth muscle contraction. Leukotriene C_4 synthase is a nuclear-membrane enzyme responsible for the conjugation of leukotriene A_4 (LTA_4) to glutathione to form LTC_4, a cysteinyl leukotriene. The mechanism of LTA_4 binding by LTC_4S has been computationally examined. Within the present computational methodology the ‘tail-to-head’ orientation appears to be the most likely substrate orientation. The mechanism by which LTB_4 is synthesized by LTA_4 hydrolase is also studied. The current proposed mechanism is unable to provide realistic Gibbs energy barriers for LTB_4 synthesis.

The catalytic mechanisms for nitrile hydratase is explored, involving cysteine-sulfenic acid acting as a nucleophile, activating a water molecule to attack nitrile and isonitrile substrates. For the nitrile substrate, the iminol intermediate undergoes tautomerization to form the amide product. The computed enthalpies are closely related to experimental values, suggesting the current mechanism with two water molecules should be further investigated.

LIST OF ABBREVIATIONS USED

ACT	Arteminisin-based combination therapy
AMBER	Assisted Model Building with Energy Refinement
CGTO	Contracted Gaussian-type orbital
DFT	Density functional theory
EE	Electronic embedding
FDA	Federal drug administration
FKBD	Fk506-binding domain
FRAP	Fk506-binding protein-rapamycin-associated protein
FRED	Fast rigid exhaustive docking
GAFF	Generalized AMBER force field
GSH	Glutathione
GTO	Gaussian-type orbital
HF	Hartree-Fock theory
*h*FKBP12	*Homo sapiens* Fk506-binding protein 12
HK	Hohenberg-Kohn
KS	Kohn-Sham
LA	Link atom
LAC	Link atom connection
LCAO	Linear combination of atomic orbitals
LDA	Local-density approximation
LT	Leukotriene
LTA_4	Leukotriene A_4

LTA_4H	Leukotriene A_4 hydrolase
LTB_4	Leukotriene B_4
LTC_4	Leukotriene C_4
LTC_4S	Leukotriene C_4 synthase
LTD_4	Leukotriene D_4
LTE_4	Leukotriene E_4
MD	Molecular dynamics
MDA	Mass drug administration
ME	Mechanical embedding
MO	Molecular orbital
MOE	Molecular operating environment
NAMD	Nanoscale molecular dynamics
NHases	Nitrile hydratases
ONIOM	Our own N-layered integrated molecular orbital and molecular mechanics
PCM	Polarizable continuum model
PDB	Protein data bank
PES	Potential energy surface
*Pf*FKBP35	*Plasmodium falciparum* Fk506-binding protein 35
PPIase	Peptidyl-prolyl *cis*/*trans* isomerase
*Pv*FKBP35	*Plasmodium viax* Fk506-binding protein 35
QM/MM	Quantum mechanics/molecular mechanics
RESP	Restrained electrostatic potential

RMSD	Root-mean-square deviation
SCF	Self-consistent field
SRCF	Self-consistent reaction field
STO	Slater-type orbital
STQN	Synchronous transit-guided quasi-Newton

Symbols

Ψ_i	Molecular wave function of the i^{th} state
Ψ_{elec}	Electronic molecular wave function
Ψ_0	Exact molecular wave function
Ψ_{trial}	Approximate molecular wave function
$\hat{H}$	Hamiltonian operator
$\hat{H}^{core}$	Core Hamiltonian operator
$\hat{H}_{elec}$	Electronic Hamiltonian operator
E_i	Energy of the system for a given wave function
E_{trial}	Energy of the system for a trial wave function
E_0	Energy of the system for the exact wave function
E_{HF}	Energy of the system for the Hartree-Fock wave function
E_{tot}	Electronic and nuclear energy
$\vec{r}_i$	Vector describing the positions of i^{th} electron
R_I	Vector describing the positions of I^{th} nucleus
s_i	Spin state of the i^{th} electron
m_i	Mass of particle i

M_I	Mass of nucleus *I*
Z_A	Nuclear charge of nucleus A
r_{ij}	Distance between electron *i* and *j*
R_{AB}	Distance between nucleus A and B
ħ	Planck's constant
$\hat{T}$	Kinetic energy operator
$\hat{V}$	Potential energy operator
$\hat{V}_{ext}$	External potential energy operator
$\hat{V}_{ee}$	Electron-electron potential energy operator
$\hat{V}_{Ne}$	Nucleus-electron potential energy operator
∇^2	$(\frac{\partial^2}{\partial x}+\frac{\partial^2}{\partial y}+\frac{\partial^2}{\partial z})$
ψ	Single molecular orbital
χ	Spin orbital
N	Normalization constant
η^{STO}	Slater-type orbital
$r^{n-1}\ e^{-\zeta r}$	Radial distribution of Slater-type orbital
$Y_{lm}\ (\Theta, \phi)$	Angular component of Slater-type orbital
l	Angular quantum number
m	Magnetic quantum number
n	principal quantum number
ϕ(r)	Atomic orbital
θ	Polar angles
Φ_{SD}	Slater determinant

δ_{ij}	Kronecker delta
G_{ijk}	Primitive Gaussian Function
F	Fock matrix
C	Orbital coefficient matrix
S	Overlap matrix
ϵ	Orbital energy matrix or dielectric constant
P_{ij}	Element of the charge density matrix
c,d,a,t	Orbital expansion coefficients
ρ_s	Electron density for a non-interacting system
ρ_0	Ground state electron density
$\hat{f}^{KS}$	One electron Kohn-Sham operator
$V_s(\vec{r})$	Effective local potential
T_s	Non-interacting kinetic energy
$F(\rho)$	Hohenberg-Kohn functional
$E_{XC}[\rho(r)]$	Exchange-correlation energy functional
$J(\rho)$	Coulomb energy
V_{xc}	Potential caused by the exchange-correlation energy
ϵ_{xc}	Exchange-correlation per particle of homogeneous electron gas
k	Spring constant
θ	Bond angle
ω	Dihedral angle
V	Force constant
N	Periodicity factor

ACKNOWLEDGEMENTS

I would first and foremost like to thank Prof. Russell Boyd for all his help and guidance through the entirety of this project. I appreciate his understanding and patience as I progress through the learning curve of this large and complex assignment. I would also like to express my gratitude to the Boyd research group for their constant support and extended conversations into the intricacies of computational chemistry. I am grateful to my co-supervisor, Prof. Axel Becke for his support and wealth of knowledge on computational methods.

I would also like to thank Prof. Donald Weaver, as the information provided in his courses was crucial in the development of many of the obtained results. I would like to thank him as well as Prof. Jan Rainey for their help in the editing and review process of this work.

I am grateful to Prof. James Gauld for welcoming me to his group at the University of Windsor in Windsor, Ontario. Shortly after meeting me, he agreed to let me visit and learn from him and his graduate students. I am especially grateful to Dr. Eric Bushnell for his helpful suggestions and conversations throughout my research, as well as his help in editing this thesis.

Natural Sciences and Engineering Research Council of Canada (NSERC), Atlantic Computational Excellence Network (ACEnet), the Douglas, E. Ryan Excellence Prize, and Dalhousie University are thanked for financial support. ACEnet, Westgrid, and SHARCNET are thanked for computational resources.

Finally, I'd like to thank my friends and family, specifically my wife, Katie. She has always believed I could handle the work in front of me, and was constantly supportive and loving. This work would not have been completed without her encouragement.

1 INTRODUCTION

Proteins (i.e., polypeptides) are large biological molecules that consist of long polymerized chains of amino acid residues (**Figure 1.1**).[1, 2] Each protein varies in its ordering of the amino acid residues found in the polypeptide chain. Such ordering defines the protein's primary structure. While there is potential for hundreds of amino acids in nature, only twenty-three of these are involved in protein synthesis (proteinogenic).[3-5] Once formed these polypeptides will fold forming specialized secondary structures, such as α-helices and β-sheets. The three-dimensional arrangement of these secondary structures results in the formation of tertiary structures. Some proteins are made from the combination of two or more tertiary structures to form a single complex. Such combinations of tertiary structures result in the formation of quaternary structures. Notably, these three-dimensional complexes (i.e., tertiary and quaternary structures) have a profound effect on protein function.[6]

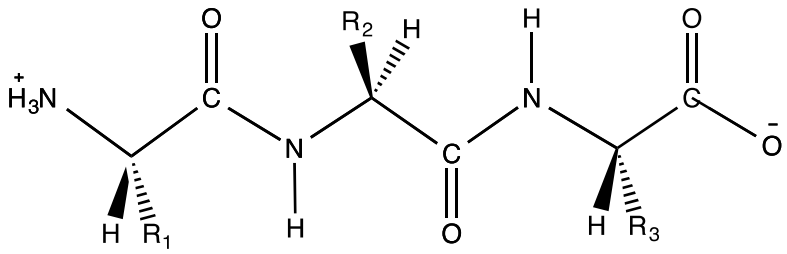

Figure 1.1 A generic three amino acid peptide chain at physiological pH.

Proteins with catalytic capabilities are further classified as enzymes.[7-9] The diverse three-dimensional structures among enzymes results in catalysts that are highly

specialized and catalyze very specific reactions. An important property of an enzyme, like all catalysts, is that it is not consumed or altered after the catalytic process; moreover, it must only reduce the Gibbs activation energy (i.e., the kinetics, $\Delta G^{\ddagger}$) (**Figure 1.2**) and not affect the thermodynamics (i.e., ΔG_r) of a given reaction. This reduction in Gibbs activation energy leads to a drastic increase (by up to many millions of times) in rate of reaction.[10] For instance a reduction of ~5.7 kJ mol^{-1} in barrier height corresponds to an increase of a factor of ten in the catalytic rate.

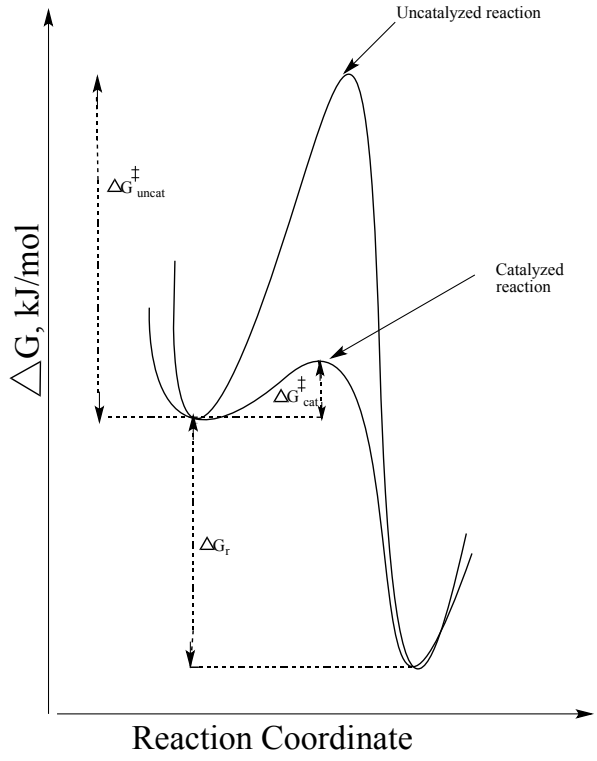

Figure 1.2 A generalized scheme for a one-step mechanism showing the change in barrier height between a catalyzed and uncatalyzed reaction.

Enzymes perform their catalytic function through complex mechanisms.[11] One method that allows enzymes to lower the activation energy of a reaction is known as

entropy reduction, where molecular fragments are brought close spatially and in the appropriate orientation to facilitate bond breaking or forming.[12-15] Another mechanism, preferential transition state binding, stabilizes the transition state greatly reducing the Gibbs activation energy by maximizing stabilizing forces such as hydrogen bonds.[16, 17] Combinations of these mechanisms, as well as steric effects,[16, 18] electrostatic effects,[13, 19, 20] and even quantum tunneling can affect rates of reaction and specificity of the enzymes.[21, 22] Studying enzymatic mechanisms can lead to further insight into important subtle residue effects, as well as potential for inhibition of specific enzymes.

The catalytic activity of an enzyme can be modified by temperature, pH, and, more importantly, active site substrate binding which as discussed in Chapter 3 and 4 has a profound affect on catalysis. After binding into the active site, molecules can induce a change in the three-dimensional structure of the protein, altering its function.[6] Such molecules that decrease the activity of enzymes are known as inhibitors, whereas those that increase the activity are known as activators.[1] Additionally, molecules can bind permanently (i.e., through covalent modification) to occupy the active sites and prevent any further catalytic activity. This method of covalent bond formation can be used as a starting point for drug discovery and drug design to be used in treating diseases.[23, 24] Of the many diseases and disorders that affect humans, the two of particular concern for this work are malaria and inflammation.

Malaria is caused by *Plasmodium* parasites. A key enzyme for the function of this parasite belongs to the peptidyl-prolyl *cis*/*trans* isomerase (PPIase) superfamily of enzymes. These enzymes are responsible for the *cis*/*trans* interconversion of amide bonds during the protein folding process (**Figure 1.3**).[25] These enzymes target X-proline amide

bonds. This specific amide bond is important for protein folding as the *cis* and *trans* forms are very similar in energy allowing for an increased population of *cis* isomers present in folded proteins such as ribonucleases and beta-lactamases.[25] The uncatalyzed *cis*/*trans* interconversion proceeds via a considerable Gibbs activation energy (~80 kJ/mol compared to ~0 kJ/mol in other amino acid residues). Hence, without the presence of a PPIase this interconversion would occur far to slowly and would in fact be the rate-limiting step for protein folding.[25] Inhibition of this group of enzymes found in malarial parasites could be a novel solution to the growing problem of malarial resistance.

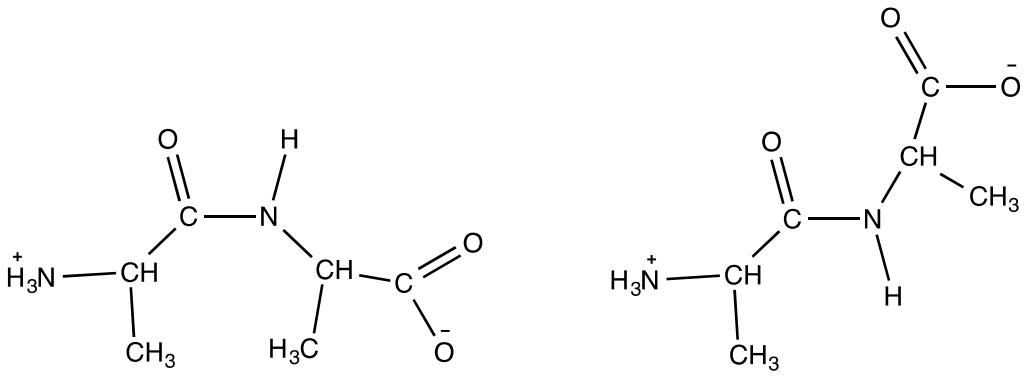

(a) (b)

Figure 1.3 The **(a)** *cis* and **(b)** *trans* amide bonds for an alanine-alanine dipeptide at physiological pH.

A common cause of inflammation is due to leukotrienes, inflammatory mediators formed by the oxidation of arachidonic acid by arachidonate 5-lipoxygenase.[26] Leukotriene A_4 (LTA_4) is the simplest leukotriene and is a precursor to all other derivatives. LTA_4 can be converted into LTB_4 by leukotriene A_4 hydrolase (LTA_4H)[27, 28] or converted into LTC_4 by leukotriene C_4 synthase (LTC_4S).[29, 30] These molecules play a

crucial role in asthma and bronchial inflammation. A better understanding of the mechanism by which leukotrienes are synthesized can lead to better inhibition and prevention of the over-production of these inflammatory mediators.

While enzymes are critical for the continuing existence of the organisms that contain them, the power of enzymes can also be used in industrial processes as biocatalysts. Nitrile hydratases are non-heme iron containing enzymes responsible for the conversion of nitrile functional groups to amides in bacteria (**Figure 1.4**). These enzymes are used industrially to synthesize acrylamide, used in waste water treatment, with nitrile as the substrate.[31] Presently, several mechanisms have been proposed for the catalytic mechanism of this enzyme group; however, only two mechanisms have experimental data to support them.[32, 33] The first proposed mechanism is where Cys_{114} (post-translationally modified to cysteine-sulfenic acid, CSO_{114}) acts as a base, abstracting a proton from a nearby water molecule.[34] This mechanism is supported by the experimental work performed by Hashimoto using time-resolved X-ray crystallography.[32] The second mechanism, however, proposes that this cysteine-sulfenic acid residue acts as a nucleophile attacking the substrate while the water molecule instead regenerates the active site after product release.[35] This mechanism has also garnered some experimental support from Martinez using kinetics and X-ray crystallography with boronic acid.[33]

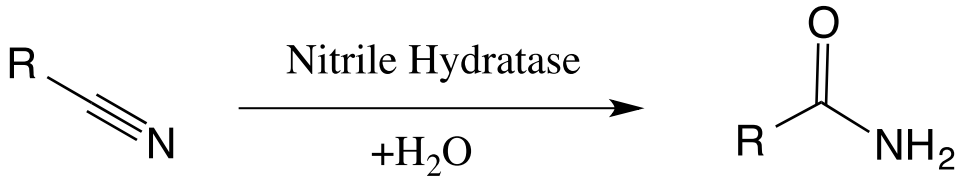

Figure 1.4 Nitrile hydration.

Regardless of whether the enzyme is used within an organism or industrially, computational chemistry (outlined in Computational Methods) provides a means to study these systems on an atomistic scale by employing highly advanced quantum mechanical methods. In particular, the three-dimensional orientation by which substrates bind into the active sites of these enzymes can be studied using docking methods. Protein dynamics and stability of docked substrates over a short time frame can be studied using molecular dynamics simulations. Finally, energy barriers of various reactions are studied to investigate their catalytic feasibility in an enzymatic environment.

Chapter 2 summarizes background information into computational chemistry. These methods serve as the backbone for the work completed in this thesis. Chapter 3 uses docking methods to dock various macrocycles into the active sites of essential human and malarial PPIases. This was done to provide insights for molecular interactions into the development of anti-malarials. Chapter 4 investigates a suicide mechanism for the inhibition of *Pf*FKBP35 from the modified natural substrate. This would provide a novel method for anti-malarial treatment.

Chapter 5 investigates the binding orientation of LTA_4 into the active site of LTC_4S in the formation of LTC_4. Advanced quantum mechanical calculations were performed to identify the binding orientation and catalytic mechanism of LTC_4 synthesis. Chapter 6 studies the catalytic mechanism of LTB_4 synthesis by LTA_4H. Insights into the production of inflammatory mediators could lead to further development of anti-inflammatory medications.

Chapter 7 investigates the enzymatic mechanism of nitrile hydratases. The hydration of t-butyl nitrile is studied and compared to previously proposed mechanisms.

2 COMPUTATIONAL METHODS

In this chapter, the underlying principles applied in the field of computational chemistry will be mentioned, as well as the application of these principles to biomolecules and proteins. Many of the details in this chapter will be used as a starting point for the presentation of results in the following chapters. For further details, standard quantum chemistry textbooks should be consulted.[36-39]

2.1 The Schrödinger Equation

In 1926, Erwin Schrödinger proposed his famous equation involving eigenvalues and eigenfunctions, shown below in its time-independent form:[37]

$$\hat{H}\Psi_i(\vec{x}_1, \vec{x}_2, \ldots \vec{x}_N, \vec{R}_1, \vec{R}_2, \ldots \vec{R}_M) = E_i\Psi_i(\vec{x}_1, \vec{x}_2, \ldots \vec{x}_N, \vec{R}_1, \vec{R}_2, \ldots \vec{R}_M) \quad (2.1)$$

where $\hat{H}$ is the Hamiltonian operator for a given molecular system with N electrons and M nuclei, $\Psi_i(\vec{x}_1, \vec{x}_2, \ldots \vec{x}_N, \vec{R}_1, \vec{R}_2, \ldots \vec{R}_M)$ is the wave function in its i^{th} state, depending on $\vec{x}$ (which is composed of x, y, and z coordinates in space ($\vec{r}_i$) and spin state (s_i) of each electron) and the spatial coordinates of the nuclei ($\vec{R}_I$). It is postulated that the wave function of a molecular system contains any and all information required to describe that system. E_i is the energy of the system for the given Ψ_i. The basis of most quantum chemical work is searching for the approximate solution to this equation. For a polyatomic system $\hat{H}$ is the sum of the kinetic and potential energy operators:

$$\hat{H} = -\frac{1}{2}\sum_{i=1}^{N}\nabla_i^2 - \frac{1}{2}\sum_{A=1}^{M}\frac{1}{M_A}\nabla_A^2 - \sum_{i=1}^{N}\sum_{A=1}^{M}\frac{Z_A}{r_{iA}} + \sum_{i=1}^{N}\sum_{j>i}^{N}\frac{1}{r_{ij}} + \sum_{A=1}^{M}\sum_{B>A}^{M}\frac{Z_A Z_B}{r_{AB}} \quad (2.2)$$

The first two terms represent the kinetic energy of electrons and nuclei, respectively. The Laplacian operators, ∇_i^2 and ∇_A^2, represents the sum of the differential operators in three-dimensional space for electron i and nucleus A, respectively:

$$\nabla^2 = \frac{\partial^2}{\partial x^2} + \frac{\partial^2}{\partial y^2} + \frac{\partial^2}{\partial z^2} \quad (2.3)$$

and M_A is the mass of the nucleus A in atomic units as multiples of the electron mass.[‡] The last three terms in eq. 2.2 represent the potential energy operators for the attractive interaction between electrons and nuclei, the repulsive interactions between electrons and the repulsive interactions between nuclei, respectively. Z_A and Z_B are the charge of nucleus A and B, r_{ij} is the distance between electrons i and j, r_{iA} is the distance between electron i and nucleus A, and r_{AB} is the distance between nuclei A and B.

[‡] Atomic units are frequently used in theoretical chemistry where fundamental constants Planck's constant ħ, the mass of an electron m_e, the charge of an electron e, and the permittivity of a vacuum multiplied by a constant $4\pi\varepsilon_0$ are all set to unity. This ensures that as these constants are refined and corrected, the computed results will remain the same and to simplify expressions in atomic physics. This formalism will be used for the duration of this document.

As mentioned previously, the basis of many quantum mechanics problems deal with approximating the exact solution to the Schrödinger equation. It is only possible to exactly solve this equation for a hydrogen-like atom (one electron and one nucleus; a two-body problem). Beyond these systems, approximations will be required to solve the Schrödinger equation.

2.1.1 The Born-Oppenheimer Approximation

The first approximation involves the consideration of the relative masses of the nuclei and an electron.[37] An electron is 1,800 times lighter than the lightest nucleus (^{1}H, a single proton) and 20,000 times lighter than a carbon nucleus. In classical mechanics, the heavier the object, the slower that object moves. The nucleus, being far heavier, will move much slower than the light electron, essentially being clamped in place. Thus, the kinetic energy for the nuclei is zero, and the potential energy for the nuclei-nuclei interactions becomes a constant. This reduces eq. 2.2 to the "electronic" Hamiltonian:

$$\hat{H}_{elec} = -\frac{1}{2}\sum_{i=1}^{N}\nabla_i^2 - \sum_{i=1}^{N}\sum_{A=1}^{M}\frac{Z_A}{r_{iA}} + \sum_{i=1}^{N}\sum_{j>1}^{N}\frac{1}{r_{ij}} = \hat{T} + \hat{V}_{Ne} + \hat{V}_{ee} \qquad (2.4)$$

where $\hat{T}$ represents the kinetic energy of the system (now completely due to the electrons), and $\hat{V}_{Ne}$ and $\hat{V}_{ee}$ represent the nuclei-electron and electron-electron potential energy operators, respectively. The electronic Hamiltonian, when used in the Schrödinger equation, generates the electronic wave function Ψ_{elec} and the electronic energy E_{elec}.

The total energy of the system is the sum of the electronic energy and the nuclear repulsion constant:

$$E_{tot} = E_{elec} + \sum_{A=1}^{M} \sum_{B>A}^{M} \frac{Z_A Z_B}{r_{AB}} = E_{elec} + E_{nuc} \quad (2.5)$$

2.1.2 The Orbital Approximation

The next approximation that can be made on the Schrödinger equation accounts for the complex nature of the wavefunction which depends of the position of each electron.[37] It is described as:

$$\Psi(\vec{r}_1, \vec{r}_2, \ldots \vec{r}_N) \quad (2.6)$$

To simplify this equation, it is assumed that the wavefunction is separable and can be described as a product of single molecular orbitals (MOs), which contains all the Cartesian coordinate information for each electron. This product assumes the electrons move independently of each other. The product of these MOs can approximate the exact wave function:

$$\Psi(\vec{r}_1, \vec{r}_2, \ldots \vec{r}_N) = \psi(\vec{r}_1)\psi(\vec{r}_2), \ldots, \psi(\vec{r}_N) \quad (2.7)$$

However, the orbitals need to also contain spin information. This is described using spin orbitals, $\chi(\vec{x})$, where $\vec{x}$ contains all coordinate information on the electron as well as spin

information, α(s) or β(s). Since electrons are fermions with spin = $\frac{1}{2}$, they can be represented by spin-up (spin = $\frac{1}{2}$, denoted α) or spin-down (spin = $-\frac{1}{2}$, denoted β):

$$\chi(\vec{x}) = \Psi(\vec{r})\alpha(s) \text{ or } \Psi(\vec{r})\beta(s) \tag{2.8}$$

changing the wave function from eq. 2.6, which now contains all spin and spatial information, to:

$$\Psi(\vec{x}_1, \vec{x}_2, \ldots \vec{x}_N) \tag{2.9}$$

2.1.3 Properties of a Wave Function

The wave function is said to hold all possible information on a given system, yet it itself is not an observable property.[37] The square of the wave function, however, defines the probability of finding an electron in different points in space. This is known as the probability density:

$$|\Psi(\vec{x}_1, \vec{x}_2, \ldots \vec{x}_N)|^2 \tag{2.10}$$

Since electrons are indistinguishable particles, this property must remain unaffected if any two electrons are interchanged:

$$|\Psi(\vec{x}_1, \vec{x}_2, \ldots, \vec{x}_i, \vec{x}_j, \ldots, \vec{x}_N)|^2 = |\Psi(\vec{x}_1, \vec{x}_2, \ldots, \vec{x}_j, \vec{x}_i, \ldots, \vec{x}_N)|^2 \tag{2.11}$$

In order for this condition to be satisfied, the two wave functions can either be symmetric or antisymmetric. However, due to the fact that electrons are fermions, these wave functions must be antisymmetric[39]:

$$\Psi(\vec{x}_1, \vec{x}_2, \ldots, \vec{x}_i, \vec{x}_j, \ldots, \vec{x}_N) = -\Psi(\vec{x}_1, \vec{x}_2, \ldots, \vec{x}_j, \vec{x}_i, \ldots, \vec{x}_N) \tag{2.12}$$

This shows that no electron can occupy the same quantum state as another, which agrees with the Pauli exclusion principle.[39]

It should also be noted that the probability of finding the N electrons over all space is 1. This imposes a normalization requirement on the wave function:

$$\int \ldots \int |\Psi(\vec{x}_1, \vec{x}_2, \ldots \vec{x}_N)|^2 d\vec{x}_1 d\vec{x}_2 \ldots d\vec{x}_N = 1 \tag{2.13}$$

2.1.4 Linear Combination of Atomic Orbitals

While the expression in 2.7 is a simplification to solve the Schrödinger equation a further approximation involves the description of each one-electron molecular wave function as a linear combination of atom-centered functions called atomic orbitals.[37] Such a method of reproducing molecular orbitals is known as the linear combination of atomic orbitals (LCAO) method. These atomic orbitals are known as basis functions, and the set of basis functions used to represent a molecular wave function is known as a basis set.

The use of a large, flexible basis set will create accurate representations of the molecular orbitals.

2.2 Basis Sets

A basis set is a set of functions which can be combined in a linear fashion to define molecular orbitals with different weighting coefficients.[36] These basis functions are used to describe the angular component, radial component, and normalization component of a given molecular orbital. The angular component describes the shape of the orbital and the radial component describes the extent of the orbital. In general, the greater the number of basis functions used, the greater the description of the system, and the greater the accuracy and computational cost.

2.2.1 Slater-type and Gaussian-type Orbitals

The most common types of orbitals used to construct basis sets are Slater-type orbitals (STOs) and Gaussian-type orbitals (GTOs).[40]

Slater-type orbitals exhibit exponential decay at long range with a cusp at short range and are represented by the equation:

$$\eta^{STO} = N\, r^{n-1}\, e^{-\zeta r}\, Y_{lm}\,(\Theta, \phi) \qquad (2.14)$$

where N is the normalization constant, r is the distance between atomic nuclei and electrons, ζ is the orbital exponent, and l, m, and n are the angular, magnetic and principal quantum numbers of the orbital being described. The $r^{n-1}\, e^{-\zeta r}$ term represents the radial distribution and the $Y_{lm}\,(\Theta, \phi)$ term represents the angular component.

While STOs offer a qualitatively correct representation of atomic orbitals, they are computationally expensive in multicentre systems due to the cusp near the nucleus. The more computationally feasible Gaussian-type orbital (GTO) model can be used instead. This orbital type has a similar shape as an STO with a continuous curve at short range. The reason for use of these Gaussians is due to the "Gaussian product theorem".[40] It states that the product of two Gaussians on two different centers is, apart from a constant, a Gaussian on a third center. This allows three- and four-centered integrals to be reduced to finite sums of two-centered integrals, greatly reducing computational cost. Gaussian-type orbitals are represented by:

$$\eta^{GTO} = N\, x^l y^m z^n\, e^{-\alpha r^2} \tag{2.15}$$

with x, y, and z being Cartesian coordinates, and l+m+n=L, where L=0, 1, 2… for s-functions, p-functions, d-functions, etc. The orbital exponent α is large for compact functions and small for diffuse functions. This equation results in a smooth, continuous curve over the nucleus which greatly decreases the computational complexity; however, the GTO does not represent the atomic orbitals accurately near a nucleus. To overcome this issue, several GTOs (primitive Gaussians) are used to more accurately represent the atomic orbitals,

$$\eta_\tau^{CGF} = \sum_a^A d_{a\tau}\, \eta_a^{GTO} \tag{2.16}$$

This is known as a contracted Gaussian-type orbital (CGTO). Several GTOs are combined with differing contraction coefficients $d_{a\tau}$ and orbital exponents α to resemble, as closely as possible, a single STO function.

2.2.2 Minimal Basis Set

A minimal basis set uses only one STO (or CGTO) to represent each core and valence atomic orbital on a given atom.[37] A minimal basis set for carbon, for example, contains 1s, 2s, $2p_x$, $2p_y$, and $2p_z$ basis functions. These basis sets are typically inadequate for most purposes, but they are sometimes used as a starting point for complex calculations. For more accurate calculations, and a better representation of the ground state wave function, more basis functions should be used to describe the valence electrons. Minimal basis sets are still acceptable for core electrons, as they are much lower in energy than valence electrons and do not participate in bonding.

2.2.3 Split-Valence Basis Set

Chemical bonds occur between valence orbitals of neighboring atoms.[37] Meanwhile, core orbitals are far lower in energy than valence orbitals; thus, they are less important for chemical bonding. To increase the speed and accuracy of molecular orbital calculations, multiple STOs or contracted GTOs can be used with varied orbital exponents to describe the valence orbitals, while core orbitals are described using a single basis function.

A split valence basis set is designed to describe the core orbitals with a single basis function, and two, three or more basis functions to describe the valence orbitals

(called double-zeta basis sets, triple-zeta basis sets, etc). This gives more radial flexibility in order to describe the electron distribution in a given environment.

For example, a 6-31G basis set for carbon uses a single basis function to describe the core orbital, whereas it uses two basis functions to describe the valence orbitals. Thus, a 6-31G basis set for carbon consists of ten basis functions. For the core inner shell (1s) orbital six primitive Gaussian orbitals are used. Three primitive Gaussian orbitals are used to describe the inner valence shell [2s(I), $2p_x$(I), $2p_y$(I), and $2p_z$(I)] orbitals, whereas one primitive Gaussian to describe the outer valence shell [2s(O), $2p_x$(O), $2p_y$(O), and $2p_z$(O)] orbitals.

2.2.4 Polarization Functions

Further flexibility can be introduced into a basis set by adding polarization functions.[37] A polarization function is a basis function that has a higher angular momentum than the basis functions in the minimal basis set, and will lead to increased accuracy and properties for the wave function.

In a molecule, orbitals deviate from their atomic orbitals. When considering a hydrogen-carbon bond, the electron density is not exactly spherical around the bound hydrogen atom, as is the 1s orbital of a free hydrogen atom. The electron density is higher between atoms due to the chemical bond, and lower on the outer edges of the atom. The best way to model this change in electron density is by adding p-type functions to allow for this flexibility. This can be done with any atom in a molecular system by adding an extra set of functions of a higher order than what is already present (for instance adding d-type functions to second row atoms and f-type functions to third row atoms).

For example, the 6-31G(d) differs from the 6-31G basis set by the addition of polarization functions to the basis set of all non-hydrogen atoms. A 6-31G(d,p) basis set adds d-type functions for all non-hydrogen atoms, and p-type functions to all hydrogen atoms. Multiple polarization functions can be added to basis sets to further increase orbital flexibility. A 6-31G(3df,2p) basis set has three sets of d-type functions and one set of f-type function on all p-block atoms, and two sets of p-type functions on all hydrogen atoms.

2.2.5 Diffuse Functions

In certain cases, such as excited states of molecules or anions (as the electron density will be more spread out across the entire molecule), the normal basis sets will not be adequate to model the system.[37] To correct this, GTOs with small exponents are used to add basis functions that are more diffuse. In a Pople-type basis set, a "+" is added to indicate that a set of diffuse functions are included in the basis set of all non-hydrogen atoms. A second "+" indicates the addition of diffuse functions to all hydrogen atoms as well. These diffuse functions are also important in describing weak interactions like hydrogen bonding.

For example, a 6-31+G basis set adds four diffuse functions (s, p_x, p_y, p_z) to all non-hydrogen atoms, while a 6-31++G basis set adds additional diffuse s functions on all hydrogens.

2.3 The Variational Principle

The variational principle states that the energy obtained using the exact wave function (Ψ_0) will always be lower in energy than that obtained with an approximate

wave function (Ψ_{trial}).[37] Importantly this allows us to variationally optimize the parameters of a trial wave function with the knowledge that the energy obtained will always be greater than the true energy:

$$\int \dots \int \Psi_{trial}^{*} \hat{H} \Psi_{trial} \, d\vec{x}_1, d\vec{x}_2, \dots, d\vec{x}_N \equiv$$

$$\langle \Psi_{trial} | \hat{H} | \Psi_{trial} \rangle = E_{trial} \geq E_0 = \langle \Psi_0 | \hat{H} | \Psi_0 \rangle \qquad (2.17)$$

where Ψ^* is the complex conjugate of the wave function, and E_0 and E_{trial} are the exact ground state and trial energies, respectively. Using this method, the components of the wave function are varied as to produce the lowest energy wave function.

2.4 The Hartree–Fock Approximation

One of the earliest electronic structure methods is the Hartree-Fock (HF) method.[37] An understanding of this method will greatly aid in the understanding of later methods, including density-functional theory.

Due to the complexity of a N-electron wave function the Hartree-Fock approximation assumes a non-interacting system of electrons. Thus, the resulting approximation to the exact, N-electron wave function is constructed from an antisymmetric product of N one-electron wave functions, $\chi_i(\vec{x}_i)$. This results in a Slater determinant, Φ_{SD}:

$$\Psi_0 \approx \Phi_{SD} = \frac{1}{\sqrt{N!}} \begin{vmatrix} \chi_1(\vec{x}_1) & \chi_2(\vec{x}_1) & \cdots & \chi_N(\vec{x}_1) \\ \chi_1(\vec{x}_2) & \chi_2(\vec{x}_2) & \cdots & \chi_N(\vec{x}_2) \\ \vdots & \vdots & \ddots & \vdots \\ \chi_1(\vec{x}_N) & \chi_2(\vec{x}_N) & \cdots & \chi_N(\vec{x}_N) \end{vmatrix} \tag{2.18}$$

where $\chi_i(\vec{x}_i)$ are one-electron spin orbitals consisting of the spatial coordinates of the electron as well as its spin function [α(s) or β(s), spin-up or spin-down], and the $\frac{1}{\sqrt{N!}}$ term ensures the wave function is normalized to ensure the probability density integrates to 1. It should also be noted that the Slater determinant is antisymmetric with respect to an exchange in spin orbitals. If any two rows or two columns are exchanged, the determinant will change sign.

The spin orbitals are orthonormalized:

$$\int \chi_i^*(\vec{x})\, \chi_j(\vec{x})\, d\vec{x} = \langle \chi_i \mid \chi_j \rangle = \delta_{ij} \tag{2.19}$$

where the Kronecker delta δ_{ij} is 1 when i=j and 0 otherwise.

Once the exact wave function has been approximated by the Slater determinant, the variational principle is applied to find the best Slater determinant (Φ_{SD} with the lowest energy). The spin orbitals are varied to minimize the energy, while remaining orthonormal:

$$E_{HF} = \min_{\Phi_{SD} \to N} E[\Phi_{SD}] \tag{2.20}$$

The energy is calculated as an expectation value of the Hamiltonian operator with the Slater determinant, and this can be shown with the expansion of the determinant with the electronic and nuclear terms of the Hamiltonian:

$$E_{HF} = \langle \Phi_{SD} | \hat{H} | \Phi_{SD} \rangle = \sum_{i}^{N} \left(i \mid \hat{h} \mid i \right) + \frac{1}{2} \sum_{i}^{N} \sum_{j}^{N} (ii \mid jj) - (ij \mid ji) \qquad (2.21)$$

where

$$\left(i \mid \hat{h} \mid i \right) = \int \chi_i^*(\vec{x}_1) \left\{ -\frac{1}{2} \nabla^2 - \sum_{A}^{M} \frac{Z_A}{r_{1A}} \right\} \chi_i(\vec{x}_1) \, d\vec{x}_1 \qquad (2.22)$$

$$(ii \mid jj) = \iint |\chi_i(\vec{x}_1)|^2 \frac{1}{r_{12}} \left| \chi_j(\vec{x}_2) \right|^2 d\vec{x}_1 d\vec{x}_2 \qquad (2.23)$$

$$(ij \mid ji) = \iint \chi_i(\vec{x}_1) \chi_j{}^*(\vec{x}_1) \frac{1}{r_{12}} \chi_j(\vec{x}_2) \chi_i{}^*(\vec{x}_2) d\vec{x}_1 d\vec{x}_2 \qquad (2.24)$$

define the kinetic energy and attraction between electrons and nuclei (eq. 2.22), the Coulomb integral (eq. 2.23), and exchange integral (eq. 2.24), respectively.

The exchange integral only accounts for interactions between parallel-spin electrons. Since the Hartree-Fock method only uses a single Slater determinant of non-interacting spin orbitals to describe the wave function, it does not properly account for interactions between opposite-spin electrons. In the next section, density-functional

theory will be used to describe these electron interactions as an improvement on Hartree-Fock methods.

2.4.1 Roothaan-Hall Equations

The Roothaan-Hall equations are used to further simplify the Hartree-Fock equations.[37] These equations are available for both open- and closed-shell systems, but only equations for closed-shell systems will be shown here (the equations for open-shell systems are called the Pople-Nesbet-Berthier equations).[41] They generalize the HF equations to a simple linear algebraic equation:

$$FC = SC\varepsilon \tag{2.30}$$

where F is the Fock matrix (which depends on C due to electron-electron interactions),

$$F_{ij} = H_{ij}^{core} + \sum_{k=1}^{K}\sum_{l=1}^{K} P_{kl}\left[(ij|kl) - \frac{1}{2}(ik|jl)\right] \tag{2.31}$$

C is the orbital coefficient matrix constructed from the molecular orbitals,

$$C = \begin{pmatrix} c_{1,1} & c_{1,2} & \cdots & c_{1,i} \\ c_{2,1} & c_{2,2} & \cdots & c_{2,i} \\ \vdots & \vdots & \ddots & \vdots \\ c_{i,1} & c_{i,2} & \cdots & c_{i,i} \end{pmatrix} \tag{2.32}$$

S is the overlap matrix of the basis functions,

$$S_{ij} = \langle \eta_i | \eta_j \rangle \tag{2.33}$$

and ε is the matrix of orbital energies. The Fock matrix (eq. 2.31) is composed of the Hamiltonian operator with slight changes. H_{ij} is a core Hamiltonian (only accounts for kinetic energy and electron-nuclear attraction), matrix element P_{kl} is a density matrix element of the occupied MOs,

$$P_{kl} = 2\sum_{i=1}^{n/2} c_{ik}^{*} c_{il} \tag{2.34}$$

and the (ij|kl) term is the two-electron repulsion integral (missing from H_{core}). It describes the Coulombic repulsion and can be written as:

$$(ij|kl) = \int\int \frac{\varphi_i^{*}(1)\varphi_j(1)\varphi_k^{*}(2)\varphi_l(2)}{r_{12}} dr_1 dr_2 \tag{2.35}$$

This term describes the repulsion between electron 1 and electron 2, where basis functions i and j are a part of the first system and k and l being a part of the second system, with the systems being a distance of r_{12} apart. Given a basis set, the (ij|kl) can be calculated; however, this equation is time-consuming and must be solved iteratively.

When i=j, the overlap matrix element will equal 1 (the basis function i will completely overlap basis function j). When $i \neq j$, there will be some degree of overlap between -1 (negative overlap) and 1 (complete overlap): $-1 \leq S_{i \neq j} \leq 1$.

2.4.2 Self-Consistent Field Procedure

As mentioned previously, $FC = SC\varepsilon$ must be solved iteratively. The spin orbitals are required to solve for the Hartree-Fock potential and the Fock operator, which, in turn, solves for the spin orbitals.[37] This issue cannot be solved in the traditional fashion. The solution is found by the Self-Consistent Field (SCF) procedure. This technique begins with an estimated set of orbitals and solves the HF equations. Using the computed set of orbitals from the previous calculation, the HF equations are solved again, computing a new set of orbitals. This procedure is repeated until the predicted change in total energy is below a certain threshold value. The set is said to have converged onto a set of self-consistent orbitals, as shown below in **Figure 2.1**:

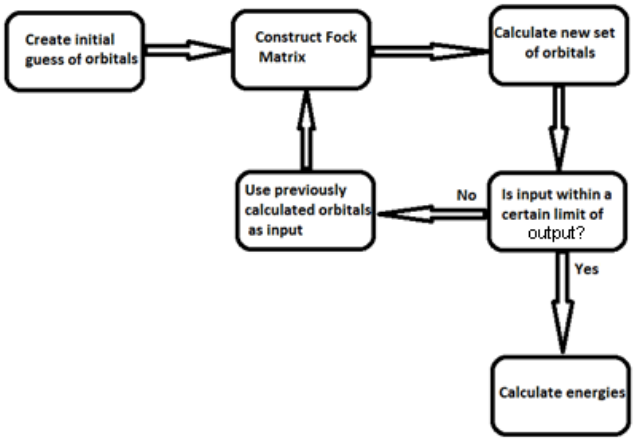

Figure 2.1 The general procedure for an SCF calculation.

2.4.3 Quadratic Convergence

An often-applied method for particularly difficult SCF convergence cases is the quadratically convergent method. This uses a linear approach when optimization is far from converging, and a Newton-Raphson[42] approach when close to convergence. Although this approach takes longer to complete, it is more robust and reliable than regular SCF methods.

2.5 Density-functional Theory

Density-functional theory (DFT) is an alternative method to Hartree-Fock theory.[37, 39] It is considerably more accurate for most molecular systems, as it accounts for electron correlation explicitly, but treats exchange approximately. Unless otherwise stated, all electron densities, $\rho(\vec{r})$, will be denoted as ρ for simplicity.

2.5.1 Hohenberg-Kohn Theorems

The first of the Hohenberg-Kohn theorems states that the electron density uniquely defines the Hamiltonian operator of a system as well as all properties of a system.[37] This can be shown by using two different external potentials, $\hat{V}_{ext}$ and $\hat{V}'_{ext}$, both generating the same electron density ρ_0 corresponding to the non-degenerate ground state of N particles.

Since the ground state energy (as well as all other molecular properties) depends on the ground state electron density of the system, it can be written as:

$$E_0[\rho_0] = T[\rho_0] + E_{ee}[\rho_0] + E_{ext}[\rho_0] \tag{2.36}$$

where $T[\rho_0]$ and $E_{ee}[\rho_0]$ are the ground state electron density-dependent kinetic and potential energy due to electron-electron repulsion, respectively. These two terms are known as "universal", as they will generate an expectation value $\langle\Psi|\hat{T} + \hat{V}_{ee}|\Psi\rangle$ when given any electron density. These two terms are independent of N, R_A, and Z_A, and define the Hohenberg-Kohn functional $F_{HK}[\rho_0]$. Eq. 2.36 can then be reduced to:

$$E_0[\rho_0] = \int \rho_0 V_{ext} d\vec{r} + F_{HK}[\rho_0] \tag{2.37}$$

This equation solves, without approximation, the Schrödinger equation. Unfortunately, the Hohenberg-Kohn functional is not explicitly known, but it can be further decomposed into an already well-known Coulombic potential $J[\rho]$, and all other unknown non-classical terms $E_{ncl}[\rho]$:

$$F_{HK}[\rho] = T[\rho] + E_{ee}[\rho] = T[\rho] + J[\rho] + E_{ncl}[\rho]. \tag{2.38}$$

A major challenge of density-functional theory is to find explicit expressions for $T[\rho]$ and $E_{ncl}[\rho]$.

The second Hohenberg-Kohn theorem is analogous to the variational principle previously described in this report. It states that the ground state energy of a system can only be given by its ground state density, and all other densities will lead to a higher energy.

2.5.2 Kohn-Sham Theory

The Kohn-Sham theorem offers a way to approximate this Hohenberg-Kohn functional, previously described in eq. 2.37.[37] It was thought that a pure density functional did not properly describe the kinetic energy of a system, and that this deficiency could be corrected by introducing orbitals for a "non-interacting" system and calculating the kinetic energy of the non-interacting system exactly. This method uses a Slater determinant (eq. 2.17) as it, by definition, represents the exact wave function of a non-interacting system. The spin orbitals are then determined by:

$$\hat{f}^{KS}\psi_i = \varepsilon_i^{KS}\psi_i \tag{2.39}$$

where f^{KS} is the one-electron Kohn-Sham (KS) operator, ψ_i is the i^{th} Kohn-Sham orbital, and $\varepsilon_i^{KS}$is the Kohn-Sham orbital energy of the i^{th} orbital. $\hat{f}^{KS}$ is defined as:

$$\hat{f}^{KS} = -\frac{1}{2}\nabla^2 + V_S(\vec{r}). \tag{2.40}$$

$V_S(\vec{r})$ is the effective local potential. This potential is such that the electron density of this non-interacting system, ρ_s, is the same as the real, fully-interacting system, ρ_0, to give:

$$\rho_0 = \rho_s = \sum_i^N \sum_s |\psi_i(\vec{r}, s)|^2 \tag{2.41}$$

This non-interacting electron density is used to calculate the non-interacting kinetic energy T_s, introducing a variation on the Hohenberg-Kohn functional, known as $F[\rho]$:

$$F[\rho] = T_s[\rho] + J[\rho] + E_{XC}[\rho] \tag{2.42}$$

where E_{XC} is the exchange-correlation energy, and accounts for the discrepancy between non-interacting and fully-interacting systems, as:

$$E_{XC}[\rho] \equiv (T[\rho] - T_s[\rho]) + (E_{ee}[\rho] - J[\rho]) = T_C[\rho] + E_{ncl}[\rho] \tag{2.43}$$

with $T_C[\rho]$ accounting for the part of kinetic energy missing from $T_s[\rho]$. It can be said that the exchange-correlation functional contains all unknown information about a system.

It can also be shown that the Kohn-Sham operator, $\hat{f}^{KS}$, can be written, using the variational principle, as:

$$\hat{f}^{KS} = -\frac{1}{2}\nabla^2 + \int \frac{\rho}{r_{12}} d\vec{r}_2 + V_{XC}(\vec{r}_1) - \sum_A^M \frac{Z_A}{r_{1A}} \tag{2.44}$$

where $V_{XC}(\vec{r}_1)$ is the potential caused by the exchange-correlation energy, and is defined as the functional derivative of the exchange-correlation energy with respect to the density:

$$V_{XC} \equiv \frac{\delta E_{XC}}{\delta \rho} \tag{2.45}$$

This approach gives the exact eigenvalues of the Hamiltonian for the Schrödinger equation, i.e. if all functionals were exactly known, this would give the exact energy of the system. Since E_{XC} and V_{XC} are unknown, this is not the case. Many methods have been developed to approximate these values.

2.5.3 Exchange-Correlation Functionals

The quality of these density-functional methods depends on how each method approximates the exchange-correlation energy.[39] One of the earliest methods to provide an accurate approximation to the exchange-correlation energy was the local-density approximation (LDA). This method approximates E_{XC} in a given chemical system by comparing it to the exchange-correlation energy per particle of a homogeneous electron gas, ε_{XC}, of density ρ:

$$E_{XC}^{LDA}[\rho] = \int \rho \, \varepsilon_{XC}(\rho) \, d\vec{r}. \tag{2.46}$$

This formalism can then be extended to the unrestricted case (chemical systems with different α or β spin-densities). This approximation is known as the local spin-density approximation (LSDA):

$$E_{XC}^{LSDA}[\rho_\alpha, \rho_\beta] = \int \rho \, \varepsilon_{XC}(\rho_\alpha, \rho_\beta) \, d\vec{r}. \tag{2.47}$$

These approximations offer results that are comparable to Hartree-Fock when considering equilibrium structures or harmonic frequencies, but are inadequate when

discussing bond energies due to overbinding. This makes this model insufficient for many areas of chemistry.

The generalized gradient approximation (GGA) offered an improvement on the LSDA by accounting for the electron density ρ as well as the gradient of the charge density ∇ρ and kinetic energy τ. This term is introduced to account for the difference in the exchange-correlation energy of the chemical system (inhomogeneous) compared to the electron gas (homogeneous),

$$E_{XC}^{GGA}[\rho_\alpha, \rho_\beta] = \int f(\rho_\alpha, \rho_\beta, \nabla\rho_\alpha, \nabla\rho_\beta)d\vec{r} \tag{2.48}$$

where f is some function of the spin densities and their gradients. These approximations lead to a large improvement in the agreement between calculated results and experimental data. These results can further be improved by adding corrections to the change in the gradient of the density ∇∇ρ. These methods are known as meta-GGA functionals.

Another approximation comes from the decomposition of the exchange-correlation energy into its exchange energy E_X and its correlation energy E_C. These components can be approximated in different ways. Some commonly-used gradient-corrected exchange functional E_X include Perdew and Wang's functional[37], as well as Becke's functional B88[43], shown below:

$$E_X^{B88} = E_X^{LSDA} - b\sum_{\sigma=\alpha,\beta}\int \frac{(\rho^\sigma)^{4/3}\chi_\sigma^2}{1 + 6b\chi_\sigma \sinh^{-1}\chi_\sigma} d\vec{r} \tag{2.49}$$

where

$$\chi_\sigma \equiv \frac{|\nabla \rho^\sigma|}{(\rho^\sigma)^{4/3}}, \tag{2.50}$$

$$E_X^{LSDA} = -\frac{3}{4}\left(\frac{6}{\pi}\right)^{1/3} \int \left[(\rho^\alpha)^{4/3} + \left(\rho^\beta\right)^{4/3}\right] d\vec{r}, \tag{2.51}$$

and b is an empirical parameter with value 0.0042.[43] There are many commonly-used gradient-corrected correlation functionals, such as the Lee-Yang-Parr (LYP) functional, the Perdew 1986 (P86), and the Becke correlation functional (B96). These exchange and correlation functionals can be combined to accurately represent the exchange-correlation energy, as with B3LYP, B3PW91, and B1B95.

2.5.4 Long-Range Corrected Functionals

While there are many methods adding improvements on previous DFT methods, the only method to be discussed in any detail will be ωB97X-D as it is used extensively throughout this project.[44] ωB97X-D is a hybrid functional (a GGA functional with a small amount of HF exchange to improve accuracy). Beginning with the B97 functional, any self-interaction errors are solved using 100% HF exchange for long-range electron-electron interactions using an error function to become ωB97. The addition of a short-range exchange parameter becomes ωB97x which smoothly transitions to the long-range functional. Finally, empirical atom-atom dispersion corrections are added to further

improve the functional without additional computational cost through the following expression:

$$E_{DFT-D} = E_{KS-DFT} + E_{disp} \tag{2.52}$$

where

$$E_{disp} = -\sum_{i=1}^{N_{at}-1} \sum_{j=i+1}^{N_{at}} \frac{C_6^{ij}}{R_{ij}^6} f_{damp}(R_{ij}) \tag{2.53}$$

and

$$f_{damp}(R_{ij}) = \frac{1}{1 + a(R_{ij}/R_r)^{-12}} \tag{2.54}$$

to form the long-range corrected ωB97X-D functional.

2.6 Force Field Methods

One of the major problems of computational chemistry is solving the electronic energy of a given nuclear conformation within a reasonable time frame. This step, as it pertains to force field methods, can be skipped. Force field methods, also known as molecular mechanics methods, refer to parameters of mathematical functions derived from high-level quantum mechanical calculations or experimental data used to describe

the potential energy of a system.[36] Force field methods differ from quantum mechanics in that they use classical Newtonian physics to describe the atoms in a molecule (spheres with mass attached to springs). The force field method being employed for this research will be the Assisted Model Building with Energy Refinement (AMBER) force field, as it has been parameterized for amino acid and protein systems.[45] This method can generate AMBER charges for each atom in the system to represent slight positive or negative charges. These charges are based on high-level quantum mechanical calculations.[46]

There are several parameters to be explored for each type of atom bonded to other atoms. These parameters are described various ways depending on the applied force field; however, the terms that will be described for the remainder of this work will be terms as described in the AMBER force field. The total force field energy of a system is given by:

$$E_{FF} = \sum E_{str} + \sum E_{bend} + \sum E_{tors} + \sum E_{vdw} \quad (2.55)$$

where these terms will be described in the following sections.

2.6.1 The Stretch Parameter

The stretch term, E_{str}, describes the energy of a bond that is stretched between atoms A and B according to Hooke's law,[36, 47] as shown in **Figure 2.2**:

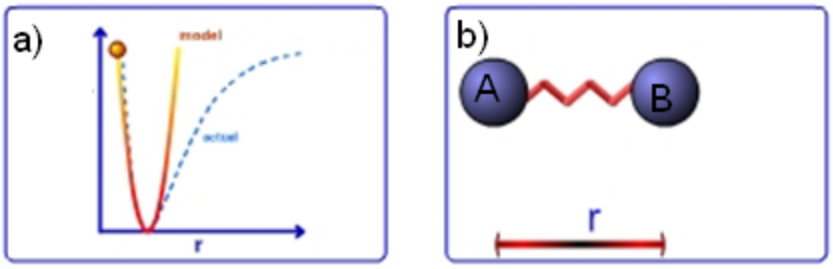

Figure 2.2 (a) Graph showing increase in energy as the bond is compressed or elongated, showing a minimum energy at intermediate bond length. **(b)** Atoms A and B connected by a spring with spring constant k and interatomic bond distance r.

$$E_{str} = k(r - r_0)^2 \tag{2.56}$$

As atoms A and B get closer, the energy of that particular system would increase due to steric repulsion. When atoms A and B are at their "equilibrium" distance r_0, the energy is lowest, as there is a slight attraction between the atoms. When these atoms get further apart, the bond breaks and the atoms are essentially isolated; however, this model treats this scenario as harmonic, as in **Figure 2.2a**. This prevents large deviations from the equilibrium bond distance due to the penalty function in eq. 2.53. This also shows that force field methods employing these simple methods are incapable of modeling bond dissociations, as they do not asymptotically decay to E=0. Each pair of atoms will have their own respective equilibrium bond distance r, and spring constant k, as determined by geometry optimizations at high levels of theory or experimental data.

2.6.2 The Bending Parameter

The bending term, E_{bend}, describes the energy as a function of the angle between atoms A, B, and C,[36, 47] as in **Figure 2.3**.

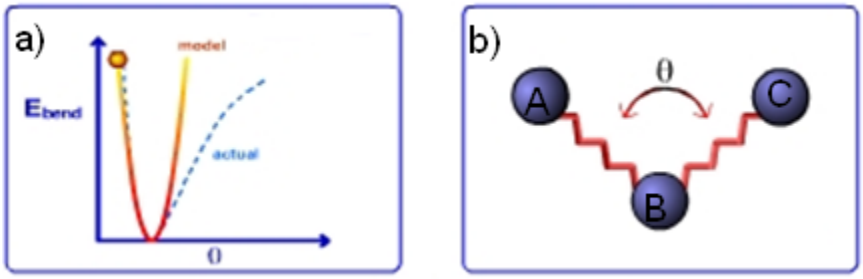

Figure 2.3 (a) Graph showing increase in energy as the bond angle is compressed or elongated, showing a minimum energy at intermediate bond angle. **(b)** Picture of atom A, B, and C with bond angle θ and spring constant k.

$$E_{bend} = k(\theta - \theta_0)^2 \tag{2.57}$$

As the bond angle θ approaches 0^0, atoms A and C will begin to experience a steric clash. This will cause the energy to increase to a maximum. The energy will decrease to a minimum as the bond angle for those particular three atoms reaches its equilibrium. As the bond angle surpasses its equilibrium angle, significant angle strain will cause the energy of the system to increase to a maximum. Eq. 2.57 treats this as a parabola, with a penalty function to prevent large deviations from the equilibrium bond angle.

2.6.3 The Torsional Parameter

The torsional term of the force field equation, E_{tors}, involves the interaction of atoms A and D, where atoms A-B, B-C, and C-D are bonded[36, 47], as in **Figure 2.4**.

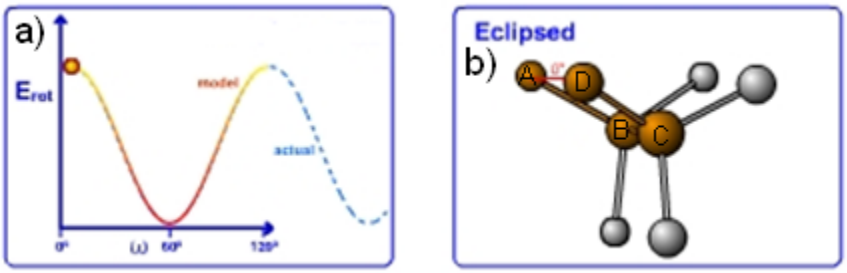

Figure 2.4 (a) Graph showing high energy when atom A (or D) eclipses another atom attached to atom B, and low energy when staggered. **(b)** Picture showing A-B, B-C, C-D bonds with dihedral angle ω, force constant V, and periodicity factor n.

$$E_{tors} = V(1 + \cos(n\omega)) \tag{2.58}$$

When atoms A and D are eclipsed, steric repulsion between the atoms gives an energy maximum. When these atoms are staggered, it gives an energy minimum. As the dihedral angle ω changes, it will vary between minimum and maximum, as shown in **Figure 2.4a**. The system will also have a force constant V, dependent on the atoms in the system. It should also be noted that the atoms A, B, C, and D do not necessarily need to be connected as shown in **Figure 2.4b**, as it can have A-B, A-C, and A-D bonds (as with the out-of-plane motion of NH_3).

2.6.4 The van der Waals Term

The van der Waals term describes the attraction or repulsion between non-bonded non-polar atoms interacting due to atomic charges.[36] These are, for example, interactions between functional groups at different parts of a molecule, or different molecules altogether.

At close inter-atomic distance, the van der Waals term is largely repulsive, as the electron clouds of the atoms overlap. At large inter-atomic distance, this penalty function approaches zero, as the systems are non-interacting. At medium distances, there is a slight attraction between electron clouds from induced dipole-dipole interactions. A popular function that obeys these rules is the Lennard-Jones potential:

$$E_{LJ}(R) = \varepsilon \left[\left(\frac{R_0}{R}\right)^{12} - \left(\frac{R_0}{R}\right)^{6} \right] \tag{2.59}$$

where R_0 is the interatomic distance for minimum energy and ε is the depth of the minimum, as shown below in **Figure 2.5**:

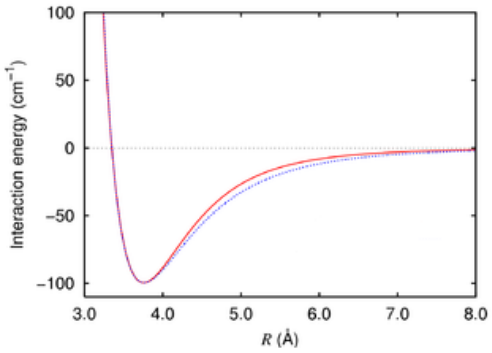

Figure 2.5 Graph showing asymptotic increase in energy as two atoms become close together, an energy minimum at ideal van der Waals distance, and energy trailing off as the atoms become infinitely far away.

2.6.5 Hydrogen Bonds

Hydrogen bonds are treated as an augmentation to the electrostatic description of the hydrogen bond. This term, as represented in AMBER, add approximately 0.5 kcal/mol to the hydrogen bond energy. This allows the majority of the description of hydrogen bonds to arise from the dipole-dipole interactions.

2.6.6 Restrained Electrostatic Potential Charges

Restrained electrostatic potential (RESP) charges are a charge method useful for allocating charges on atoms in molecules.[46] This model succeeds by sampling thousands of points near the molecule and creating an electrostatic potential caused by the molecule. This potential, created primarily from atoms closest to the surface of the molecule, will create faulty partial charges on the "buried" atoms. To accommodate for this error, a hyperbolic penalty function can be added to non-zero partial charges to ensure that only atoms that contribute to the electrostatic potential have charges significantly different

than zero. The RESP model also places certain constraints on the system, such as ensuring that both oxygens on a carboxylate functional group have the same partial charge, and that all charges on a group sum to zero.

2.7 OMEGA Software

One further method to be discussed is implemented by the OMEGA software, developed by OpenEye Scientific.[48, 49] This program performs very rapid (1-2 second) systematic conformational searches of a given molecule. OMEGA produces a large library of possible drug candidates and generates multi-conformer databases. This software has been used to reproduce conformations of known bioactive drugs, and these libraries can be used as input for the Fast Rigid Exhausted Docking software (discussed below).

2.7.1 Molecular Docking

Molecular docking is a computational method used to determine the optimal alignment between two molecules interacting with each other, i.e. fitting a small substrate molecule into a large protein active site.[50] This can be done using an X-ray crystal structure of a given protein with a substrate bound into the active site. In drug design, the substrate can be removed and other molecules fit into the active site to identify potential new drug candidates.

2.7.2 Fast Rigid Exhaustive Docking

Fast Rigid Exhaustive Docking (FRED) is a computational protein-ligand docking program.[50] It uses a protein structure [typically a Protein Data Bank (PDB) file] as input and fits small molecules into the active site based on a variety of fitting parameters.

A protein structure with bound ligand and crystallographic waters is input into the FRED program. During this step, the protein and water molecules are specified as being fixed, while the ligand is flexible. The active site is then defined placing a "box" over the bound ligand. This defines the three-dimensional position where new ligands can bind. All amino acids as part of the protein can then be "tweaked". Since the protein is held rigid, freely-rotatable groups (such as the alcohol groups on tyrosine and serine) need to be adjusted to maximize hydrogen bonding and other favourable interactions. Other issues with binding such as protonation are corrected by the user.

The next step is to create an active site potential. This is done by docking small molecular probes to the active site of the protein to detect likely sites for binding. This method takes longer than using carbon probes, but offers fewer, higher quality sites. This method offers an "inner" and "outer" contour of the shape potential. At least one heavy atom from the substrate needs to be within the inner contour at all times and all heavy atoms from the substrate need to be within the outer contour. This creates a restraint on the available positions for the substrate to limit computational time.

The last step involves loading a variety of new substrates to dock into the active site. These docked substrates will be given a score based on a variety of scoring functions.

2.7.3 Chemgauss Scoring Function

The scoring function implemented by the FRED software is Chemgauss3, developed by OpenEye Scientific.[51] It uses Gaussian functions to describe the chemistry and shape of given molecules. This method generates a score for each pose of a substrate based on a variety of scoring criteria.

The Chemgauss scoring function identifies each heavy atom as 'steric' (having a certain mass and size). These heavy atoms can also be described as a hydrogen bond acceptor or donor (strong, moderate or weak), coordinating groups, or metals. In addition to these heavy atom types, certain positions around these atoms can be identified: lone pairs, polar hydrogens, water positions, and chelator coordination. These terms are combined in such a way to generate appropriate scoring functions for each molecule being docked to the target protein.

2.8 Molecular Dynamics

Molecular mechanics methods suggest that a given system is stationary; for example, a given water molecule has a set bond length and bond angle.[36, 38] In reality, this does not occur. Even at 0 kelvin all systems vibrate and at elevated temperatures these systems are in constant motion, rapidly changing between one molecular conformation to another. Molecular dynamics (MD) methods account for these movements by solving Newton's equation of motion for molecules on the potential energy surface (PES) using the position and velocities of the atoms in the system.

The goal of molecular dynamics is to sample all possible conformations of a given system; however, depending on system size, this will take a very long time to

simulate. In addition if energy barriers exist between conformations the simulation may not properly sample the phase space; thus, only the local surrounding area of the potential energy surface is explored. However, high temperatures can be used to overcome these large energy barriers.

Molecular dynamics is often used for sampling the conformational space of large molecular systems. It can be especially useful when using a starting geometry from experimental data, i.e. X-ray crystal structures. The main disadvantage to this method is the need for very high temperatures to overcome large energy barriers, and relatively short time scales (on the order of 10-100 ns).

2.9 Geometry Optimization Methods

The methods previously discussed are used to optimize the geometry of a given molecular system.[52] These systems are optimized to an equilibrium geometry. These states are important to determine molecular properties. There are many computational methods and tools available to determine this minimum-energy geometry. Only a brief introduction to the material will be discussed, and any further reading will be the responsibility of the reader.

The molecular wave function is a function of the nuclear coordinates of a given molecular system. This means that all geometries of a molecule will generate a different wave function, and each wave function will produce a different energy. These energies can be used to create a multi-dimensional surface for the potential energy of a system called the potential energy surface (PES). Geometry optimization methods will search along the PES for a valley along the surface (where the energy of the system is lowest).

This energy minimum will give the best approximation to the ground-state molecular properties such as energy.

Minima along the potential energy surface represent low energy structures for the molecular system.[52, 53] A transition state is a high-energy conformation between two minima along the PES, and the energy difference between minima and transition state is the energy barrier for the reaction. These transition structures are more difficult to obtain compared to minima, as they are saddle points on the potential energy surface. They are first-order saddle points, as the PES is a maximum in one direction and a minimum in all other directions.

2.9.1 Synchronous Transit-Guided Quasi-Newton Method

The Synchronous Transit-Guided Quasi-Newton (STQN) method[53] uses a linear approach to classify transition states. It will converge efficiently on the transition structure, provided reliable reactant and product structures are available. It is also helpful if a transition state guess is provided from experimental data. This enables only a small portion of the PES to be explored and greatly reduces computational time required.

2.9.2 Ultrafine Grids

Two-electron integrals are calculated using numerical integration grids. Smaller grids (fine grids) are used by default, with a minimal number of points required to be sufficiently accurate. The number of points can be increased by using ultrafine grids to provide a greater accuracy in systems with many tetrahedral centers and larger, floppy potential energy surfaces with low frequency modes.

2.10 ONIOM

One of the main goals in computational chemistry is to find a proper balance between accuracy of computed results and computational cost.[54-57] Ideally, high-accuracy methods (i.e. density-functional theory) would be used to model very large systems, but this is not practical within the limits of computational resources available. This restricts the number of biochemically-relevant systems available for study.

"Our own N-layered Integrated molecular Orbital and molecular Mechanics" (ONIOM) is a method developed by Morokuma and coworkers.[54, 57-61] It allows highly-accurate methods to be applied to the chemically-relevant part of a system (i.e. the active site of an enzyme, where bonds are breaking and forming) and allows the rest of the system to be treated at the molecular mechanics level. It does this by allowing the user to define several "layers" and these layers are treated at differing levels of theory.

The high layer is used to define the area of the system where bond breaking and formation occur and is known as the 'model' system. The low layer consists of the entire molecule and is treated at a low level of theory, such as molecular mechanics or a semi-empirical method. It is known as the 'real' system.

ONIOM approximates the energy of the real system as a combination of both layers:

$$\mathrm{E}^{\mathrm{ONIOM}} = \mathrm{E}^{\mathrm{low}}(\mathrm{R}) + \mathrm{E}^{\mathrm{high}}(\mathrm{M}) - \mathrm{E}^{\mathrm{low}}(\mathrm{M}) \qquad (2.60)$$

This means that the energy of the entire system can be regarded as being the energy of the real system at low level of theory [$\mathrm{E}^{\mathrm{low}}(\mathrm{R})$] added to the energy of the model system

at high level of theory [$E^{high}(M)$] with the energy of the model system at low level of theory subtracted [$E^{low}(M)$]. This method greatly reduces computational resources required to accurately model large biochemically-important systems.

This model raises an interesting issue: what happens when bonds are cut between real and model systems (for example, in a carbon-carbon bond)? This would suggest one of the carbon atoms would be placed in the high layer and the other in the low layer, each treated with separate methods, and as tri-valent atoms. This issue is negated by the addition of link atoms (LA). These atoms are added to the atoms on the boundary of the model system (link atom connection, LAC) to satisfy any issues with valency, as shown in **Figure 2.6**.

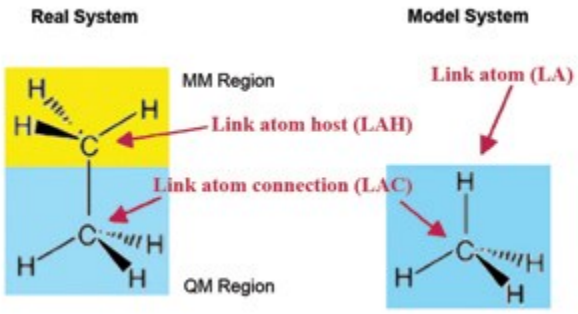

Figure 2.6 Image depicting the use of link atoms in between real and model systems.[62]

The ONIOM method can be used to perform geometry optimizations, compute energies, and predict vibrational frequencies; however, this method has the drawback of requiring each layer to be defined completely by the user. If the model system contains too many atoms, the calculations will be unnecessarily complex. If the model system does not include enough atoms, essential biochemical processes may not be modeled with desired accuracy.

2.11 Solvent Methods

All previously discussed methods occur *in vacuo*, meaning that the methods act on the isolated molecules in an ideal gas, and do not involve any solvent. Since many chemical and biological systems are not isolated from solvent, these types of gas phase calculations do not provide a realistic representation of many molecular systems.

The best way to model a chemical reaction would be using an explicit solvation model. This is done by introducing explicit solvent molecules to interact with the model system.[39] This may be considered one of the more accurate solvent models, but it is computationally demanding. For instance, in the case of water, as each solvent molecule is added the size of the system increases by ten electrons. Even after the addition of ten water molecules, the system would become dramatically larger, and calculations on even small systems may not be computationally feasible.

There are many ways to model solvation on model systems, but one of the more reliable methods is the implicit solvation model. This model places the molecule of interest in a spherical cavity inside the solvent with dielectric constant ε_r. An improvement on these simple models uses smaller spheres centered on top of each individual atom instead of a spherical cavity to represent the entire solute. This creates a much more physically reasonable cavity.

Once this step is finalized, the total energy of the system (solute and solvent) is calculated as:

$$E^{total} = E^{elec} + E^{NN} + E^{int} + E^{pol} \tag{2.61}$$

where E^{elec} is the electronic energy of the system, E^{NN} is the Coulombic repulsion of the nuclei, E^{int} is the solute-solvent interaction, and E^{pol} is the energy required to polarize the solvent.

3 MOLECULAR DOCKING OF PLASMODIUM FALCIPARUM FK506-BINDING PROTEIN 35

3.1 Introduction

Malaria is a world-wide epidemic affecting nearly 250 million people each year.[28, 63-66] Of those afflicted, nearly one million are African children, and these cases nearly always result in death.[28] It is a life-threatening disease caused by *Plasmodium* parasites. There are five types of malaria affecting humans; the most common and most deadly being *Plasmodium vivax* and *Plasmodium falciparum*, respectively. Symptoms of malaria include anemia, fever, headache, and nausea, and can be as severe as convulsions, coma, or death.[65]

Although human immunity reduces the risk of severe disease due to the parasite, it does not offer complete protection. The only reliable treatment, as with many diseases, is the persistent use of drugs, or anti-malarials. Chloroquine is the typical anti-malarial used in the treatment of *P. vivax*, *P. ovale*, *P. malariae*, and, up until the recent widespread resistance, *P. falciparum*.[67, 68] Upon first being discovered, it went unused for a decade, as it was thought to be too toxic for human use. The main issue related to using chloroquine is the rapid and significant resistance developed by *P. falciparum* in recent years. This could possibly be due to mass drug administrations (MDAs).[69]

As there has yet to be a viable vaccine for malaria,[70, 71] the current treatment for all types of malaria is a potent combination of artemisinin-based combination therapy (ACTs).[64, 72, 73] It is used for multi-drug resistant *P. falciparum* worldwide. Artemisinin and its derivatives can be administered orally or through intra-muscular injection, are fast

acting, and have a high likelihood of curing malaria. The parasites, however, have been slowly developing resistance to artemisinin and its derivatives in Cambodia and along the Thailand border. This has led to the recommendation that artemisinin-based monotherapies no longer be used and be exclusively replaced by ACTs.[74] ACTs are typically a combination of artemisinin (or a derivative, i.e. dihydroartemisinin, artesunate, etc.) and a drug from a different class (mefloquine, piperaquine, etc.). This has led to a reduced likelihood of developing resistance.

There are several issues with the current method of treatment for malaria: the drugs are non-specific (often treating malaria as well as a variety of other diseases), the drugs can be very toxic to humans, and the parasites can develop a resistance to the drugs after a short period of time.[75] Another fear is that certain drugs that treat malaria have similar mechanisms of action in the parasite. This is a serious concern; if the parasite develops resistance to one drug's mechanism of action, it could be resistant to several others. This highlights the need for a novel malaria treatment, and the investigation of peptidyl-prolyl *cis*/*trans* isomerases may offer new insight.

Peptidyl-prolyl *cis*/*trans* isomerases (PPIases) are a powerful enzyme superfamily capable of the rapid interconversion of *cis* and *trans* amide bonds in proteins and peptides.[76-78] Although this group of enzymes was believed to be the only biocatalyst whose sole purpose is the *cis*/*trans* interconversion of peptide bonds, new discoveries show that PPIases are also involved in such cellular processes as apoptosis or protein synthesis. These enzymes are present in many forms of life, ranging from bacteria to mammals. They are also found in all intracellular compartments and are not tissue

specific. Without the help from PPIase activity, proteins would fold improperly, take too long to fold, or never fold at all.[76]

Fk506-binding proteins (FKBPs) are the largest and most varied of the PPIases.[76-78] Containing between 107 and 580 amino acids, they can contain between one and four domains with isomerase activity. Every FKBP has a FKBP12 binding domain, which is homologous to FKBP12 found in the human body (*h*FKBP12). This well-known domain is made from a five-strand β-sheet with an alpha helix that forms the binding site for Fk506 (tacrolimus) and rapamycin. Tacrolimus is a small molecule that binds reversibly to FKBPs and inhibits isomerase activity. The mechanism by which *h*FKBP12 isomerizes proline residues in peptide chains has now been determined.[79-82]

The FKBP of particular interest to this work is FKBP35, commonly found in *P. vivax* and *P. falciparum* (*Pv*FKBP35 and *Pf*FKBP35, respectively). Due to the increasing anti-malarial resistance in these species in particular, FKBP inhibition is a novel concept for this issue: if the FKBPs can be inhibited and prevented from performing their isomerase activity, essential malarial proteins would not fold properly and the parasite would cease normal function and die. An important issue with this approach is: if the drugs inhibit FKBP35, what prevents them from inhibiting *human* FKBPs as well? It has recently been suggested that the *h*FKBP12 domain present in all FKBPs is noticeably absent from FKBP35 (**Figure 3.1**).[83, 84] His_{87} and Ile_{90} present in *h*FKBP12 are replaced by cysteine and serine in *Plasmodium* FKBP35 active site (Cys_{106}/Ser_{109} and Cys_{105}/Ser_{108} in *Pf*FKBP35 and *Pv*FKBP35, respectively). This implies that one active site could be selectively inhibited, while leaving the other unaffected. The next step in

this process would be to determine how different substrates interact in each active site and comparing these results using docking methods.

3.2 Docking Study

The emphasis of this work is, ultimately, to find the ideal drug candidate that will inhibit *Pv*FKBP35 and *Pf*FKBP35 enzymes while having little affect on the *h*FKBP12 enzyme. This can be explored through the implementation of docking studies.

Docking studies allow the comparison between different substrates binding into the active site of a given enzyme. Using these methods, a variety of known available substrates (**Figure 3.2**)[50] can be docked into the active site of *Pv*FKBP35, *Pf*FKBP35, and *h*FKBP12 (PDB code: 3IHZ, 2VN1, 1FKJ, respectively).[84-86] For additional completeness, the substrates were also docked into the active site of *h*FKBP12 with bound FKBP-rapamycin-associated protein (FRAP, PDB code: 1FAP).[87] These active sites with bound natural substrates are outlined in **Figure 3.1**. This enzyme was included as these substrates would be expected to bind favourably into this active site as well as the active sites discussed previously. This additional enzyme complex has been included to verify docking methods: rapamycin and its derivatives would be expected to bind more favourably to the Fk506-binding domain and FRAP (FKBD+FRAP) than FKBP alone, and this should be reflected in the docking scores.

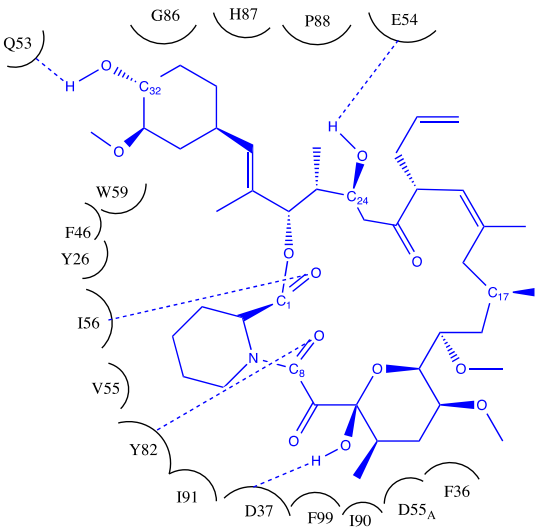
G86
H87
P88
E54
Q53
W59
F46
Y26
I56
V55
Y82
I91
D37
F99
I90
D55A
F36

(a)

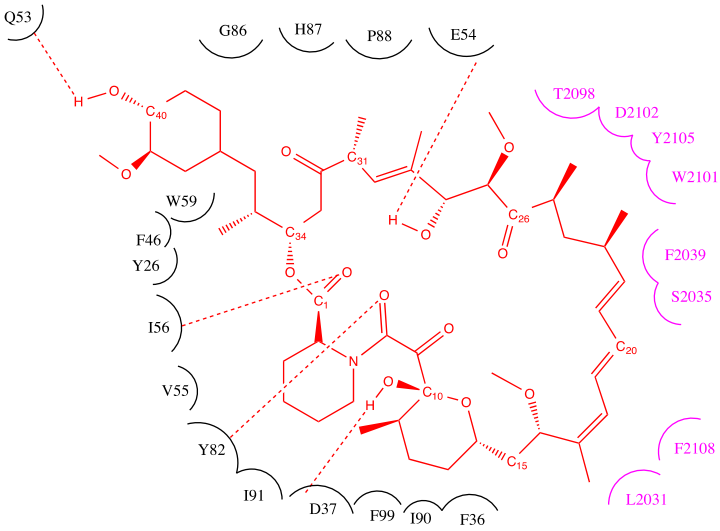
Q53
G86
H87
P88
E54
T2098
D2102
Y2105
W2101
W59
F46
Y26
F2039
S2035
I56
V55
Y82
F2108
I91
D37
F99
I90
F36
L2031

(b)

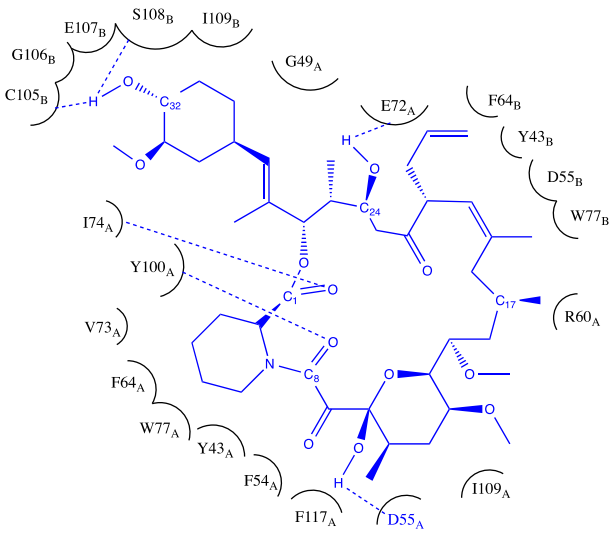

(**c**)

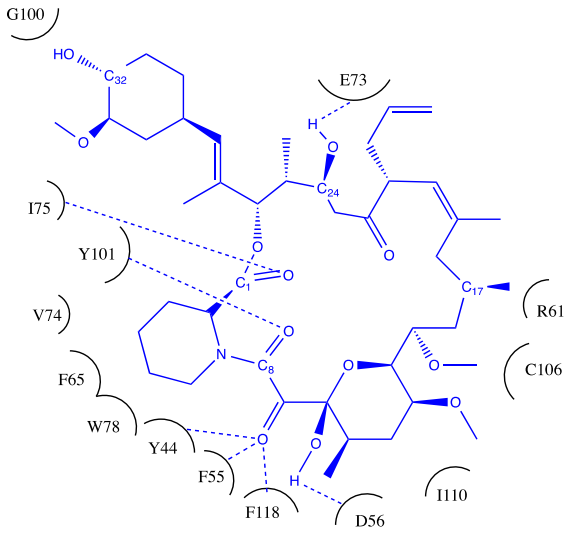

(**d**)

Figure 3.1 Active site illustrations for **(a)** *h*FKBP12, **(b)** *h*FKBP12+FRAP, **(c)** *Pv*FKBP35, and **(d)** *Pf*FKBP35. All active sites have bound Fk506 (blue) or rapamycin (red). Active site residues are outlined around the substrate. Purple residues represent the FRAP complex interacting with rapamycin. Residues without hashed lines represent nonpolar contact residues and hashed line represent hydrogen bonding residues. Residues

marked with “A” or “B” belong to the “A” or “B” peptide chain. These active sites were used as receptors for the docking of various macrocycles.

For the best results, a particular substrate would give a very large negative (strongly binding) score when docked to parasitic enzymes with a non-binding or weakly-binding (large positive) score when docked to human enzymes. This would suggest a substrate could selectively inhibit *Pf*FKBP35 and *Pv*FKBP35 and could be used as a starting point for drug discovery while having little effect on the human isomerases. The substrates used for docking to the active sites are shown below, as several of these compounds have shown inhibitory responses to differing isomerases and are derivatives of previously synthesized drug candidates.[84] The goal of this study is to discover a substrate that binds very strongly with *Pv*FKBP35 or *Pf*FKBP35 while having very little or no binding affinity for the active site of *h*FKBP12. This work could be used to find exploitable differences in the protein active sites to be used in further drug development.

Comparisons of binding scores of ligands between different proteins happen very little in the described work. Much of the work described is the comparison of qualitative docking scores of ligands within certain proteins, which has been shown to be acceptable.[88-90] This work does not attempt to compare binding scores of specific ligands across proteins. The only comparisons between proteins are overall qualitative trends (i.e. Fk506 and its derivatives bind stronger than rapamycin and its derivatives, etc.), stating that changes in binding affinity of ligands within proteins is consistent across all proteins used. In this work, we are concerned with the overall qualitative trend, not with the absolute binding score.

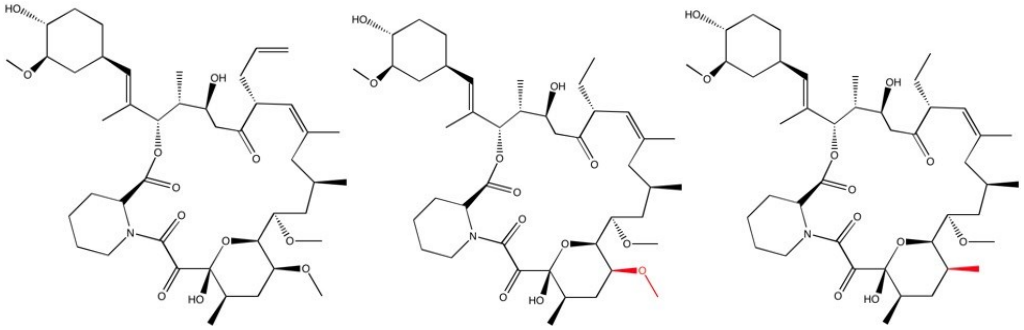

(a) **(b)** **(c)**

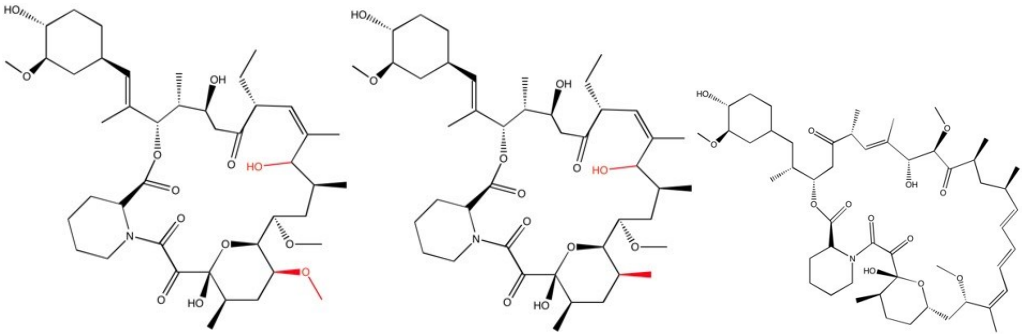

(d) **(e)** **(f)**

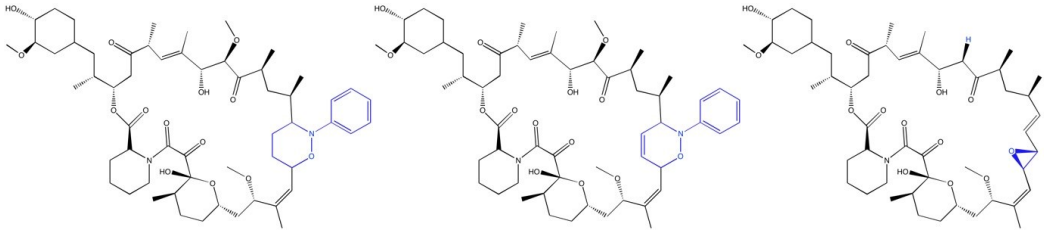

(g) **(h)** **(i)**

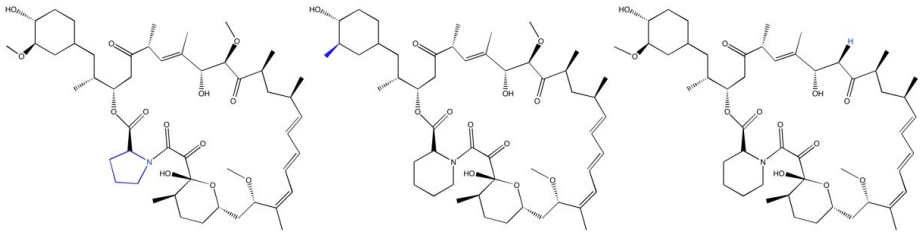

(j) **(k)** **(l)**

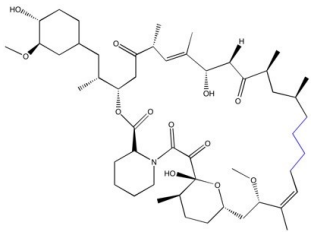

(m)

Figure 3.2 Substrates used in docking study: **(a)** Fk506, **(b)** Fk520, **(c)** 13-dM(Me)-Fk520, **(d)** 18-OH-Fk520, **(e)** 13-dM(Me)-18-OH-Fk520, **(f)** rapamycin, **(g)** ILS-920, **(h)** WYE-592, **(i)** WAY-179639, **(j)** prolylrapamycin, **(k)** desmethylrapamycin, **(l)** desmethoxyrapamycin, and **(m)** 40-Sub-1,2,3,4-tetrahydrorapamycin. These substrates were docked into the active sites of *h*FKBP12, *h*FKBP12+FRAP, *Pv*FKBP35 and *Pf*FKBP35 and the docking scores compared. The red and blue sections of the figure represent the modifications made to the substrate.

3.3 Computational Methods

All substrates outlined in **Figure 3.2** were docked into the active sites of *h*FKBP12, *h*FKBP12 binding domain and bound FRAP (FKBD+FRAP), *Pv*FKBP35 and *Pf*FKBP35 (**Figure 3.1**, PDB codes: 1FKJ, 1FAP, 3IHZ, and 2VN1, respectively).[84-87] The active site was defined in all enzyme systems as the residues directly interacting with the bound Fk506 substrate. This gives the docked substrates a very small active site volume, and allows for very fast docking into the chosen active site.

All molecular docking calculations were performed with the FRED receptor software developed by OpenEye Scientific.[50] The scoring function used for the FRED receptor software was Chemgauss3, also developed by OpenEye Scientific.[51, 91] The FRED

receptor program has been shown to be a reliable docking method for quickly binding various substrates into different enzymes.[88, 92] The ChemGauss3 scoring function can accurately predict binding modes and qualitatively predict binding strength for competing substrates.[51, 91] This scoring function is used as a simplified protein-ligand binding energy which has been shown to be a reasonable approximation to experiment.[91, 92]

A high quality potential was generated for the active site for all four enzymes in the docking study. All substrates were built using Fk506 and rapamycin as a template with functional group changes performed using the Avogadro graphical interface.[93] Although all substrates are rigid macrocycles, all rotatable bonds were allowed to optimize with respect to the active site. All amino acids near the active sites were 'tweaked' to maximize hydrogen bonding potential. When residues are 'tweaked, this allows all terminal rotatable bonds (alcohols, thiols, etc.) to change their geometry to optimize available hydrogen bonds between active site and docked substrate. All crystallographic waters were included as part of the protein. This docking method has been used previously with considerable success.[51, 88, 92, 94]

3.4 Results and Discussion

The results of the docking study are tabulated in **Table 3.1**. Comparatively, more negative scores indicate more stabilizing forces and better binding. It is noted that while these values are likely not quantitatively accurate (due to differing substrate-protein interactions), they likely provide a correct qualitative ordering of the ligands tested.[51, 88, 92, 94] Some important comparisons can be made between substrates.

Substrate	*h*FKBP12		*Pv*FKBP35	*Pf*FKBP35
	FKBD	FKBD+FRAP	FKBD	FKBD
Fk506	-25.21	-87.53	-110.06	-103.41
Fk520	-24.32	-89.07	-104.56	-102.37
13-dM(Me)-Fk520	-24.74	-91.97	-110.93	-100.65
18-OH-FK520	-24.32	-89.07	-104.56	-102.37
13-dM(Me)-18-OH-Fk520	-24.74	-91.97	-110.93	-100.65
Rapamycin	-1.93	-150.17	-33.24	-33.64
ILS-920	34.24	-120.09	-67.28	-10.74
WYE-592	34.24	-120.09	-67.28	-10.74
WAY-179639	-1.93	-150.17	-33.24	-33.64
Prolylrapamycin	-3.11	-148.29	-24.73	-28.52
Desmethylrapamycin	-4.16	-153.67	-29.56	-32.93
Desmethoxyrapamycin	-3.17	-149.70	-31.61	-35.30
40-Sub-1,2,3,4-tetrahydrorapamycin	-3.17	-149.70	-31.61	-35.30

Table 3.1 Results obtained from docking study of various substrates into the Fk506-binding domain (FKBD) of *h*FKBP12, *Pv*FKBP35, *Pf*FKBP35, as well as the binding domain of *h*FKBP12 with the FKBP12-rapamycin-associated protein (FRAP). A strong interaction between substrate and receptor is shown with a large negative docking score while weakly or non-interacting substrates will have a positive docking score.

3.4.1 Docking Study for *h*FKBP12

As seen in **Table 3.1**, the substrates that bind strongest in the Fk506-binding domain (FKBD) of *h*FKBP12 are Fk506 and its derivatives. All derivatives have similar docking scores, while Fk506 is given the best score. This implies that the deviations made to Fk506 are less favourable for inhibition than the original substrate. Identical binding scores of -24.32 are given for Fk520 and 18-OH-Fk520. For 13-dM(Me)-Fk520 and 13-dM(Me)-18-OH-Fk520, both have binding scores of -24.74. The marginal differences in binding score imply that the addition of an alcohol group at carbon 18 or the presence of a vinyl group at carbon 21 does not provide a significant improvement for inhibition through hydrogen bonds or sterics.

Rapamycin and its derivatives bind less favourably than Fk506, as to be expected. ILS-920 and WYE-592 have identical binding scores of 34.24, which would imply that the change from alkane to alkene would have no effect on inhibition; however, it is important to remember that the Chemgauss3 scoring function only takes into account heavy atoms (except in the cases for hydrogen bond donor/acceptor). This means there is little difference for docking for an sp^3 or sp^2 carbon. For this same reason, identical scores are given to desmethoxyrapamycin and 40-Sub-1,2,3,4-tetrahydrorapamycin (-3.17). Lastly, rapamycin and WAY-179639 have identical scores (-19.3), suggesting the addition of an epoxide has little effect on inhibition. The trends for substrates with identical scores are mirrored for all enzymes used in the docking study.

3.4.2 Docking Study for *h*FKBP12+FRAP

Rapamycin and Fk506 are both immunosuppressive drugs that can bind to FKBP12 and inhibit its PPIase activity. The rapamycin-FKBP12 complex can bind with the FKBP12-rapamycin-associated protein (FRAP, PDB code: 1FAP) in humans. This will cause cell-cycle arrest. Rapamycin will bind into a hydrophobic binding pocket of both FKBP12 and FRAP, forming a dimer.

Rapamycin binds much more favourably with FKBD+FRAP than Fk506 (-150.17 compared to -87.53); this is expected, as it has been experimentally shown that the Fk506-FKBP12 complex will not bind FRAP. This is shown through the comparatively low docking score. The best substrate to bind and inhibit the FKBD+FRAP is desmethylrapamycin with a docking score of -153.67, suggesting that the substitution of a methyl group for the ether at carbon 42 improves binding affinity, and the addition of the bulky groups at carbon 19 lowers binding affinity, as with ILS-920 and WYE-592 (-120.09).

3.4.3 Docking Study for *Pv*FKBP35 and *Pf*FKBP35

Docking all substrates into the active sites of *Pv*FKBP35 and *Pf*FKBP35 yields comparative results. In both enzymes, Fk506 and its derivatives have better scores than rapamycin and its derivatives, with Fk506 being the best inhibitor for both enzymes with a docking score of -110.06 and -103.41, respectively. One anomaly was found while docking ILS-920 and WYE-592 to both enzymes. The docking scores of ILS-920 and WYE-592 are far more favourable than rapamycin in *Pv*FKBP35 (-67.28 compared to -33.24), while the same substrates are far less favourable than rapamycin in *Pf*FKBP35 (-

10.74 compared to -33.64). While these active sites are conserved, there is evidence to suggest that the *Pv*FKBP35 active site can favourably accommodate a bulky group at carbon 19 while this is detrimental for inhibition of *Pf*FKBP35.

3.5 Conclusions

Of particular interest is the difference in docking score for ILS-920 and WYE-592 in the *Plasmodium* FKBP35 enzymes. The current work suggests *Pf*FKBP35 cannot favourably accommodate a bulky group on carbon 19, while this addition seems to improve inhibition for *Pv*FKBP35. It is also important to note the change from rapamycin to ILS-920 or WYE-592 (the addition of a nitrosobenzylated moiety) in *h*FKBP12 results in a decrease in docking score. This would suggest the addition of a bulky moiety on carbon 19 could lead to novel inhibitors of *P. vivax* without negatively affecting the most common *Homo sapiens* Fk506-binding protein binding domain. These results provide insight into the molecular interactions that in turn may be important for the development of anti-malaria drugs.

4 COMPUTATIONAL INSIGHTS INTO THE SUICIDE INHIBITION OF *PLASMODIUM FALCIPARUM* FK506-BINDING PROTEIN 35

4.1 Introduction

Malaria (genus *Plasmodium*) is a mosquito-borne parasite effecting millions of people each year in Sub-Saharan Africa, Asia and South America.[63, 69, 73, 75] *Plasmodium falciparum* and *Plasmodium vivax* are by far the most common strains of malaria, with *Plasmodium falciparum* being the most virulent.[66, 84, 95-98] Female *Anopheles* mosquitoes transmit the parasite from host to host. This allows sporozoites to travel through the blood stream of the host to the liver, where they reproduce asexually and continues to infect red blood cells. The asexual reproduction continues until the red blood cells lyse and infect other red blood cells. The new parasites are ready for uptake upon subsequent mosquito meals to be transferred to a new host. Common symptoms of malaria include headaches, anemia, nausea, recurring fever and chills, which can, if untreated, lead to the death of the infected individual.[65]

The available treatment for malaria has been a growing concern in the 20th and 21st centuries, as the parasites have been developing an increased immunity to the currently used drugs.[99] A common treatment for malaria is artemisinin-combination therapy (ACT), a potent mix of anti-malarials such as amodiaquine, lumefantrine, and pyrimethamine [64, 72-74]. This combination of anti-malarials lowers the risk of parasitic immunity to one specific drug; however, parasites have been observed that show

immunity to many of the presently used drugs.[99, 100] This concern over growing immunity has inspired an interest into research focusing on novel anti-malarials.

The use of anti-malarials to target an enzyme superfamily present in all forms of life, peptidyl-prolyl *cis*/*trans* isomerases (PPIases),[76-78] will be discussed. In particular, the Fk506-binding proteins (FKBPs)[76-78] are the focus of this study. FKBPs are responsible for the *cis*/*trans* interconversion in peptide chains for protein folding and without them nascent peptide chains would fold improperly or take too long to fold, resulting in cell death. The natural substrate for FKBPs is tacrolimus (Fk506) and is shown in **Figure 4.1**.[101] It has been proposed that inhibition of this enzyme *in vivo* would deform the enzyme, prohibit the enzymatic isomerase activity, and prevent the parasite from surviving.[95]

Figure 4.1 Fk506 (tacrolimus), the natural substrate of Fk506-binding proteins.

While different types of inhibition exist suicide inhibition is a form of enzyme inhibition where a covalent bond is formed between substrate and enzyme.[102, 103] This covalent bond forms an irreversible product complex during the normal catalysis reaction

to form an inhibitor-enzyme complex. This causes the enzyme to be unable to release the newly-formed product and thus unable to continue its function as an enzyme.[104]

Suicide inhibition is used in rational drug design where extensive information is known about substrate binding or the catalytic mechanism for a chosen enzyme. With this information, a novel substrate can be synthesized similar to natural substrates with slight variation. These changes can be exploited to form covalent bonds between a novel substrate and enzyme.[105]

In this work, suicide inhibition will be used to explore new possible treatments for malaria. The PPIases that will be investigated are human FKBP12 (*h*FKBP12) as well as *Pf*FKBP35 and *Pv*FKBP35 found in *Plasmodium falciparum* and *Plasmodium vivax*, respectively. It is noted that these three enzymes have highly conserved active sites.[83, 84, 96, 97] While this makes it particularly difficult to specifically target a particular enzyme it is important to realize that the parasitic enzymes have a cysteine amino acid residue (for instance Cys_{106} in *Pf*FKBP35) in place of the histidine found in *h*FKBP12 (i.e., His_{87}) (**Figure 4.2**).[84, 95] This subtle difference opens up the possibility of using this cysteine residue as a nucleophile to form a covalent bond between the enzyme and substrate, preventing the enzyme from performing its isomerase function. This can be achieved by adding an electrophile such as a Michael acceptor to position 42 on the natural substrate, Fk506.[95, 101] Notably, this Michael acceptor can act as an electrophile for the nearby cysteine in the parasitic enzymes. This bond would not be formed in *h*FKBP12 as histidine cannot act as a nucleophile. While the cysteine residue is found in both *Pv*FKBP35 and *Pf*FKBP35, only *Plasmodium falciparum* is a valid target for this

approach, as the cysteine is involved in a disulfide bridge in *Pv*FKBP35 and therefore unable to act as a nucleophile.

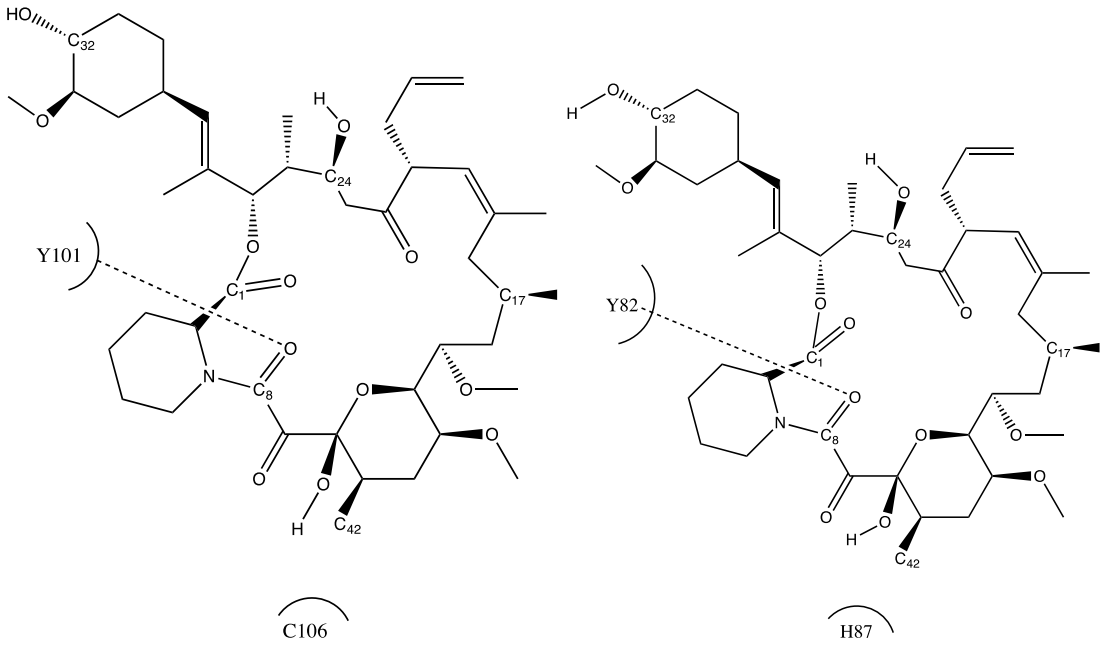

Figure 4.2 Active sites of **(a)** *Pf*FKBP35 with bound Fk506, showing important cysteine and tyrosine residues, and **(b)** *h*FKBP12 with bound Fk506, showing histidine and tyrosine residues.

This work aims to answer the question: provided there was a substrate with an appropriately positioned electrophile, could Cys_{106} perform a nucleophilic attack and form a covalent bond with the natural substrate? This type of targeted covalent inhibition has been achieved with a cysteine residue in a major oncology drug target.[106] This approach modeled a quinazoline inhibitor and added an electrophile to form a covalent bond with the cysteine residue. This form of suicide inhibition has been repeated with

other endogenous cysteine residues in various enzyme systems with positive results.[44, 59, 99, 107, 108] Tacrolimus is already approved by the FDA for human use[109], so if this rational drug design approach is valid, it could be a relatively cheap and safe alternate treatment for malarial infection.

4.2 Computational Methods

The molecular operating environment (MOE)[110] program was used for model preparation, energy minimization and assessment of the generated trajectories. Molecular dynamics (MD) simulations were performed using the NAMD program.[111]

4.2.1 Molecular Dynamics and Model Preparation

The Fk506-FKBP35 X-ray crystal structure from *Plasmodium falciparum* was used for all calculations (PDB ID: 2VN1).[86] Protonate3D was used to add hydrogen atoms to the crystal structure.[112] The system was solvated using a 7 Å spherical layer of water molecules. An MD simulation was then performed for 11 ns on the solvated system. As noted above, MD simulations were performed using the NAMD program to obtain the trajectories.[111] A constant temperature of 300 K and a time step of 0.5 fs were used with the AMBER99[113] force field for the simulation. From the trajectories the RMSD of the substrate and active site were then calculated with respect to the structure at t=0. These RMSDs where then clustered into 5 groups. An average structure from the most populated cluster was then energy minimized and then used as the starting structure for subsequent QM/MM calculation (see below). The minimization was done using the AMBER99[113] force field until the root mean square gradient of the energy fell below 1

kcal mol^{-1} $Å^{-1}$. It is noted that similar protocols have been previously successfully implemented.[114, 115]

4.2.2 QM/MM Modeling

The Gaussian 09 program[116] was used for all two-layer ONIOM[54, 58-61, 108, 117-119] QM/MM calculations. Structures were optimized at the ONIOM(B3LYP/6-31G(d):AMBER96) level of theory in the mechanical embedding (ME) formalism.[44, 107, 120-122] The transition state geometry was calculated using the opt=ts keyword in Gaussian after calculating force constants with an initial guess at the transition state geometry. Frequency calculations at this level of theory were done to verify the nature of the stationary points on the PES as well as to obtain Gibbs energy corrections. Single point energies for stationary points on the PES were obtained at the ONIOM(B3LYP/6-311+G(2df,p)//AMBER96) level of theory with electronic embedding and Gibbs energy corrections added (see above).[44, 107, 120-122] The AMBER force field used contained all necessary parameters for the calculations, while any additional parameters required due to truncating the protein or splitting the high and low layers in the ONIOM model have been supplemented by the generalized AMBER force field (GAFF).

Using the minimized structure obtained from the MD simulations, a QM/MM model was generated. From this model, the Michael-acceptor is added to carbon 42, as shown in **Figure 4.3**. The QM layer includes a large portion of the Fk506 substrate (including the Michael acceptor), the R-group of a nearby tyrosine residue (Tyr_{101}), and the R-group of the cysteine to be used as nucleophile (Cys_{106}). The MM layer includes all residues that surround the QM layer and all water molecules that interact with the QM

layer. To maintain the structure of the active site, all α-carbons within the backbone of the protein were held fixed at their MM-optimized positions.

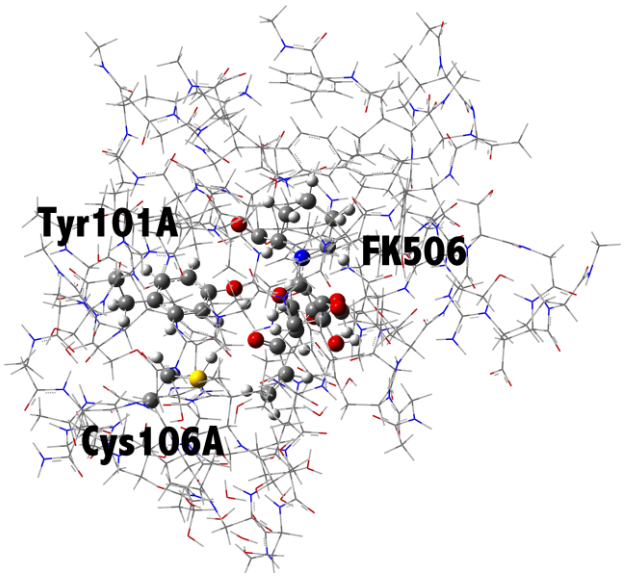

(a)

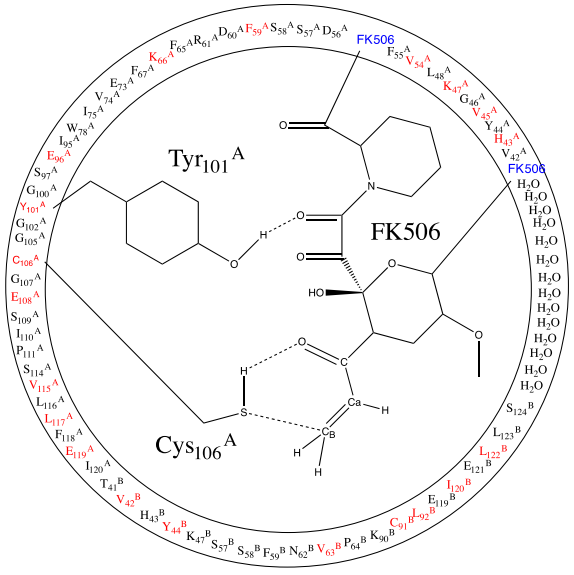

(b)

Figure 4.3 (a) The QM/MM model used to investigate the suicide inhibition of *Pf*FKBP35 with modified Fk506 substrate. **(b)** Schematic representation of the QM/MM

model: groups in the inner and outer circles have been modeled at the B3LYP/6-31G(d) and AMBER96 levels of theory, respectively. Residues written in black are included in the MM layer entirely, residues in red only have their peptide backbone included, and residues in blue represent the remainder of Fk506 not included in the QM region. The superscript "A" and "B" denote to which chain the residue belongs.

4.3 Results and Discussion

The reactant complex, transition state, and product complex for the above calculations with bond lengths of interest are shown in **Figure 4.4**, **Figure 4.5**, and **Figure 4.6**.

The optimized reactant complex (**Figure 4.4**) confirms the nearby Cys_{109} is in a position to interact with the modified Michael acceptor. The cysteinyl sulfur has an interatomic bond distance of 3.76 Å from the terminal end of the Michael acceptor $r(S_{Cys}\cdots C_{\beta})$. The hydrogen atom to be transferred to the carbonyl of the Michael acceptor has $r(H_{Cys}\cdots S)$ of 1.34 Å and $r(H_{Cys}\cdots O)$ of 2.37 Å. This moiety likely forms a hydrogen bond between cysteine and the Michael acceptor with a feasible interatomic distance to allow for bond formation. For the allylic ketone functional group in the Michael acceptor being attacked, the vinyl bond length $r(C_{\beta}\cdots C_{\alpha})$ and alpha carbon-carbonyl bond length $r(C_{\alpha}\cdots C)$ are 1.34 Å and 1.48 Å, respectively. The combination of the carbonyl and allene functional groups lead to a slightly shorter than typical C-C bond length between all three sp^2 hybridized carbons. In the case of the carbonyl (C=O) bond length it is calculated to be 1.23 Å, which corresponds to a typical length for such a bond.[123] Because

this is the reactant complex the single point energy with Gibbs thermal corrections is set 0.0 kJ/mol. The energies of all other stationary points on the PES are relative to this 0.0 kJ/mol.

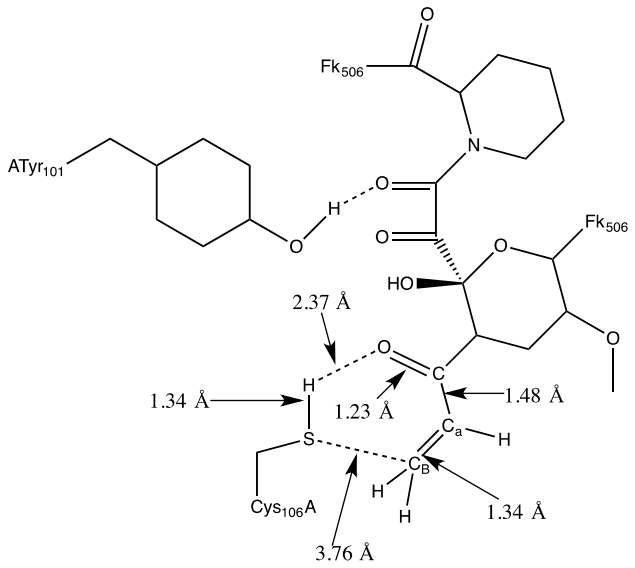

Figure 4.4 The reactant complex for modified Fk506 bound into the active site of *Pf*FKBP35.

The transition state is representative of the bond formation between the cysteinyl sulfur and the terminal end of the Michael acceptor while simultaneously transferring a proton from the cysteinyl thiol to the carbonyl group of the Michael acceptor (**Figure 4.5**). As $r(S_{Cys}\cdots C_{\beta})$ shortens to 2.31 Å, $r(S_{Cys}\cdots H_{Cys})$ lengthens to 1.50 Å. Concomitantly, a proton transfers to the forming enolate, where $r(H_{Cys}\cdots O)$ shortens to 1.42 Å. For this transition state an imaginary frequency of i931.89 cm^{-1} is obtained that

corresponds to the simultaneous sulfur-carbon bond formation and proton transfer. The Gibbs energy for this step relative to the reactant complex was found to be 91.3 kJ/mol.

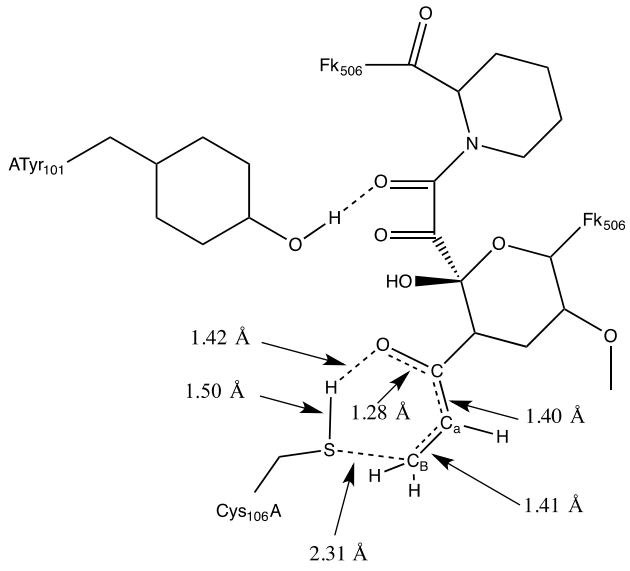

Figure 4.5 The transition state for the nucleophilic addition of cysteine to the modified Fk506 substrate.

Upon product complex formation (**Figure 4.6**), the sulfur-carbon bond has formed with $r(S_{Cys}\cdots C_{\beta})$ shortening to 1.87 Å while complete proton transfer from the cysteine residue to the carbonyl oxygen forming an alcohol has occurred (i.e., $r(H_{Cys}\cdots O) = 0.98$ Å). Upon sulfur-vinyl bond formation, $r(C_{\beta}\cdots C_{\alpha})$ elongates to 1.51 Å, which is to be expected as the beta carbon changes from sp^2 hybridized to sp^3 hybridized. This forces $r(C_{\alpha}\cdots C)$ to shorten to 1.35 Å as it changes from a single bond to a double bond, and $r(C\cdots O)$ to elongate as it changes from a carbonyl group to an alcohol. This final product complex has a Gibbs energy of 6.7 kJ/mol when compared to the reactant complex. Thus, at standard conditions the reaction is slightly endergonic.

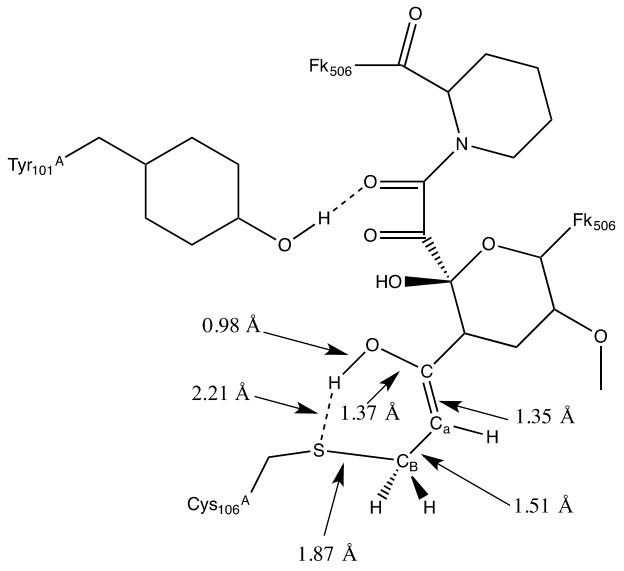

Figure 4.6 The product complex formed after the nucleophilic addition of cysteine to the modified Fk506 substrate.

Overall from this mechanistic pathway shows that suicide inhibition using cysteine as a nucleophile could be a valid direction for malaria treatment. The work performed could act as a proof of concept, showing how macrocycles of varying size and structure could be modified with different electrophiles to perform suicide inhibition. This method could have a few concerns, namely the issue of stability and synthesis of the modified substrate, the nucleophilicity of Cys_{106}, the electrophilicity of the Michael acceptor, and the toxicity of the Michael acceptor. This method does not discuss the stability of the modified Fk506, or the synthetic plausibility of this modification, as the addition of the Michael acceptor at carbon 42 would be difficult. What is important, however, is that macrocycles that would fit into both active sites (such as derivatives of

rapamycin and Fk506)[95] could be modified with various electrophilic functional groups to further exploit this active site difference.

As for the nucleophile, endogenous cysteines have been used for suicide inhibition in a variety of reactions and enzymes.[124-128] The nucleophile could also be modified through deprotonation of the cysteine to further strengthen the formed covalent bond. Considering the electrophile, a derivative of the chosen Michael acceptor (3-buten-2-one) has been shown to have greater reactivity than its aldehyde or ester equivalents, with a predicted log K of 3.51 when reacted with glutathione.[129] This structure also has a log EC of -4.51 for *Tetrahymena pyriformis* after 48 hour exposure, indicating this Michael acceptor has a comparatively smaller toxicity than other similar Michael acceptors (1-penten-3-one, 1-hexen-3-one, and 1-octen-3-one have comparable log K and log EC values).[129] This Michael acceptor would also be anchored to a large natural product, limiting its ability to react in tight protein pockets.

Further concerns arise with respect to the toxicity of the Michael acceptor.[130] As electrophilic agents, certain Michael acceptors can form covalent bonds with DNA and proteins, causing carcinogenicity.[131] This would cause a serious issue with modifying a tacrolimus substrate with an extremely reactive Michael acceptor; however, similar Michael acceptors have been used as a treatment for cancer.[127] It has also been shown that endogenous cysteinyl thiols can prevent carcinogenesis when reacting with certain Michael acceptors. This places further emphasis on the choice of Michael acceptor being crucial in the inhibition of *Pf*FKBP35.

4.4 Conclusion

The work performed explores the possibility for new potent anti-malarials. Using the natural substrate as a potential drug molecule, a Michael acceptor is added to the carbon 42 position. This substrate modification allows for a nucleophilic attack from a nearby cysteine residue present only in *Plasmodium* FKBPs. The formation of a covalent bond between enzyme active site and substrate will permanently inactivate the enzyme from performing its isomerase function.

This process has been shown to have a Gibbs energy change of 91.3 kJ/mol and the product complex formed has a Gibbs energy change of 6.7 kJ/mol. This work suggests suicide inhibition by the addition of an electrophile to a macrocycle in a position to interact with the nucleophilic cysteine could be a feasible pathway to novel anti-malarials.

5 THE CATALYTIC FORMATION OF LEUKOTRIENE C_4: A CRITICAL STEP IN INFLAMMATORY PROCESSES

5.1 Introduction

First discovered in 1938, leukotrienes are known to play a key role in smooth muscle contraction.[132-139] In particular, the cysteinyl leukotrienes (cys-LTs; **Figure 5.1**), comprised of leukotriene C_4 (LTC_4) and its metabolite derivatives D_4 and E_4, have been shown to have critical roles in a broad range of allergic diseases. For instance, these biologically-active small molecules are involved in bronchoconstriction during asthma attacks and the slow, painful constriction of smooth muscle.[133] Importantly, therapeutic intervention in the biosynthesis or bioactivity of cys-LTs has been shown to provide a means of alleviating a broad range of allergic diseases.[140-143] For instance in mouse models the disruption of leukotriene synthesis reduced antigen-induced inflammation in lung cells.[144-146] LTC_4 is enzymatically synthesized in humans by leukotriene C_4 synthase (LTC_4S, EC 4.4.1.20)[147] via the conjugation of a glutathione[148] (GSH) and leukotriene A_4 (LTA_4). Notably, given its central role in cys-LT biochemistry, it has been proposed[135, 136, 138] that inhibition of LTC_4S is a viable solution to the treatment of asthma and inflammatory responses.

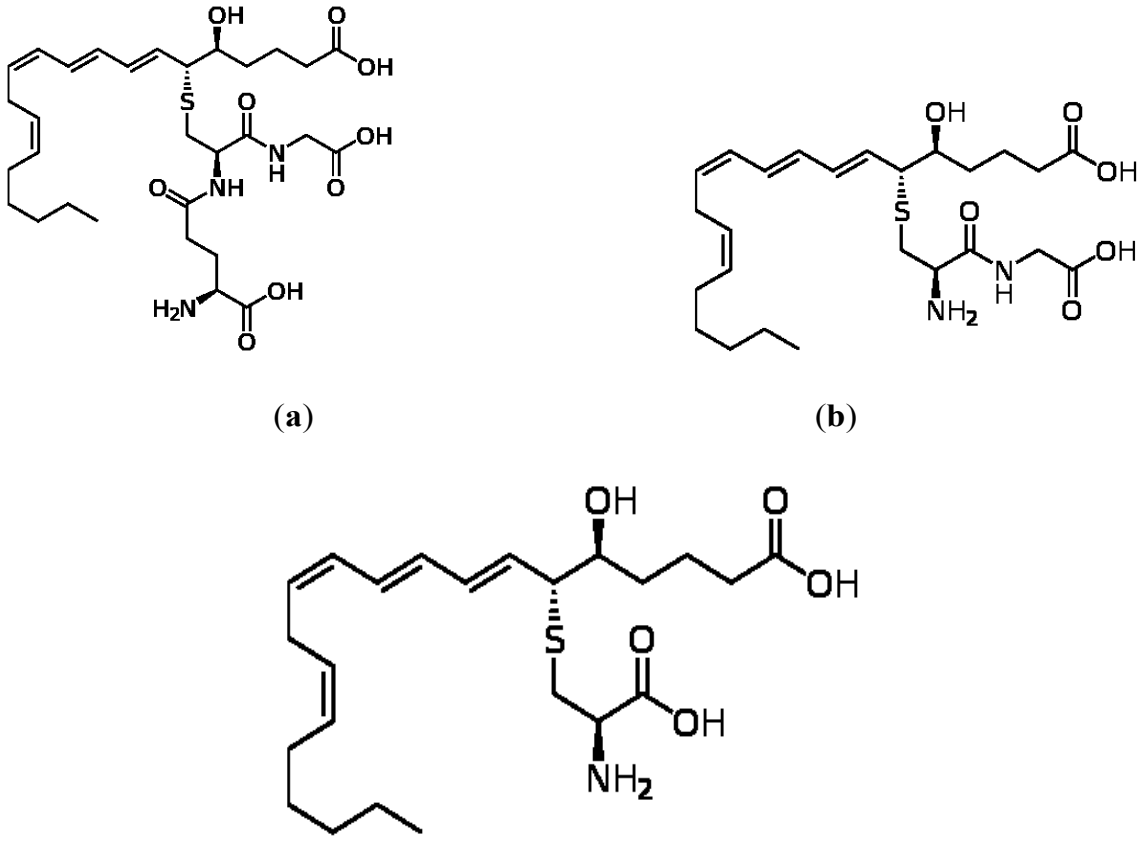

Figure 5.1 Schematic representations of leukotriene **(a)** C_4, **(b)** D_4 and **(c)** E_4.

While the exact catalytic mechanism of LTC_4S still remains unknown, experiment has provided some insight. In particular, previous X-ray crystal structures[29, 30] have shown that LTC_4S exists as a trimer, where the active site is formed at the interface of two of the three monomers. Moreover, nine amino acid residues from two subunits are involved in binding glutathione within the active site. A site-directed mutagenesis study[146] suggested that of these, an arginine residue (Arg_{104}) was critical. In particular, it was suggested that its guanidinium side chain hydrogen bonds to the sulfur of GSH. Consequently, it is able to facilitate activation of the GSH, deprotonation of its thiol by

stabilizing the resulting thiolate and allowing it to act as a nucleophile. Unfortunately, there is presently no available X-ray crystal structure of an LTA_4-bound LTC_4S, likely due to the reactivity of LTA_4.[11] Nevertheless, based on the binding of the analogous hydrocarbon tail of dodecyl maltoside within LTC_4S, a possible binding mode has been proposed for LTA_4.[29, 30] In particular, the hydrocarbon tail of dodecyl maltoside was observed to bind within a hydrophobic pocket. At the deepest point within this pocket it interacts with a tryptophan residue (Trp_{116}) that presumably helps hold the ligand within the active site.[29, 30] It has been suggested that if LTA_4 were to bind in an analogous manner, a catalytically important arginine residue (Arg_{31}) would be able to directly interact with its epoxy functional group.[143] Furthermore, such an interaction would also orient the LTA_4 substrate for nucleophilic attack at its C_6 center by the thiolate of glutathione. Experimentally,[143] substitution of Arg_{31} by glutamine and alanine reduced the rate of reaction by 70% and 88%, respectively, suggesting this residue plays an important role in substrate binding. Moreover, it was suggested that Arg_{31} protonates the forming alkoxide upon C-S bond formation (**Figure 5.2**).[143] While such a proposal explains the observed stereochemistry of the product formed, the exact orientation of LTA_4 within the active site as well as the catalytic involvement of Arg_{31} in LTC_4S remains debated. For instance, both structural and mutational X-ray data obtained in the work of Haeggström and Funk[149] have been inconclusive with respect to the involvement of Arg_{31}.

Using a combination of computational methods, we have investigated both the binding of LTA_4 and the catalytic mechanism of LTC_4S.[139] More specifically, docking of LTA_4 within the active site has been done in order to gain a better understanding of its

possible binding modes. In addition, MD simulations have been performed to investigate the dynamics of the active site and key interactions that may be involved in the binding of both the LTA_4 and GSH substrates. Lastly, using an ONIOM(QM/MM) approach the catalytic mechanism of LTC_4S has been examined.

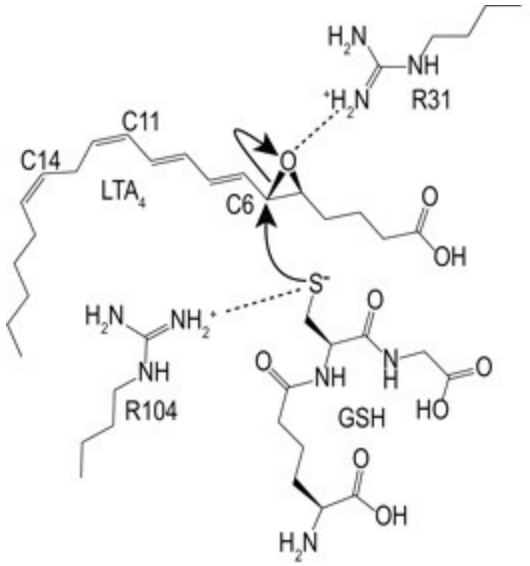

Figure 5.2 Schematic of proposed[143] catalytic architecture for the active site of leukotriene C_4 synthase (LTC_4S) with glutathione and LTA_4.

5.2 Computational Methods

The molecular operating environment (MOE)[110] program was used for model preparation, energy minimization and assessment of the generated trajectories. Molecular dynamics (MD) simulations were performed using the NAMD program.[111]

5.2.1 Docking

As a template the GSH-LTC_4S X-ray crystal structure from *Homo sapiens* (PDB ID: 2PNO)[29] was used.[139] The LTA_4 molecule was then docked within the active site using a Proxy Triangle[110, 150] placement to form the reactant complex (i.e., LTC_4S with bound GSH and LTA_4). The generated poses were then scored using a London dG scoring function where the top thirty poses were kept.[151] Of these thirty complexes, two conformations were kept that differed in the orientation of the substrate. The first was oriented such that the hydrocarbon tail was exposed to the solvent and the polar head was hydrogen bonding with Arg_{104}, known as the 'tail-to-head' orientation (**Figure 5.3a**). The second pose had an orientation such that the polar head was exposed to the solvent and the hydrocarbon tail was in a hydrophobic pocket of the enzyme with its terminal carbon interacting with Trp_{116}. Such a binding mode is very similar to that proposed by Molina *et al*.[30] As noted in the introduction this is known as the 'head-to-tail' orientation (**Figure 5.3b**). The 'head-to-tail' orientation was the top scoring pose from the dataset. Other conformations were rejected as being either simply variations of the top scoring pose or as being inappropriate for catalysis. For example, poses that contained long glutathione-$S^-\ldots C_6$ interatomic distances or epoxide geometries that do not allow the reaction to occur, and thus were excluded. In both orientations, the epoxide-Arg_{31} and glutathione–$S^-\ldots C_6$ bond distances were appropriate for catalysis to give the expected products.

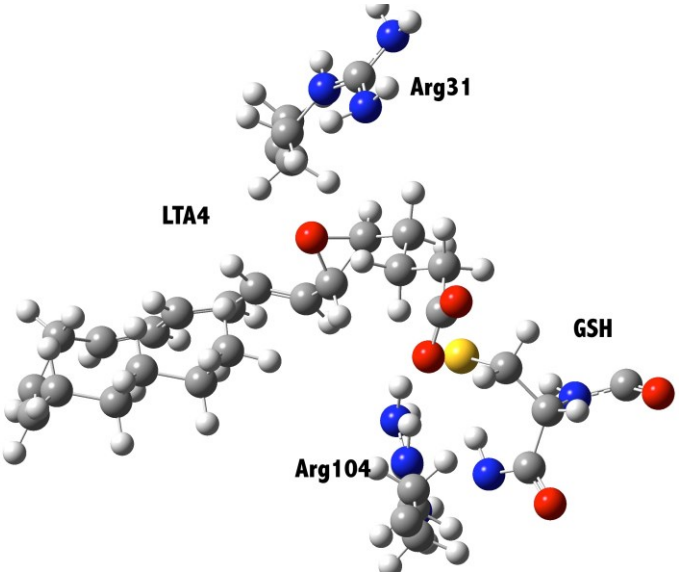

(**a**)

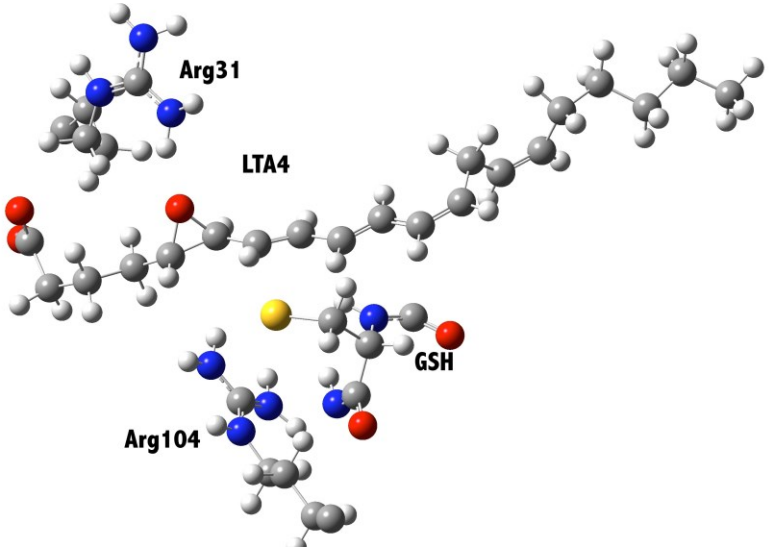

(**b**)

Figure 5.3 Representation of the active site of LTC_4S with LTA_4 in the **(a)** 'tail-to-head' orientation and the **(b)** 'head-to-tail' orientation. Important residues such as Arg_{104}, Arg_{31}, glutathione (GSH) and LTA_4 are shown.

5.2.2 Molecular Dynamics (MD) Simulations

To solvate the systems, a 7 Å spherical layer of water molecules was used. MD simulations were then performed for each orientation in stages. The first stage was a MD simulation where the glutathione–S^-…C_6 interatomic distance was restrained to be 3.50 Å. This was to ensure the LTA_4 did not leave the active site before the amino acids could rearrange and accommodate the new molecule. This simulation was performed for 11 ns. The final structures from each simulation was energy minimized using the AMBER99[113] force field until the root mean square gradient of the energy fell below 1 kcal mol^{-1} $Å^{-1}$. These optimized 'head-to-tail' and 'tail-to-head' complexes were then re-simulated for a period of 11 ns where the glutathione–S^-…C_6 restraint was removed. As noted above, MD simulations were performed using the NAMD program to obtain the trajectories.[111] A constant temperature of 300 K was used with the AMBER99[113] force field for the simulation. A time step of 0.5 fs was used. From the trajectories the RMSD of the substrate and active site were then calculated with respect to the structure at t=0. These RMSDs where then clustered into 5 groups. An average structure from the most populated cluster was then energy minimized and these structures were then used as the starting structure for subsequent QM/MM calculation. Similar protocols have been previously successfully implemented. [114, 115] [38]

5.2.3 QM/MM Calculations

The Gaussian 09 program[116] was used for all two-layer ONIOM[54, 58-61, 108, 117-119] QM/MM calculations. Structures were optimized at the ONIOM(ωB97X-D/6-31G(d):AMBER96) level of theory in the mechanical embedding (ME) formalism.[44, 107,

[120-122] Frequency calculations at the same level of theory as the optimization were done to verify that transition states had a single imaginary frequency. Single point energies for reactants, products, and transition states were obtained at the ONIOM(ωB97X-D/6-311+G(2df,p)//AMBER96)-ME level of theory.[44, 107, 120-122] It is noted that the energies reported are electronic energies only. The AMBER force field used contained all necessary parameters for the calculations, while any additional parameters required due to truncating the protein or splitting the high and low layers in the ONIOM model have been supplemented by the generalized AMBER force field (GAFF).

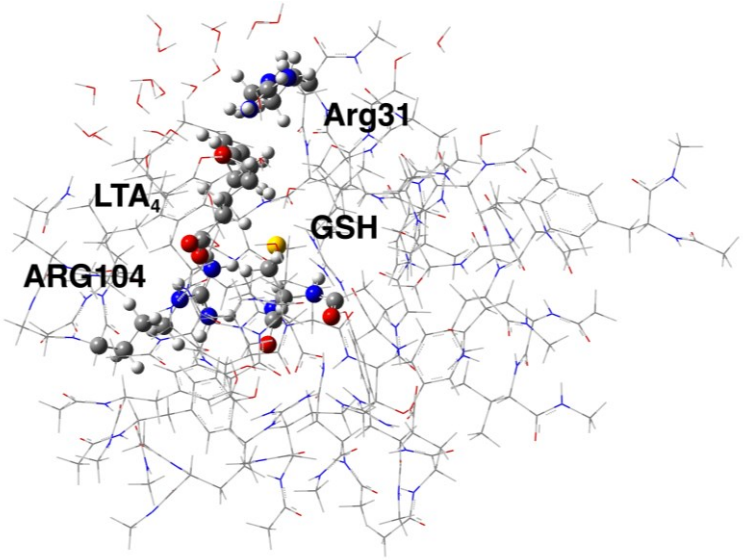

(**a**)

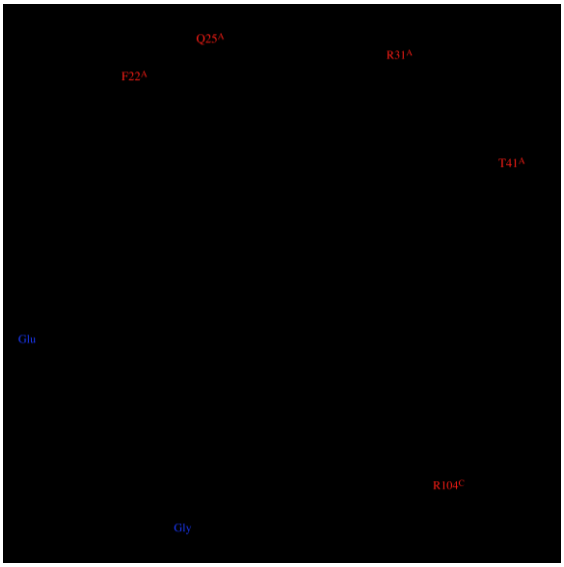

(**b**)

Figure 5.4 (a) The QM/MM model used to investigate the catalytic mechanism of leukotriene C_4 synthase with 'tail-to-head'-docked LTA_4. **(b)** Schematic representation of the QM/MM model: groups in the inner and outer circles have been modeled at the ωB97X-D/6-31G(d) and AMBER96 levels of theory, respectively. Residues written in black are included in the MM layer entirely, residues in red only have their peptide backbone included, and residues in blue are the residues included as part of glutathione. The superscript "A" and "C" denote to which chain the residue belongs.

Using the optimized structure obtained from the unrestrained MD simulations (*cf.*, above) a QM/MM model was generated. An example of this model for the 'tail-to-head' orientation is shown in **Figure 5.4**. The QM layer includes part of the leukotriene A_4 substrate (C_1 through C_{10}, the polar head, epoxide ring, and all attached hydrogen atoms), the cysteinyl moiety of glutathione, and the R-groups of Arg_{31} and Arg_{104}. The MM layer includes all residues that surround the QM layer and all water molecules that interact with

the QM layer. To maintain the structure of the active site, all α-carbons within the backbone of the protein were held fixed at their MM-optimized positions.

5.3 Results and Discussion

5.3.1 MD Simulations

For the MD simulations of the unrestrained 'head-to-tail' and 'tail-to-head' complexes we have used the trajectories to calculate the RMDSs of the substrate and active site residues with respect to the complex at t=0. The graphs of which are given in **Figure 5.5**.[139]

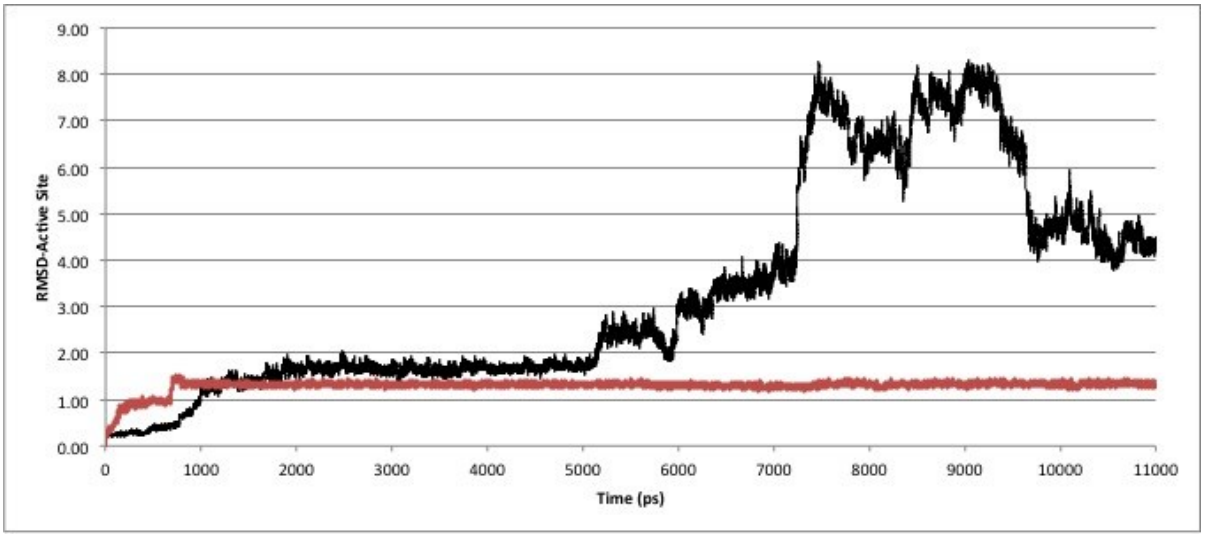

Figure 5.5 Plots of calculated RMSD of the active site versus time (ps) obtained from MD simulations of LTC_4S with glutathione bound and LTA_4 bound in a 'tail-to-head' (red) or 'head-to-tail' (black) orientation.

As seen above, there are vastly different results for the two orientations. In the case of 'tail-to-head' orientation the simulation appears to suggest that the active site remains stable over the course of the 11 ns simulation. This is interesting given that the tail of the substrate does not lie within the hydrophobic pocket of the active site. In particular, by 2 ns of the simulation we see very little deviation in the calculated RMSDs where it remains around a value of 1.29 with respect to the starting complex. Over the course of this simulation, r(glutathione–$S^{-}\cdots C_6)_{Avg}$ was 3.78 Å. This is a reasonable interatomic bond distance where these atoms could interact in a favorable way. In contrast, the MD simulation for the 'head-to-tail' orientation is erratic with an average RMSD of 3.32 and average r(glutathione–$S^{-}\cdots C_6)_{Avg}$ of 6.63 Å. In this model, after approximately 7.5 ns, the substrate effectively leaves the active site and as a result has a very long (as high as 9 Å) glutathione– $S^{-}\cdots C_6$ interatomic distance. As noted above this binding mode was similar to that proposed by Molina *et al.*[30], where the tail of the substrate interacts with Trp_{116}. It is noted that for the 'head-to-tail' model no interaction between the carboxylate head and Arg_{104} is formed. Such an interaction appears critical in proper placement of the substrate for catalysis. Thus, for the MD simulations it seems that the former orientation is more likely to lead to LTC_4 synthesis. This model will be used for further QM/MM calculations.

5.3.2 QM/MM Calculations for the 'Tail-To-Head' Model

As noted in Computational Methods an average structure from the MD simulation for the 'tail-to-head' system was minimized and used as a model for the subsequent QM/MM calculation. Following optimizations, r(glutathione–$S^{-}\cdots C_6$) was found to be

3.78 Å (**Figure 5.6a**) which is the same as the average value of 3.78 Å observed during the MD simulations. With respect to the carboxylate head an average distance of 1.78 Å was calculated for r($CO_2^-\cdots Arg_{104}^+$) suggesting a strong ionic interaction is formed. However, in the case of the epoxide group a weak interaction is formed with Arg_{31} where r($Arg_{31}^+\cdots O$) was found to be 3.08 Å. To stabilize the anionic thiolate of GSH the guanidinium of Arg_{104} forms a hydrogen bond with a distance of 2.35 Å. Such an interaction is likely to affect the pKa of the cysteinyl moiety of glutathione enabling it to be deprotonated for catalysis.

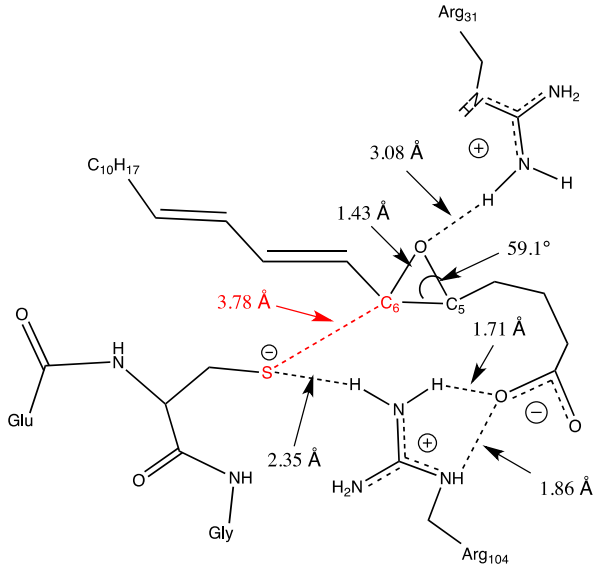

(a)

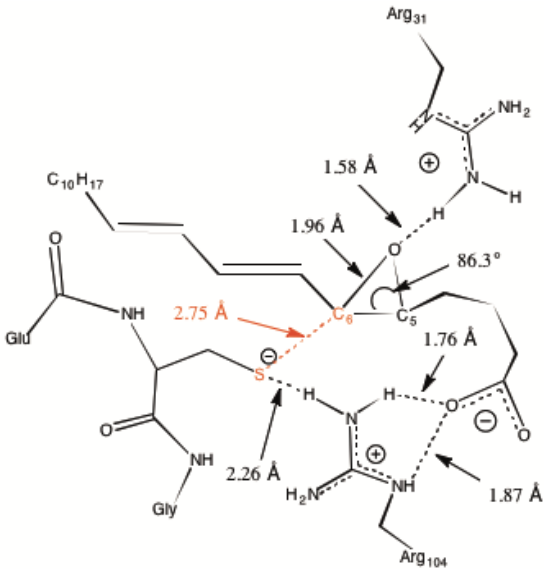

(**b**)

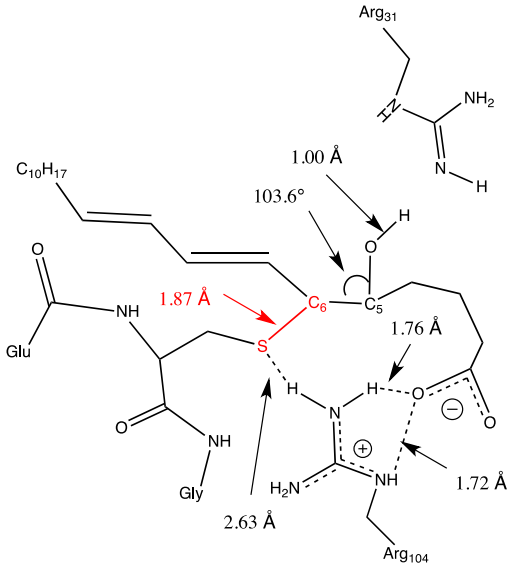

(**c**)

Figure 5.6 Optimized structures of **(a)** reactant, **(b)** transition state, and **(c)** product complexes of the 'tail-to-head' substrate orientation obtained at the ONIOM(ωB97X-D/6-31G(d)//AMBER96)-ME level of theory with selected distances (in angstroms) and bond angles (in degrees) shown.

The transition state for the nucleophilic attack of the GSH is shown in **Figure 5.6b**. An imaginary harmonic frequency (i399.05 cm^{-1}) representing the simultaneous epoxide ring opening to form a hydrogen bond with Arg_{31} and S–C bond formation was observed. As can be seen r(glutathione–$S^{-}\cdots C_6$) and r($Arg_{31}^{+}\cdots O$) have become considerably shorter. In particular, for the former bond length a change of 1.03 Å is observed while for the latter a change of 1.50 Å is observed. In the case of the breaking C–O bond of the epoxide a lengthening of 0.53 Å is observed. This lengthening results in the increase of the C_6-C_5-O angle by 27.2º. With the forming C–S bond r($GSH^{-}\cdots Arg_{104}^{+}$) was found to shorten slightly by 0.07 Å. However, for r($CO_2^{-}\cdots Arg_{104}^{+}$) no significant change was observed. The relative energy of the TS to the reactant complexes was found to be 102.0 kJ mol^{-1}. A possible explanation for this large, albeit not unreasonable, activation energy could be due to the loss of a formally-negative sulfur—Arg_{104} hydrogen bond and the gain of a thioether—Arg_{104} hydrogen bond. The transition state also contains a long alkoxide—Arg_{31} hydrogen bond and requires the breaking of the Arg_{31} H-N bond. Thus at the current level of theory it appears that (for the 'tail-to-head' orientation) following the binding of LTA_4 and GSH the reaction would occur readily.

For the optimized product complex (**Figure 5.6c**) r(C···S) is 1.87 Å thus, indicating the formation of the C–S bond. Because of disappearance of the anionic thiolate r($GSH^{-}\cdots Arg_{104}^{+}$) has lengthened by 0.37 Å to a final length of 2.63 Å. With complete cleavage of the C–O bond of the epoxide the C_6-C_5-O angle is now 103.6º, however in the optimization of the product complex a proton on Arg_{31} is transferred to the alkoxide without barrier forming the alcohol. The relative energy of the product

complex with respect to the reactant complex was found to be -135.5 kJ mol^{-1}. Thus, it appears that in the case of the 'tail-to-head' orientation S–C bond formation is energetically favourable.

5.4 Conclusion

For the leukotriene C_4 synthase (LTC_4S) enzyme, docking, molecular dynamics simulations, and QM/MM methods were applied to investigate the orientation of leukotriene A_4 (LTA_4) binding to the active site with an already-bound glutathione, and to show a possible enzymatic pathway for leukotriene C_4 (LTC_4) synthesis.

The docking approach coupled with MD simulations showed two possible appropriate 3-dimensional structures for the binding of LTA_4 to the active site of LTC_4S. This structure had not previously been isolated, as LTC_4 is quickly formed after binding. It shows that the 'tail-to-head' orientation of binding for LTA_4 is preferred over the 'head-to-tail' orientation. This result is likely due to the extra hydrogen bond formed between the polar head of LTA_4 and Arg_{104}.

The ONIOM QM/MM method was used to identify the reactant, product, and transition state complexes. The thiolate sulfur as part of the glutathione was found to be 3.75 Å away from carbon 6 of LTA_4 in the reactant complex. When these two atoms were brought closer to undergo the reaction, it forms the transition state complex with a thiolate-carbon 6 bond length of 2.75 Å. As the thiolate sulfur forms a bond with carbon 6 of LTA_4 (1.87 Å), the epoxide ring opens, forming an alkoxide. This alkoxide is concertedly neutralized by the nearby protonated Arg_{31} to form the LTC_4 complex.

6 COMPUTATIONAL INSIGHTS INTO THE CATALYTIC FORMATION OF LEUKOTRIENE B_4

6.1 Introduction

First discovered in 1938, leukotrienes are important inflammatory mediators.[132-138] Leukotriene A_4 (LTA_4, **Figure 6.1**), the simplest of the leukotrienes, is a precursor to cysteinyl leukotrienes (cys-LTs; **Figure 6.2**), important mediators for human bronchial asthma. Leukotriene C_4 (**Figure 6.2a**) is formed from a condensation type reaction between LTA_4 and glutathione in the active site of leukotriene C_4 synthase. Leukotriene D_4 (**Figure 6.2b**) is then formed from the loss of a glutamate. The subsequent loss of glycine, results in formation of leukotriene E_4 (**Figure 6.2c**). These final leukotrienes are synthesized through an unknown receptor pathway.[152, 153]

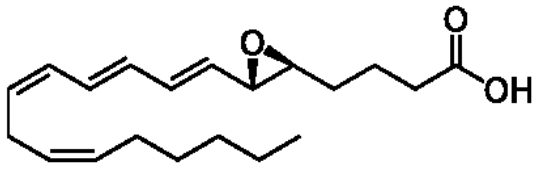

Figure 6.1 Leukotriene A_4.

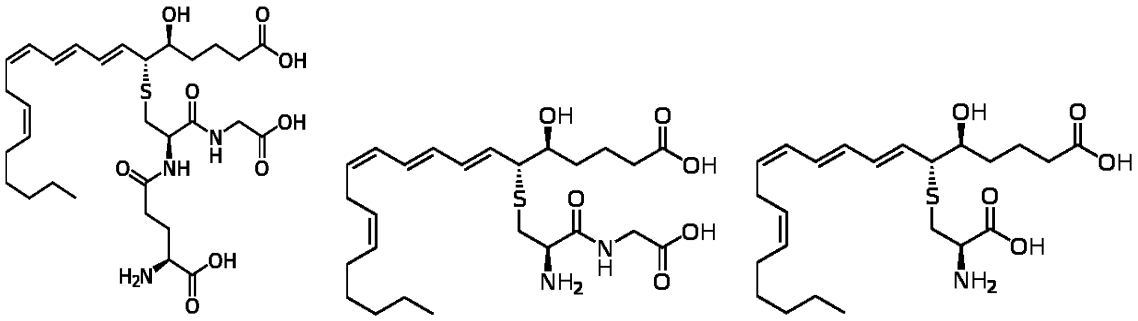

(**a**) (**b**) (**c**)

Figure 6.2 Cysteinyl leukotrienes: **(a)** leukotriene C_4, **(b)** leukotriene D_4, and **(c)** leukotriene E_4.

In addition to the conversion of cysteinyl leukotrienes, LTA_4 can be converted to leukotriene B_4 (LTB_4; **Figure 6.3**) through the addition of a water molecule. This reaction is catalyzed by leukotriene A_4 hydrolase (LTA_4H).[27, 154] The active site of LTA_4H contains a Zn^{2+} atom coordinated by His_{295}, His_{299}, and Glu_{318}. Other nearby amino acids, such as Glu_{296} and Tyr_{383}, have been shown to be catalytic in peptide cleaving activity, stabilizing the transition state.[155] LTB_4 is produced in the leukocytes and is formed in response to inflammatory mediators, resulting in a build-up in leukotrienes in inflamed tissues. Further insight into the mechanism by which LTA_4 hydrolase synthesizes LTB_4 could lead to suggestions for the treatment for inflammatory diseases.

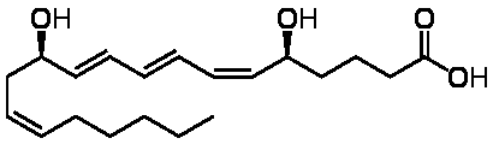

Figure 6.3 Leukotriene B_4.

The mechanism for LTB_4 synthesis has previously been proposed by Haeggström[156] and Paige.[28] In this mechanism, LTA_4 binds into the active site of LTA_4 hydrolase with the polar head of the substrate interacting with two nearby positively charged residues, Lys_{565} and Arg_{563}, whereas the epoxide ring is interacting with the Zn^{2+} (**Figure 6.4**).[157] This leaves the rest of the non-polar chain to lie in the nearby hydrophobic pocket. It is noted that mutagenesis studies suggest Asp_{375} is important for the catalytic formation of LTB_4.[156] In particular, it has been proposed that the water that attacks C_{12} is activated via deprotonation by the nearby polar-negative Asp_{375} residue. With attack of the water molecule the epoxide ring opens and is protonated by a nearby Zn-ligated water molecule which also forms a hydrogen-bond to Glu_{271} (**Figure 6.4**). This has been supported with mutagenesis studies.[158] The desired LTB_4 product coordinates to the nearby Zn^{2+} via the newly formed hydroxyl functional group (**Figure 6.4**).[158]

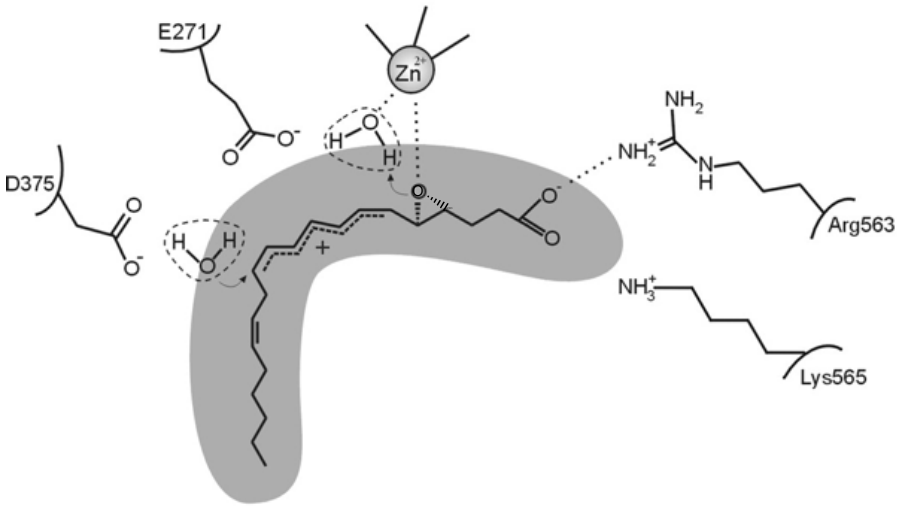

Figure 6.4 The proposed binding orientation of LTA_4 in the active site of LTA_4 hydrolase.[156, 158]

This chapter explores the proposed mechanism through computational methods such as docking, molecular dynamics, and QM/MM modeling. Specifically, the involvement of Asp_{375} and Glu_{271} in the catalytic mechanism of LTA_4H is examined to determine if these residues hydrolyze water to add to carbon 12 (C_{12}) and protonate the epoxide of LTA_4 to synthesize LTB_4.

6.2 Computational Methods

The molecular operating environment (MOE)[110] program was used for model preparation, energy minimization and assessment of the generated trajectories. Molecular dynamics (MD) simulations were performed using the NAMD program.[111]

6.2.1 Molecular Dynamics (MD) Simulation

As a template the LTA_4 hydrolase X-ray crystal structure from *Homo sapiens* (PDB ID: 4DPR)[29] was used. Prior to docking the inhibitor molecule captopril was deleted from the crystal structure. The LTA_4 molecule was then docked within the active site using a Proxy Triangle[110, 150] placement algorithm to form the reactant complex (i.e., LTA_4H with bound LTA_4). The generated poses were then scored using a London dG scoring function where the top thirty poses were kept.[151] The pose being investigated involved the polar head of LTA_4 interacting with two nearby polar groups (specifically Lys_{565} and Arg_{563}) while the epoxide is within reasonable distance to the Zn^{2+}, as outlined in previous work.[156, 157] This particular pose was in the top 10 poses scored, and the only pose with the Zn^{2+} within 5 Å of the epoxide oxygen, as proposed.

To solvate the system, a small 7 Å spherical layer of water molecules was used. A short 11 ns molecular dynamics (MD) simulation was performed to equilibrate the newly docked substrate. Such a simulation was done to ensure stability of the docked substrate. From the trajectories the RMSD of the substrate and active site were calculated with respect to the structure at t=0. These RMSDs were then clustered into 5 groups. An average structure from the most populated cluster was energy minimized and used as the starting structure for subsequent QM/MM calculations, which was then energy minimized using the AMBER99[113] force field until the root mean square gradient of the energy fell below 1 kcal mol^{-1} $Å^{-1}$. As noted, the MD simulation was performed using the NAMD program to equilibrate the system.[111] A constant temperature of 300 K and time step of 0.5 fs was used with the AMBER99[113] force field.

6.2.2 QM/MM Calculations

The MD simulated (and subsequently MM minimized) LTA_4-protein complex was used for subsequent QM/MM calculations. The Gaussian 09 program[116] was used for all two-layer ONIOM[54, 58-61, 108, 117-119] QM/MM calculations. Included in the QM region were Zn^{2+}, LTA_4, Glu_{271}, Glu_{296}, Glu_{318}, His_{295}, His_{299}, Asp_{375}, and two water molecules. The rest of the surrounding protein was placed in the MM region (**Figure 6.5**). Structures were optimized at the ONIOM(ωB97X-D/6-31G(d,p):AMBER96) level of theory in the mechanical embedding (ME) formalism.[159-162] Frequency calculations at the same level of theory as the optimization were done to verify the nature of the stationary points and for Gibbs thermal corrections. Single point energies for reactants, products, and transition states were obtained at the ONIOM(ωB97X-D/6-311+G(2df,p):AMBER96//ωB97X-D/6-31G(d,p):AMBER96) level of theory within the electronic embedding formalism with Gibbs energy corrections.[44, 107, 120-122] It is noted that additional parameters required due to splitting the high and low layers in the ONIOM model have been supplemented by the generalized AMBER force field (GAFF).

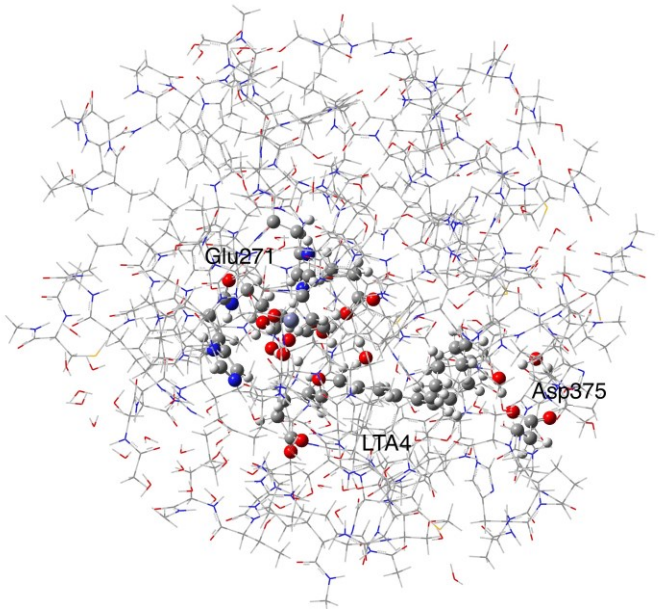

(a)

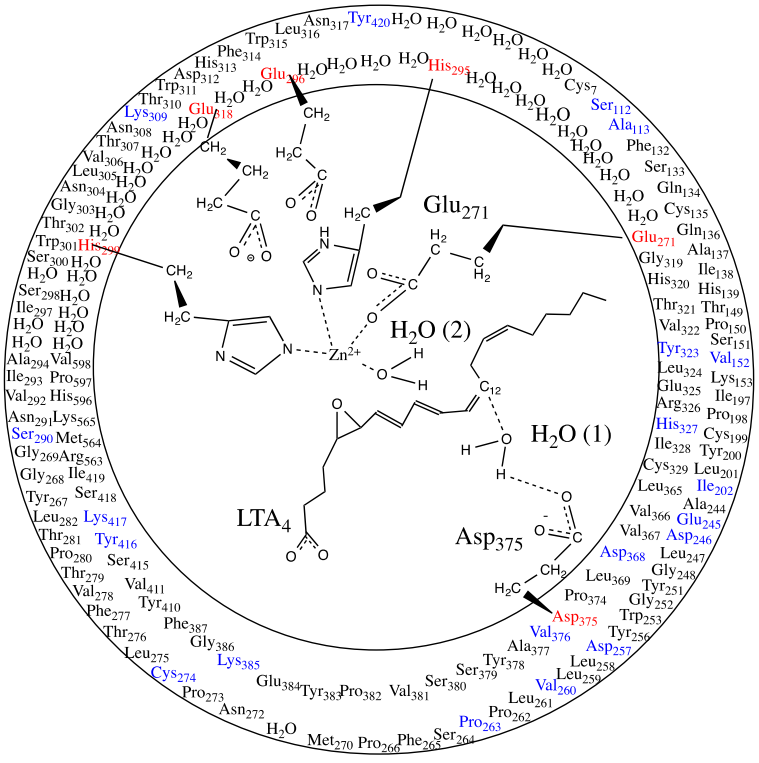

(b)

Figure 6.5 (a) The QM/MM model used to investigate the catalytic mechanism of leukotriene A_4 hydrolase with docked LTA_4. **(b)** Schematic representation of the

QM/MM model: groups inside the inner circle have been modeled at the ωB97X-D/6-31G(d,p) and groups inside the outer circle have been modeled at the AMBER96 level of theory. Residues written in black are included in the MM layer entirely, residues in red have their R chains included in the QM region and backbone included in the MM region, and residues in blue only have their backbone modeled in the MM region.

6.3 Results and Discussion

With the docking of LTA_4 into the active site of LTA_4 hydrolase the modeled pose was found to be very similar to binding orientation proposed by Haeggström.[157] In particular, the polar head of LTA_4 interacts with Arg_{563} and Lys_{565} through hydrogen bonding interactions (**Figure 6.6a**). This orientation serves to anchor the substrate into the active site for catalysis. Notably, the interaction between the polar head of LTA_4 and Arg_{563} and Lys_{565} results in the epoxide between C_5 and C_6 on LTA_4 to sit within a reasonable distance of 3.17 Å to the Zn^{2+} (**Figure 6.6b**).[158] Thus. there is ample space for a water molecule to coordinate to the metal centre between the epoxide functional group and Glu_{271}. As noted above Glu_{271} likely helps the water ligate to Zn^{2+} and orient the water molecule to protonate the opening epoxide ring while the hydroxyl ion remains coordinated to the metal centre.

For this top scoring conformer LTA_4's hydrophobic chain was found to bind into the enzyme's hydrophobic pocket. It is noted that this pocket, however, forces a slight bend along the non-polar chain of the substrate starting at approximately C_{12}, resulting in the active site Asp_{375} to be within 7 Å and exposing C_{12} for possible nucleophilic attack. As noted above, it has been suggested[156] that Asp_{375} catalyzes the addition of a nearby

water molecule to C_{12}. It is noted that such a water molecule was not present in the crystal structure due to the presence of captopril, but the space between C_{12} and Asp_{375} could accommodate one water molecule (**Figure 6.6c**).

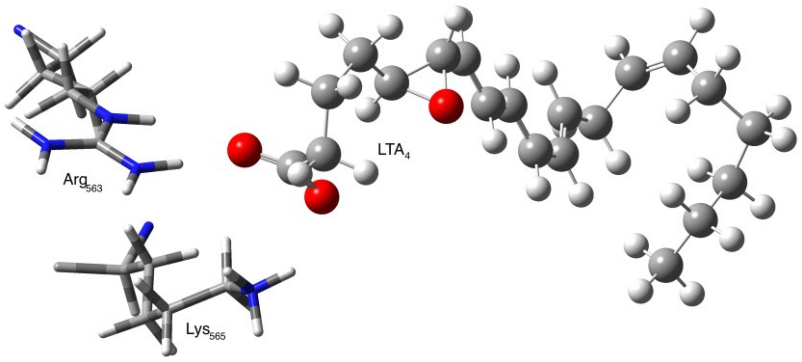

(a)

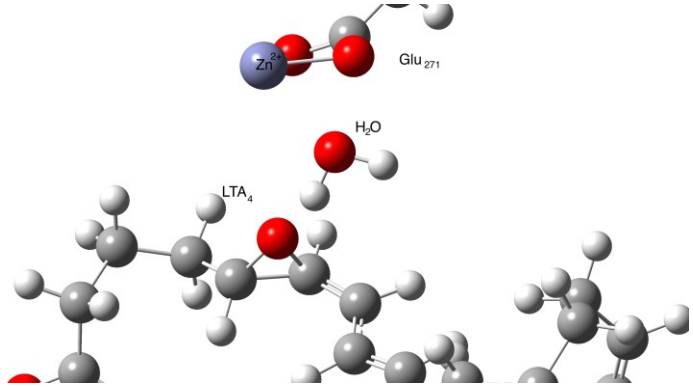

(b)

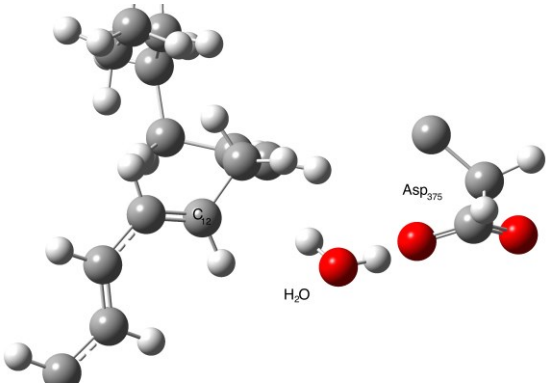

(c)

Figure 6.6 The interactions between the protein environment and the docked LTA_4 substrate for the **(a)** polar head, **(b)** epoxide ring with **(c)** one water molecule between C_{12} and Asp_{375} after energy minimization.

Indeed, upon the addition of the solvation sphere on the docked enzyme complex prior to MD simulation one water molecule was positioned between C_{12} and Asp_{375}. This could allow the reaction to occur through a one-water proton transfer chain. Throughout the MD simulation this water was found to be hydrogen bonded to Asp_{375} and maintained an interatomic C-O_{w1} bond distance between 3 and 4 Å.

From the final MM minimized complex the reaction mechanism for LTB_4 synthesis was investigated using an ONIOM formalism. The stationary states for this reaction are provided in **Figure 6.7**, **Figure 6.8**, and **Figure 6.9**.

The reactant complex (**Figure 6.7**) has one water molecule forming a hydrogen bond network connecting C_{12} to Asp_{375} (H_2O (1)). This water molecule is in an orientation to facilitate proton transfer to Asp_{375} and C-O bond formation with r($H_1 \cdots O_{Asp}$) being 1.65 Å and r($C_{12} \cdots O_{w1}$) being 3.11 Å. At this step in the reaction, the epoxide ring between C_5 and C_6 is still fully formed with a C_5-C_6-O bond angle of 59.5º From **Figure 6.7** there is one nearby water molecule which may likely protonate the epoxide oxygen after ring opening. The water molecule most likely to protonate the epoxide from mutagenesis studies is denoted in **Figure 6.7** and is positioned between LTA_4 and Glu_{271} (H_2O (2)).[158] This allows the carboxylate functional group to activate the water molecule, promoting ionization of the water with r($H_2 \cdots O$) of 2.91 Å. This

reactant complex is assigned a Gibbs energy of 0.0 kJ/mol after Gibbs corrections to be compared to subsequent steps.

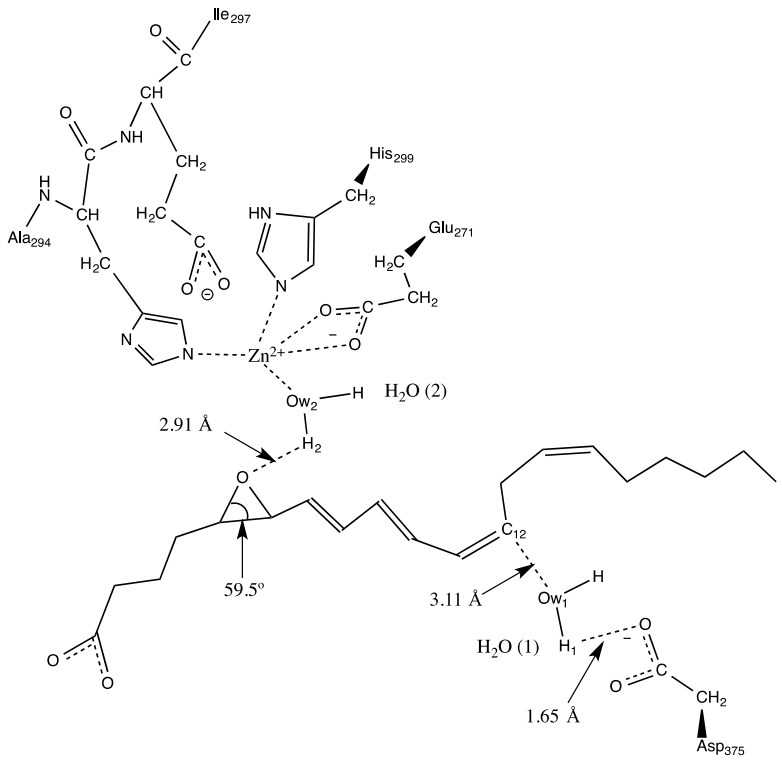

Figure 6.7 Reactant complex when LTA_4 binds into the active site of LTA_4 hydrolase.

The transition state corresponding to the proton transfer from H_2O (1) to Asp_{375} and the simultaneous C_{12}-Ow_1 bond formation is provided in **Figure 6.8**. In the case of the forming carbon-oxygen bond r($C_{12}\cdots O_{w1}$) is 1.48 Å. It is noted that for TS with the formation of the $C_{12}\cdots O_{w1}$ bond the epoxide ring at C_5 and C_6 is opening with a bond angle of 83.4°. The alkoxide will then be protonated by H_2O (2) with r($H_2\cdots O$) of 1.36 Å. The position of H_2O (1) will form exclusively the R enantiomer at C_{12} while the position of H2O (2) will form exclusively the S enantiomer at C_5, producing LTB_4 and a hydroxide ion coordinated to the metal centre. This geometry has an imaginary frequency

of i333.0 cm^{-1} representing the simultaneous C-O_{w1} bond formation and epoxide ring opening. This step along the reaction mechanism has a relative Gibbs energy of 235.4 kJ/mol. This Gibbs energy will be discussed below.

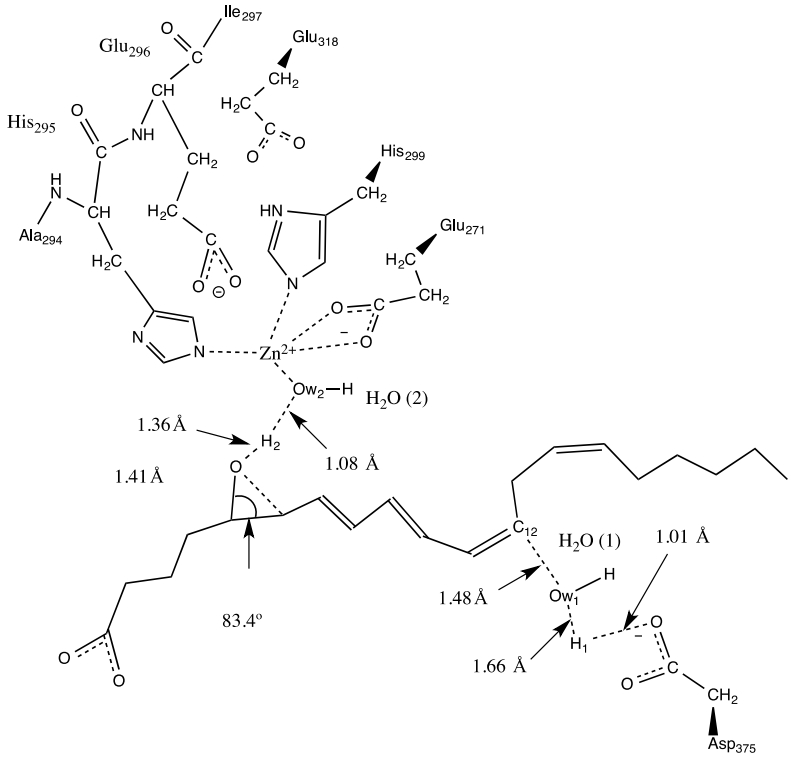

Figure 6.8 The transition state of LTB_4 synthesis through the addition of water to C_{12} of LTA_4.

The LTB_4 product complex for this mechanism (**Figure 6.9**) features a completely formed bond at C_{12} with a C-O bond length r(C_{12}···O_{w1}) of 1.46 Å and protonated Asp_{375}. This bond formation opens the epoxide ring with a C_5-C_6-O bond angle of 105.6º. This alkoxide is then protonated by H_2O (2) with r(O···H_2) of 1.00 Å and r(H_2···O_{w2}) of 1.62 Å. This process has a relative Gibbs energy of 221.2 kJ/mol, indicating the product complex is far too high in energy to realistically form. This

suggests that with the present model the proposed mechanism is not feasible for LTB_4 synthesis. The most likely cause for these high Gibbs energies would be the Asp_{375} residue responsible for water ionization. The relatively low pKa for aspartic acid (~3.78) is likely to prevent ionization of water and prevent LTB_4 synthesis. Another residue along the hydrophobic pocket, such as Tyr_{383}, may be more suitable for promoting LTB_4 synthesis. Additionally, another residue that has not been included in the model could have stabilized the aspartic acid to lower the Gibbs energies. The current methods also suggest the mechanism for LTB_4 synthesis is a concerted mechanism and not stepwise as suggested in Refs. 11 and 12.

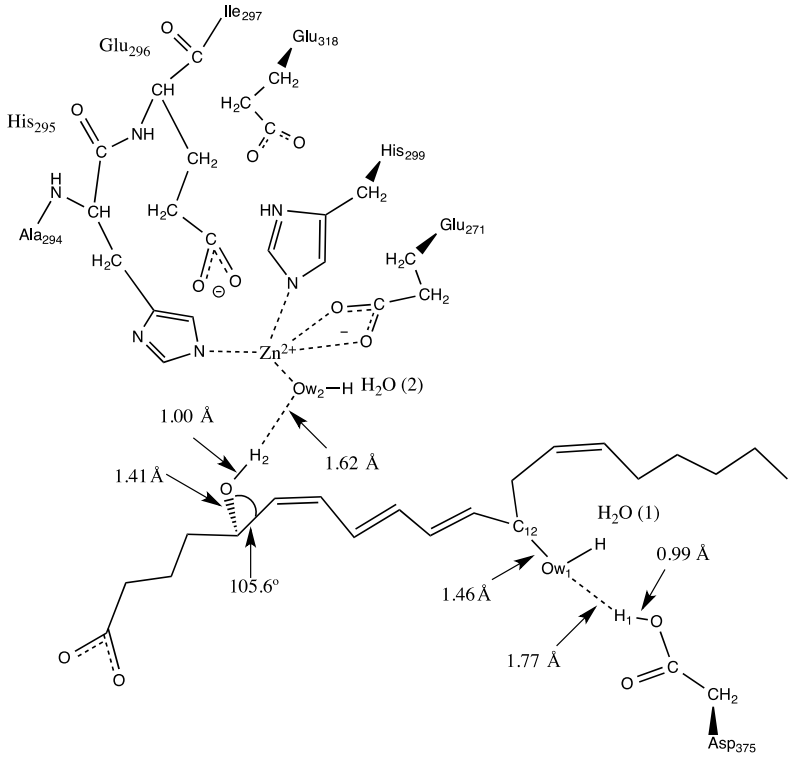

Figure 6.9 Product complex formed after synthesis of LTB_4 by LTA_4 hydrolase.

6.4 Conclusion

The current chapter investigates the synthesis of LTB_4 from LTA_4 and LTA_4 hydrolase. While the current mechanism has been supported by experimental evidence, the current computational methods suggest this mechanistic pathway will not occur. This is likely due to the pKa of aspartic acid 375 and its inability to accept a proton from water. This will cause the product complex to have an unreasonably high Gibbs energy. Another polar residue along the hydrophobic pocket would be more able to activate a water molecule for ionization with lower barriers.

7 COMPETING NITRILE HYDRATASE CATALYTIC MECHANISMS: IS CYSTEINE-SULFENIC ACID ACTING AS A NUCLEOPHILE?

7.1 Introduction

Nitrile hydratases (NHases, EC 4.2.1.84)[32, 34, 35, 163-168] are a class of enzymes involved in the carbon and nitrogen metabolic pathways of some bacteria; however, they are also used in industrial applications to catalyze the conversion of a variety of nitrile functional groups to amides (**Figure 7.1**). Nitrile hydratases have a highly-conserved active site, containing a non-heme Fe^{3+} or non-corrin Co^{3+} in a distorted octahedral geometry.[32, 169] The ligand residues involved in the active site are the side chains of Cys_{109}, Cys_{112}, Cys_{114}, and the deprotonated backbone amide nitrogens of Ser_{113} and Cys_{114}.[32, 34, 168] However, it is noted that the side chains of Cys_{112} and Cys_{114} are post-translationally modified to cysteine-sulfinic acid (CSD_{112}) and cysteine-sulfenic acid (CSO_{114}, **Figure 7.2**), respectively. The sixth coordination site (*trans* to Cys_{109}) is open for substrate binding.

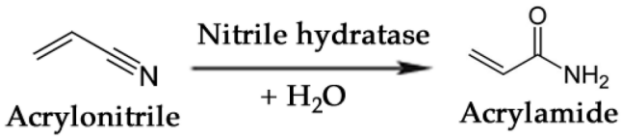

Figure 7.1 Conversion of acrylonitrile to acrylamide catalyzed by nitrile hydratase.

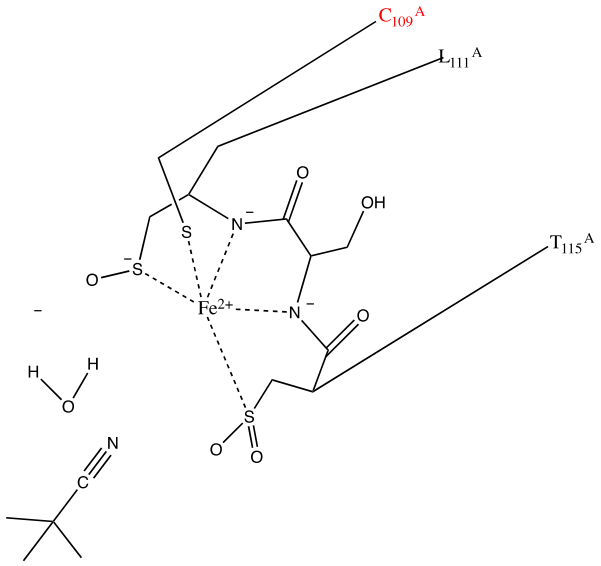

Figure 7.2 Distorted octahedral geometry of nitrile hydratase active site with bound t-butyl nitrile.

While the enzymatic mechanism of nitrile hydratases has been studied experimentally and computationally, the reaction mechanism remains debated where several reaction mechanisms have been proposed.[33] One mechanism involves the direct binding of the nitrile molecule to the metal center, followed by the nucleophilic attack of a nearby water molecule.[34] This mechanism has been supported with experimental data by time-resolved X-ray crystallography.[32] An alternative mechanism involves the binding of this water molecule to the metal center instead, which is followed by deprotonation (forming the hydroxide ion) allowing for the nucleophilic attack on the nearby nitrile molecule.[35]

A third mechanism that has been recently studied theoretically[167] proposes that the oxygen of the sulfenic acid CSO_{114} nucleophilically attacks the nitrile molecule

resulting in formation of a disulfide bridge between Cys_{109} and CSO_{114} and formation of the amide. This bridge would then be hydrolyzed via the addition of a water molecule, regenerating the enzyme's active site. The theoretical calculations offer a reaction profile showing how their unusual disulfide bridge formation and regeneration of the enzyme can be energetically feasible, with enthalpies and electronic energies which agree with the experimental activation barriers of 13-15 kcal/mol (54-63 kJ/mol). It is noted that recent experimental work supports the notion of such a disulfide mechanism.[33]

Hopmann *et. al* have been publishing theoretical work in the area for several years.[34, 35, 167, 168] Primarily, the theoretical research (wherein the first-shell ligands Cys_{109}, CSD_{112}, Ser_{113}, CSO_{114}, the iron centre and two water molecules are used as a model for the active site) suggests the first mechanism of NHase-mediated nitrile hydration (where CSO_{114} acts as a nucleophile; **Figure 7.3**) is preferred. The inclusion of second shell ligands (Arg_{56} and Arg_{141}), the proposed mechanism suggests the binding of a water molecule first, either deprotonating the water molecule to act as a nucleophilic OH^- or allowing the cysteine-sulfenic acid to act as the nucleophile (**Figure 7.4**).

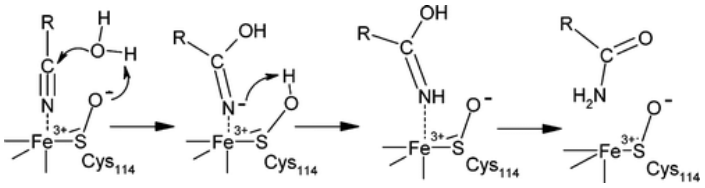

Figure 7.3 Proposed water-mediated mechanism for nitrile hydration.

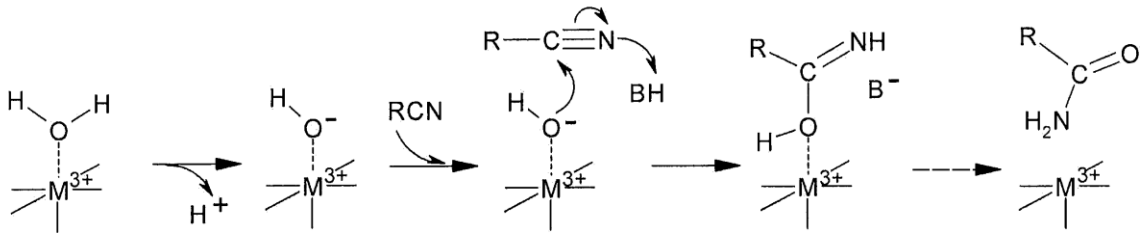

Figure 7.4 Alternate proposed mechanism for the hydroxide-mediated mechanism for nitrile hydration, where M^{3+} represents iron or cobalt.

While the mechanism of nitrile hydration by nitrile hydratases has been shown to have a viable pathway through a disulfide bridge, the previously-discussed mechanism of the water molecule acting as a nucleophile has only been modeled by a very small active site without the surrounding residues while being directly bound to the iron centre. This model system neglects the effect of the protein environment.

The purpose of this work is to study the proposed nucleophilic water mechanism using a quantum mechanics/molecular mechanics model. These calculations will compare molecular embedding and electronic embedding methods to determine how important protein environment is for this mechanism. This work will then be compared to the work by Hopmann *et. al* to determine if there is another feasible mechanism for nitrile hydration.

An important distinction is that Hopmann uses a large QM model with an implicit solvation model (to simulate the dielectric of the surrounding protein), while this work uses a large QM/MM model where the rest of the surrounding protein is modeled at the molecular mechanics level. This work is not primarily used to determine which mechanism is most feasible; however, it will determine if there are multiple mechanistic pathways for nitrile hydration.

7.2 Computational Methods

The molecular operating environment (MOE)[110] program was used for model preparation, energy minimization and assessment of the generated trajectories. Molecular dynamics (MD) simulations were performed using the NAMD program.[111]

7.2.1 Model Preparation

The X-ray crystal structure of nitrile hydratase with bound t-butyl isonitrile and nitric oxide (PDB ID: 2ZPE) was used as a template for the proceeding calculations.[32] It is noted that the nitric oxide molecule in the sixth ligand position is in fact a competitive inhibitor used to inactivate the enzyme with a t-butyl isonitrile molecule nearby (the isonitrile fragment pointed away from the iron, **Figure 7.5a**). Thus, the nitric oxide was removed using MOE to open the ligand position in favor of t-butyl isonitrile. The substrate was rotated and placed in the ligand position so the isonitrile functional group is in a position to interact with the iron active site.

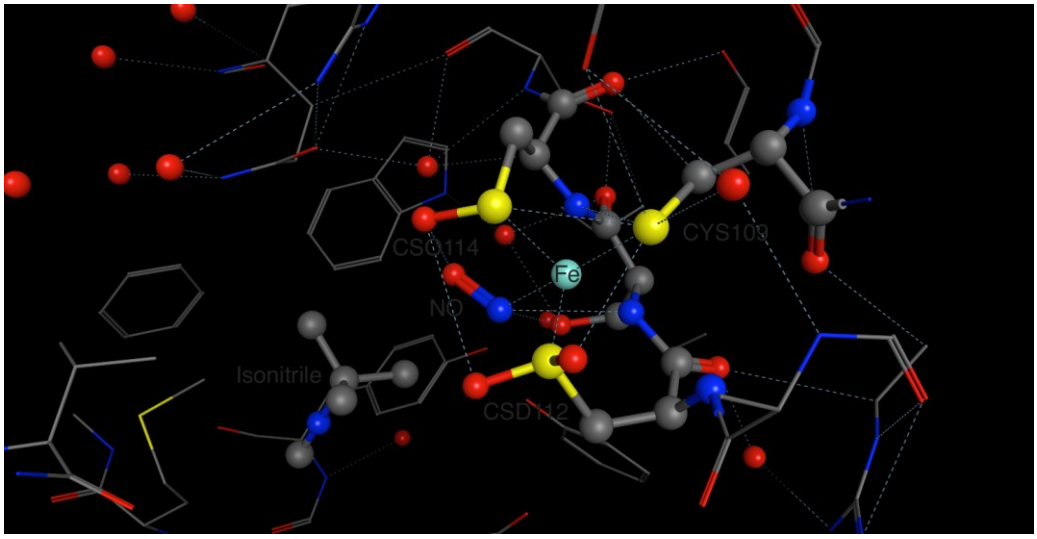

Figure 7.5 The crystal structure for the active site of nitrile hydratase with nitric oxide (NO) bound into the sixth ligand position of the non-heme iron and unbound t-butyl isonitrile (Isonitrile).

7.2.2 Molecular Dynamics (MD) Simulation

Prior to simulation a 7 Å spherical layer of water molecules was added to solvate the active site. The protonation states for all residues were corrected using Protonate 3D.[112] MD simulations were then performed for 11 ns with a 0.5 fs time step at a constant temperature of 300 K. The AMBER99 force field was used for the simulation. From the trajectories, the RMSD of the substrate and segments of the active site were calculated with respect to the structure at t=0. These RMSDs were then clustered into 5 groups. An average structure from the most populated cluster was then energy minimized using the AMBER99 force field until the root mean square gradient of the energy fell below 1 kcal mol^{-1} $Å^{-1}$. This optimized structure was used to modify the substrate from an isonitrile functional group to a nitrile functional group (Nitrile, **Figure 7.6**) for subsequent calculations.

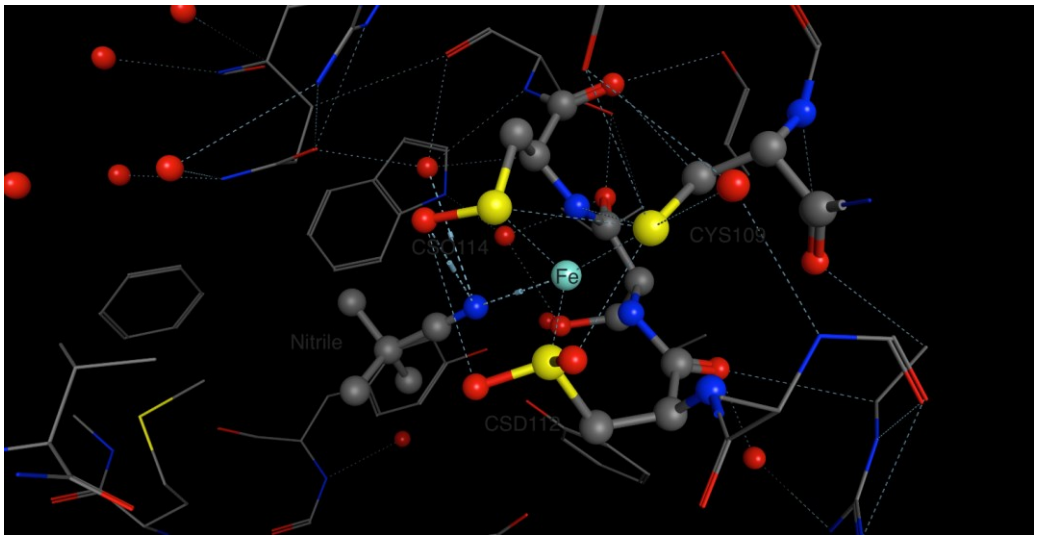

Figure 7.6 Active site of nitrile hydratase with t-butyl nitrile (Nitrile) in the sixth ligand site. All hydrogen atoms were removed for the graphic.

7.2.3 QM/MM Calculations

The Gaussian 09 program was used for all two-layer ONIOM QM/MM calculations.[116] Stationary points were obtained at the ONIOM(ωB97X-D/6-31G(d,p):AMBER96) level of theory in the mechanical embedding (ME) formalism.[44, 107, 120-122] Frequency calculations at the same level of theory were done to verify the nature of the stationary points and to obtain the respective enthalpy corrections. Single point electronic energies were obtained at the ONIOM(ωB97X-D/6-311+G(2df,p)//AMBER96) level of theory with mechanical embedding (ME) and electronic embedding (EE) formalism for comparison.[170] These energies were corrected to enthalpies via the addition of the enthalpy corrections. All calculations were performed with a multiplicity of 2 unless otherwise stated.

The QM/MM model for the nitrile hydratase with nitrile substrate is shown in **Figure 7.7a** with the schematic representation of the QM/MM model is shown in **Figure 7.7b**.

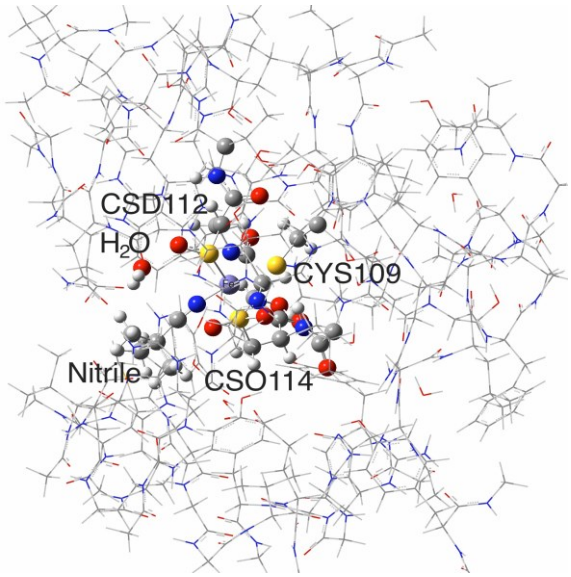

(**a**)

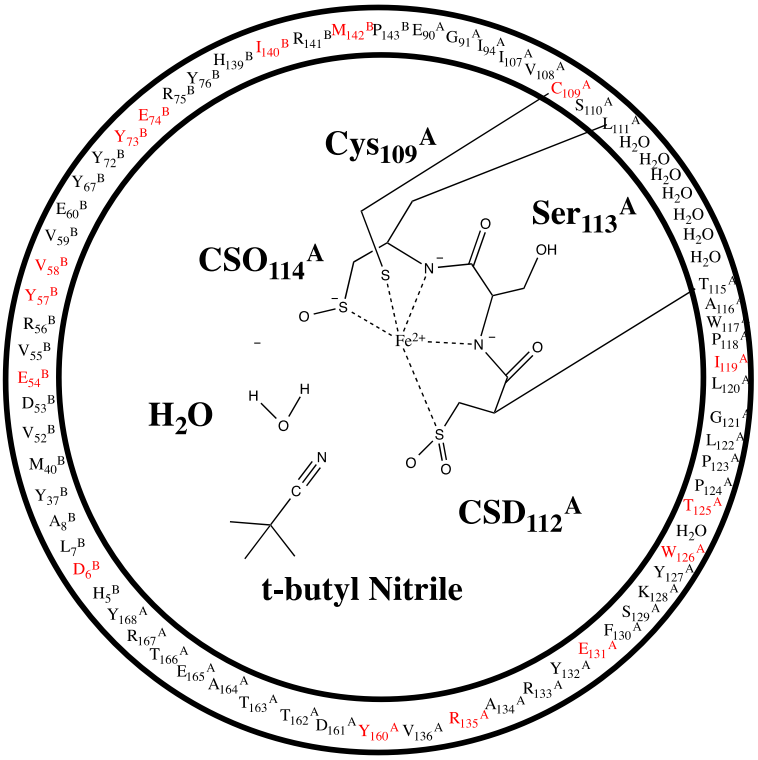

(**b**)

Figure 7.7 (a) The QM/MM model used to investigate the enzymatic mechanism of nitrile hydratase with bound t-butyl nitrile. **(b)** Schematic representation of the QM/MM model: groups in the inner and outer circles have been modeled at the ωB97X-D/6-31G(d,p) and AMBER96 levels of theory, respectively. Residues written in black are included in the MM layer entirely, residues in red only have their peptide backbone included. The superscript "A" and "B" denote to which chain the residue belongs.

7.3 Results and Discussion

7.3.1 Complex Geometries

The structures of the stationary points obtained at the ONIOM(ωB97X-D/6-31G(d,p):AMBER96)-ME level of theory are provided in **Figure 7.8** through **Figure 7.15**. The enthalpy surfaces obtained at the ONIOM(ωB97X-D/6-311+G(2df,p)//AMBER96)-ME and ONIOM(ωB97X-D/6-311+G(2df,p)//AMBER96)-EE levels of theory are provided in **Figure 7.16a** and **Figure 7.16b**, respectively. The third transition state calculation was omitted for reasons that will be outlined below.

As shown in **Figure 7.8** all nearby binding residues (Cys_{109}, CSD_{112}, Ser_{113}, CSO_{114}) form a distorted octahedral complex with the iron centre allowing for the nitrile substrate to bind in the sixth coordination site. The substrate binds with an interatomic distance r(N···Fe^{2+}) of 1.93 Å and r(C···N) of 1.16 Å (**Figure 7.8**). It has been proposed that a nearby water molecule will ionize, transferring the hydroxide ion to the substrate and the hydrogen ion (H_1) to the nearby CSO_{114}. Such a water molecule with r(C···O_w) of 2.85 Å is within a reasonable distance to allow bond formation after loss of a proton to the sulfenic acid where r(H_1···O_{CSO}) is calculated to be 2.85 Å (**Figure 7.8**). All stationary points energies are relative to the enthalpy of reactant complex (RC), which has a relative energy of 0.0 kJ/mol.

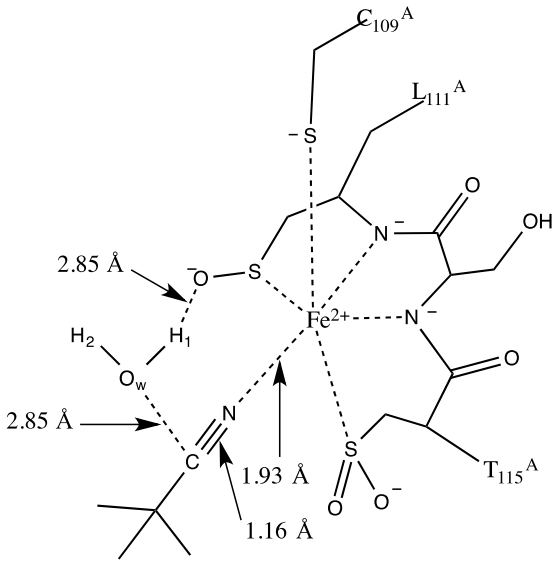

Figure 7.8 Reactant complex (RC) formed when t-butyl nitrile binds into the active site of nitrile hydratase.

In the transition state for the first step of the reaction (TS1) the r(C···O_w) is shortened considerably from 2.85 Å to 1.89 Å, whereas r(C···N) is found to lengthen by 0.03 Å (**Figure 7.9**). Moreover, r(H_1···O_{CSO}) is found to be 1.21 Å which corresponds to the proton transfer from water to cysteine-sulfenic acid. An imaginary harmonic frequency (i768.54 cm^{-1}) representing this ionization of water is observed. This step occurs with an enthalpy of 84.8 kJ/mol relative to RC.

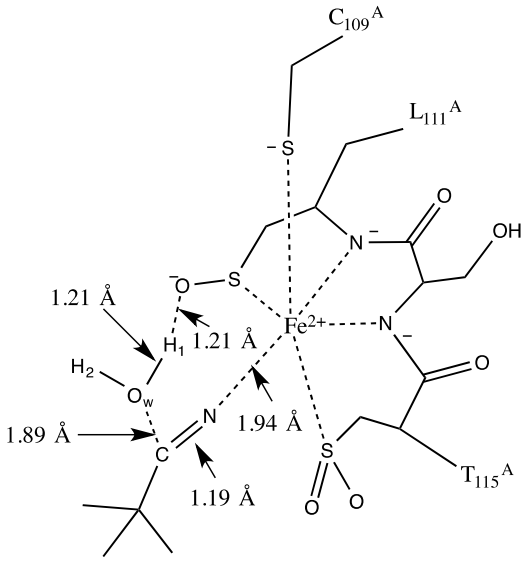

Figure 7.9 The initial transition state (TS1) for the addition of water catalyzed by cysteine-sulfenic acid to t-butyl nitrile.

The first intermediate complex formed during this reaction (I1; **Figure 7.10**) is formed after the addition of the hydroxide ion to the nitrile functional group. This addition elongates r(C···N) to 1.24 Å to form a carbon-oxygen bond r(C···O_w) of 1.45 Å. The hydrogen ion transferred from the ionized water has completely transferred to the cysteine-sulfenic acid with r(H_1···O_{CSO}) of 1.00 Å. Relative to the RC, this intermediate complex lies 71.3 kJ/mol higher in enthalpy.

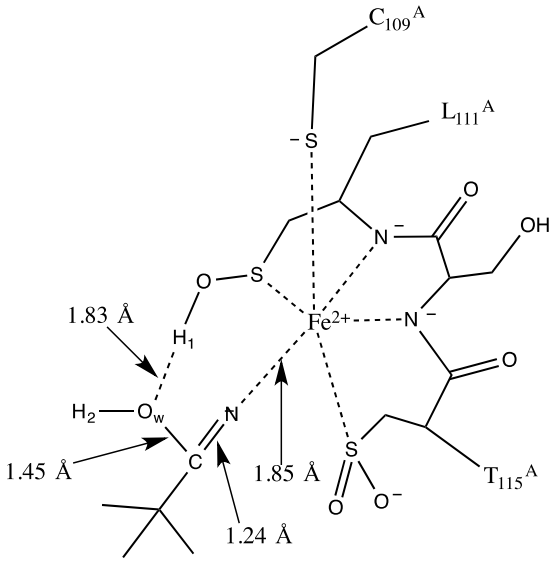

Figure 7.10 The first intermediate (I1) formed after the addition of water catalyzed by cysteine-sulfenic acid.

At this point in the mechanism, the proton bound to the cysteine-sulfenic acid (H_1) transfers to the nitrogen of the nitrile substrate via TS2. As shown in **Figure 7.11** $r(H_1 \cdots O_{CSO})$ and $r(H_1 \cdots N)$ are calculated to be 1.32 Å and 1.21 Å, respectively. The transition state for this proton transfer occurs with one imaginary frequency ($i907.89\ cm^{-1}$) and lies 162.2 kJ/mol higher in energy than the RC.

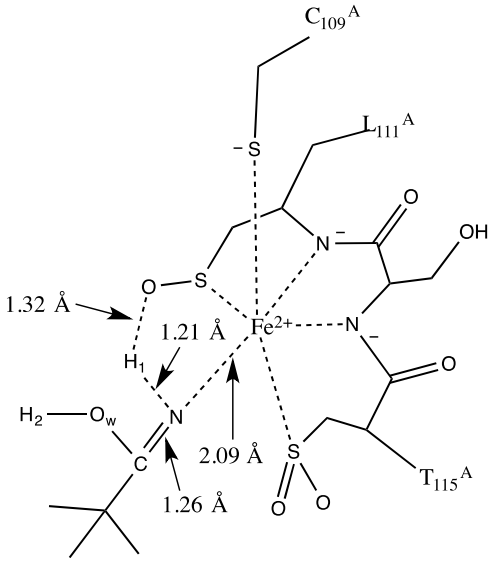

Figure 7.11 The second transition state (TS2) resulting from the proton transfer from CSO_{114} to the substrate.

With the complete proton transfer to the nitrile nitrogen, the second intermediate (I2) is found to have a slightly elongated r(N···Fe^{2+}) of 2.09 Å (**Figure 7.12**). This is likely due to the strain caused by the change from sp to sp^2 nitrogen, as well as the change in formal charge of nitrogen (from -1 to 0) and the steric interaction from H_1. In the case of the sulfenic acid r(O_{CSO}···H_1-N) is found to be 3.29 Å. This complex has a relative enthalpy of 156.1 kJ/mol.

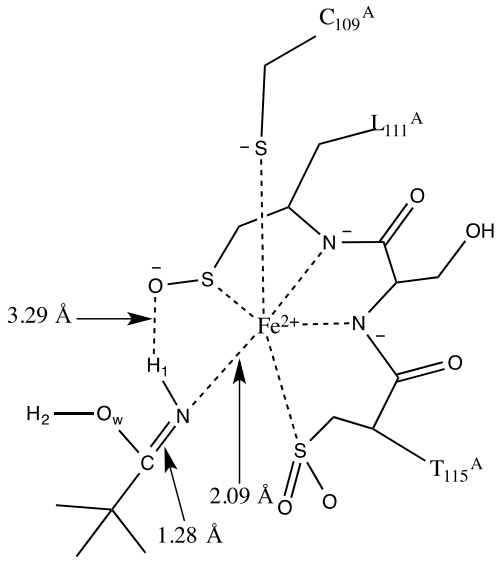

Figure 7.12 The second intermediate (I2) formed for the hydration of t-butyl nitrile.

The next transition state involves the rotation of the H_1 attached to the nitrogen such that it isomerizes from *cis* to *trans* to the alcohol bound to the nitrile carbon (**Figure 7.13**). As previously discussed this step will readily occur with a small activation energy barrier.[171, 172] Thus, we did not calculate a transition state for this step. The resulting intermediate complex (I3) lies 117.6 kJ/mol lower in energy than I2 and now only lies 38.5 kJ/mol higher in energy than RC.

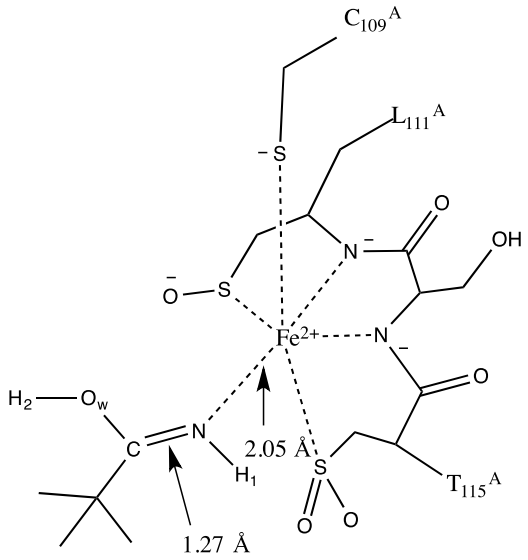

Figure 7.13 The third intermediate (I3) formed for the hydration of t-butyl nitrile.

The final step of the mechanism is the transfer of the second hydrogen (H_2) from the imidate to form the desired amide product (TS3; **Figure 7.14**). This step is accompanied by an increase in r(H_2···O) and decrease in r(H_2···N). This shift lengthens r(C···N) to 1.33 Å as the nitrogen changes from sp^2 to sp^3 and r(C···O_w) shortens to 1.30 Å as the carbonyl functional group forms. This transition state has an enthalpy of 202.3 kJ/mol relative to the reactant complex, and represents the rate-limiting step for this mechanism. This considerable energetic cost is likely due to the breaking of a hydrogen bond between the iminol and Gln_{90}, and the four-membered transition state which are well known to be very high in energy for amide-iminol tautomerization reactions.[34]

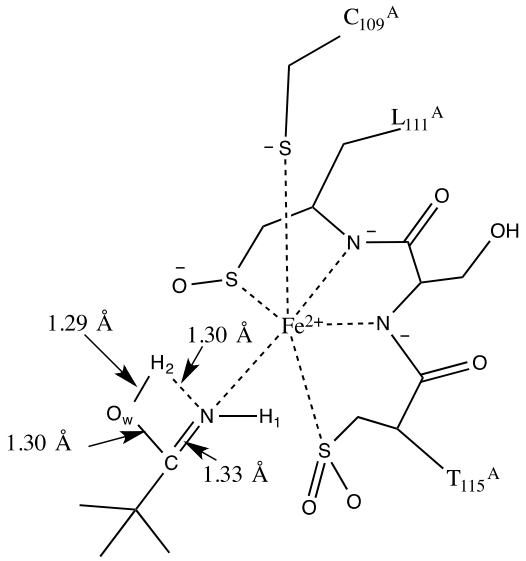

Figure 7.14 The third transition state (TS3) formed from t-butyl nitrile in the nitrile hydratase enzyme.

The final product complex (PC) is shown in **Figure 7.15**. This product has r($C^{\cdots}O_w$) and r($C^{\cdots}N$) of 1.24 Å and 1.35 Å, as expected for an amide functional group. As can be seen r($N^{\cdots}Fe^{3+}$) is 4.77 Å, suggesting the amide is no longer bound to the metal centre. With formation of the amide the active site is returned to its catalytic form to allow for further catalysis. Relative to RC this product complex has an enthalpy of -775.3 kJ/mol.

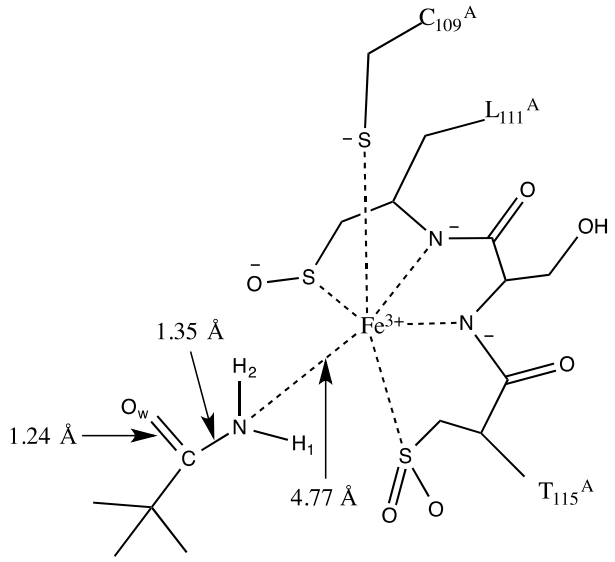

Figure 7.15 The final amide product complex (PC) formed by nitrile hydratase.

7.3.2 Mechanical Embedding and Electronic Embedding

At the ONIOM(ωB97X-D/6-311+G(2df,p)//AMBER96)-ME level the calculated reaction enthalpies for several stationary points are far too high to be enzymatically feasible (**Figure 7.16a**). Indeed, TS3 has the highest relative energy for this reaction of 202.3 kJ/mol relative to RC, which suggests the product could never be formed through this particular mechanism.

These calculations, however, were performed using mechanical embedding. This process performs calculations on the QM region in the absence of the MM system, i.e. the QM region is not polarized by the AMBER point charges from the surrounding environment. However, the enzyme environment is a crucial aspect of catalysis, which allows the reaction to occur, often having a large impact on computed energies. In order to account for the polarization due to the remainder of the enzyme system, electronic

embedding single point calculations were also performed with enthalpy corrections on the geometries obtained using mechanical embedding (**Figure 7.16b**).

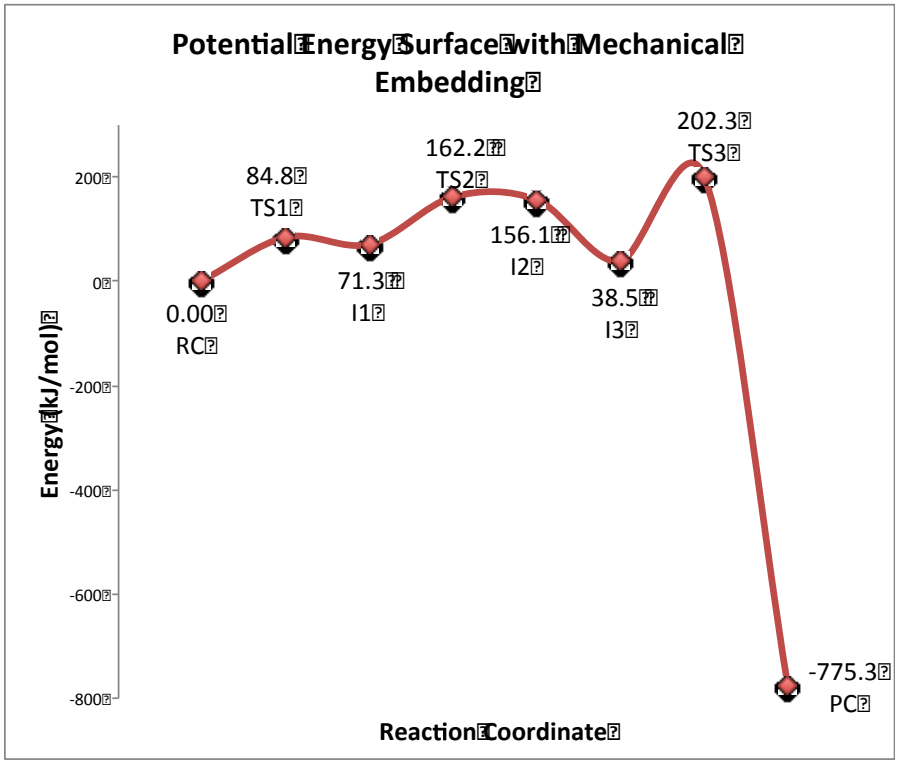

(a)

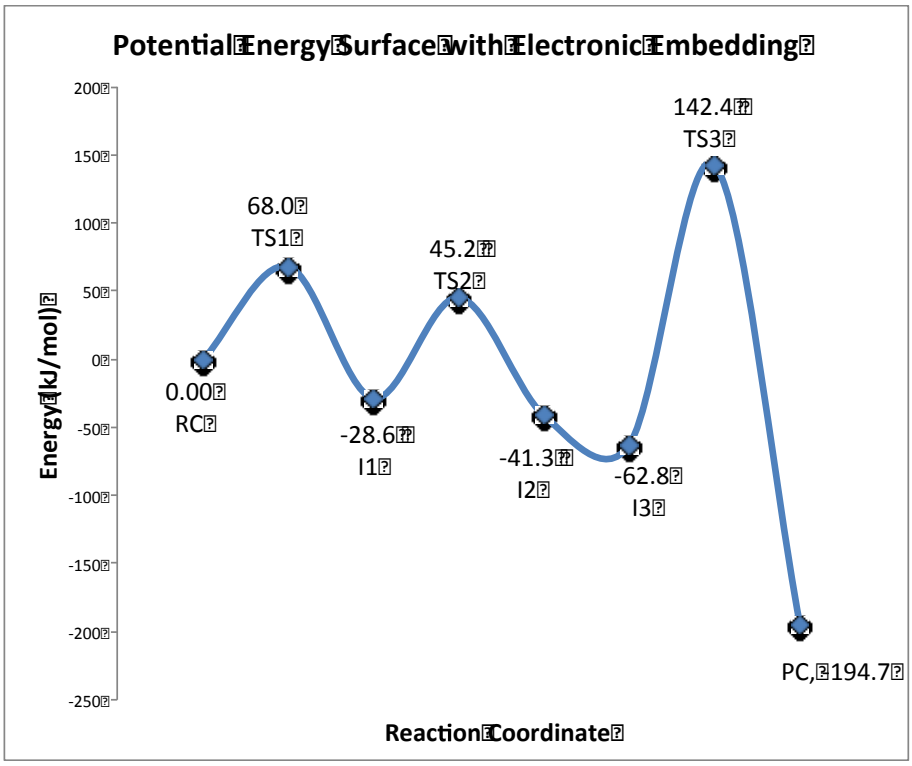

(b)

Figure 7.16 Potential energy surface for nitrile hydration by t-butyl nitrile hydratase. All energies given are single point energies with enthalpy corrections and **(a)** mechanical embedding and **(b)** electronic embedding, in kJ/mol.

As shown in **Figure 7.16b** the reaction enthalpies for this enzyme mechanism have been dramatically improved by electronic embedding. The mechanism is now three distinct steps (ionization of water in TS1, proton transfer in TS2 and amide-iminol tautomerization in TS3) with enthalpies of 68.0 kJ/mol, 73.8 kJ/mol and 205.2 kJ/mol relative to RC, respectively. The details of which will be discussed below.

The overall reduction in enthalpies between reactants and transition states is likely due to the stabilizing effects of nearby polar residues from the MM region introducing hydrogen bonds to the QM region, such as Gln_{90} (accepting a hydrogen bond from

water), Glu_{165} (accepting a hydrogen bond from water) and Arg_{167} (donating a hydrogen bond to CSO_{114}) on chain A and Arg_{141} on chain B (donating a hydrogen bond to CSD_{112} and CSO_{114}). During the first step of the mechanism (ionization of water), Glu_{165} maintains its hydrogen bond with the water molecule, stabilizing the transiently formed hydroxide ion. The proceeding intermediate (I1) is stabilized by the alcohol-Gln_{90} hydrogen bond formed. The second step in the mechanism involves the transfer of a proton from CSO_{114} to the substrate's terminal nitrogen. This process is likely stabilized due to the hydrogen bonds donated by Arg_{167} and Arg_{141} to the oxygen of CSO_{114}, promoting proton transfer. The final step in this mechanism (amide-iminol tautomerization) is only slightly stabilized by the surrounding environment, as there are no additional hydrogen bonds formed during this intramolecular rearrangement. While the enthalpies for the complexes have been improved after the addition of electronic embedding, the energies are still larger than the experimental energies of ~54-63 kJ/mol.[34] While the relative energies of TS1 and TS2 are in reasonable agreement, the relative enthalpy of TS3 still remains to high to be enzymatically feasible. However, given that TS3 is a four-membered transition state the addition of a second water molecule would likely have a significant effect on the energetics of this step.

The addition of a second water molecule will change the four-membered transition state to a six-membered transition state and dramatically lower the relative enthalpy for TS3. Such a reduction in energy has been previously shown for the isolated iminol-amide tautomerization.[34]. At the CPCM-B3LYP/6-31G(d,p) level of theory (with zero-point vibrational corrections), the four membered transition state for this process occurred with a barrier of ~142 kJ/mol. However, with the addition of a second water

molecule, the barrier drops to just ~10 kJ/mol. Thus, in the present case the addition of a second water would be expected to have similar effects in the relative enthalpy of TS3.

Provided the relative energy of TS3 is reduced the mechanism studied in this chapter would agree with experimental energies and be a competing mechanism for the currently accepted mechanism, which involves a disulfide switch.[167]

7.4 Conclusion

The catalytic mechanism for nitrile hydration by nitrile hydratases has been studied using advanced computational methods. The proposed mechanism where cysteine-sulfenic acid acts as a nucleophile has been examined with a large portion of the protein active site modeled. Previous models of this mechanism have neglected the effect of surrounding protein environment. After the inclusion of the protein environment, the enthalpies of all complexes have been lowered to within 10 kJ/mol of experimental barriers. However, while TS3 still remains far too high in energy the presence of a second water would likely reduce the energetic cost for this four-membered TS considerably. Thus, further investigation into the addition of a second water molecule in the active site of this enzyme is needed.

8 CONCLUSION

8.1 Conclusions

In chapter 3, the FRED receptor program was used to bind various substrates into four FKBP enzymes. The current work compares the binding scores of various similar macrocyclic substrates into the active site of *h*FKBP12, *Pv*FKBP35, and *Pf*FKBP35. While ILS-920 and WYE-592 bind less favourably than rapamycin in *h*FKBP12 and *Pf*FKBP35, the addition of a nitrosobenzylated moiety to carbon 19 of rapamycin has an increase in docking score. This small but significant modification to the macrocycle could be used as a starting point for novel drug design of antimalarials.

In chapter 4, the work performed investigates the plausibility of suicide inhibition for a new class of anti-malarial. To explore this, a Michael acceptor was added to carbon 42 of the natural substrate, Fk506. This modification allows for covalent bond formation between Cys_{106} of *Plasmodium falciparum* FKBP35 and the substrate through a one-step mechanism, forming the inhibitor-enzyme complex. While the activation energy barrier is relatively high, this shows the possibility for modified macrocycles acting as suicide inhibitors for treatment of malaria caused by *Plasmodium falciparum*.

Chapter 5 studies the enzymatic pathway of leukotriene C_4 synthase for the conversion of leukotriene A_4 to leukotriene C_4 using docking, molecular dynamics and QM/MM methods. The employed methods suggest the substrate binds in a ‘tail-to-head’ orientation to better interact with the enzyme and bound glutathione. This substrate orientation is likely preferred over the ‘head-to-tail’ orientation due to the extra hydrogen bond formed between the polar head of leukotriene A_4 and Arg_{104}. A better understanding

of the binding orientation could lead to novel anti-inflammatory mediators for the treatment and prevention of asthma and bronchoconstriction.

In chapter 6, the enzymatic pathway of leukotriene B_4 synthesis from the precursor leukotriene A_4 with leukotriene A_4 hydrolase was studied using docking, molecular dynamics, and QM/MM methods. The mechanism proposes Asp_{375} promotes water ionization, adding a hydroxide ion to carbon 12. This bond formation causes the epoxide ring between carbon 5 and 6 to open and be protonated by a nearby water molecule to form the desired product. The methods performed for this work suggests the enthalpy of the product complex, LTB_4, is far too high in comparison to the reactant, LTA_4. It is likely that Asp_{375} will not accept a proton from water to catalyze water splitting for the first step of the mechanism, and perhaps another nearby residue would be more appropriate.

In chapter 7, the proposed mechanism of nitrile hydratase with a t-butyl nitrile substrate was investigated using docking, molecular dynamics and QM/MM methods. This mechanism, in the presence of one water molecule, offers enthalpies far higher than realistic when compared to the alternate mechanism, which occurs through a disulfide switch. The enthalpies for the current mechanism are greatly improved after the addition of the polarizing effect of the protein environment. It has also been suggested the addition of a second water molecule to the active site would greatly reduce the enthalpy of the transition states, as similar proton transfers have been shown to be facilitated through water chains and four-membered transition states for iminol-amide tautomerism are changed to six-membered transition states. The decrease in enthalpies would show good

enough agreement with experiment to warrant further investigation of a two-water mechanism.

8.2 Future Work

Chapter 3 outlines potential new lead compounds for anti-malarials. While a few of these macrocycles have been tested in various FKBPs in various different organisms, a systematic approach to testing IC_{50} and EC_{50} values for all available, FDA-approved macrocycles with *h*FKBP12, *Pv*FKBP35, *Pf*FKBP35, and any other prevalent PPIase in the human body would be required to further this research. This work would solidify which moieties are most effective in inhibition, and if this inhibition would harm the patient with malaria.

Chapter 4 explores the plausibility of suicide inhibition for treatment of *Plasmodium falciparum* malaria. This method could be expanded through the modification of various other macrocycles aside from Fk506, as they have also been shown to have inhibitory properties.[95] This could also involve other electrophiles other than Michael acceptors of varying electrophilicities. The strength of the formed covalent bond could also be improved through the deprotonation of Cys_{106}. This could be accomplished by changing the local environment around the nucleophile, perhaps by adding formally positive charges along the active site. These changes could lead to a much stronger covalent bond with a smaller activation energy.

Chapter 5 investigates the enzymatic mechanism of leukotriene C_4 synthesis, a molecule important in inflammatory response and asthma. Determining another potential binding orientation for the substrate in this enzyme provides additional information that could be used in the design of novel anti-inflammatory drugs. If leukotriene C_4 synthase

can be inhibited and prevented from binding leukotriene A_4, this can prevent leukotriene C_4 from causing unwanted bronchoconstriction in asthmatic patients.

Chapter 6 studies the enzymatic mechanism for leukotriene B_4 synthesis, a molecule involved with inflammation. The work performed in this chapter did not conclusively determine that Asp_{375} was able to catalyze the water splitting required for the formation of leukotriene B_4. Further studies would be required to determine if another residue would be most appropriate for water ionization, or what factors would need to change in order for this residue to be catalytic. This information could lead to further drug development of anti-inflammatory medications.

Chapter 7 investigates one of the competing mechanisms for nitrile hydration for a t-butyl nitrile substrate by nitrile hydratase. The one-water mechanism offers enthalpies much higher than experiment. While it has been proposed the addition of a second water molecule would lower enthalpies to be in excellent agreement with experimental barriers, the calculations would need to be performed to verify how the second water molecule would lower the barriers of tautomerism and proton transfers.

REFERENCES

1. Nelson, D. L.; Cox, M. M., *Lehninger's Principles of Biochemistry, 4th Edition*. New York., 2005.

2. Sousa, S. F.; Fernandes, P. A.; Ramos, M. J., Computational enzymatic catalysis--clarifying enzymatic mechanisms with the help of computers. *Phys. Chem. Chem. Phys., **2012**, 14,* 12431-41.

3. Hertweck, C., Biosynthesis and charging of pyrrolysine, the 22nd genetically encoded amino acid. *Angew. Chem. Int., **2011**, 50,* 9540-9541.

4. Pollegioni, L.; Servi, S., eds, *Unnatural Amino Acids.* Humana Press.: 2012.

5. Jakubke, H.-D.; Sewald, N., *Peptides from A to Z: A Concise Encyclopedia*. 2008.

6. Gutteridge, A.; Thornton, J. M., Understanding nature's catalytic toolkit. *Trends Biochem. Sci., **2005**, 30,* 622-9.

7. Liu, H.; Gauld, J. W., Substrate-assisted catalysis in the aminoacyl transfer mechanism of histidyl-tRNA synthetase: a density functional theory study. *J. Phys. Chem. B., **2008**, 112,* 16874-82.

8. Ramos, M. J.; Fernandes, P. A., Computational enzymatic catalysis. *Acc. Chem. Res., **2008**, 41,* 689-98.

9. Fedor, M. J.; Williamson, J. R., The catalytic diversity of RNAs. *Nat. Rev. Mol. Cell Biol., **2005**, 6,* 399-412.

10. Radzicka, A.; Wolfenden, R., A proficient enzyme. *Science., **1995**, 267,* 90-3.

11. Prabhakar, R.; Morokuma, K.; Musaev, D. G. Computational insights into the structural Pproperties and catalytic functions of selenoprotein glutathione peroxidase

(GPx). In *Computational Modeling for Homogeneous and Enzymatic Catalysis*; Wiley-VCH Verlag GmbH & Co. KGaA: 2008, pp 1-25.

12. Bruice, T. C., Some pertinent aspects of mechanism as determined with small molecules. *Annu. Rev. Biochem., **1976**, 45,* 331-374.

13. Warshel, A., Electrostatic origin of the catalytic power of enzymes and the role of preorganized active sites. *J. Biol. Chem., **1998**, 273,* 27035-27038.

14. Villà, J.; Štrajbl, M.; Glennon, T. M.; Sham, Y. Y.; Chu, Z. T.; Warshel, A., How important are entropic contributions to enzyme catalysis? *Proc. Natl. Acad. Sci. U.S.A., **2000**, 97,* 11899-11904.

15. Villà, J.; Warshel, A., Energetics and dynamics of enzymatic reactions. *J. Phys. Chem. B., **2001**, 105,* 7887-7907.

16. Pauling, L., Molecular architecture and biological reactions. *Chem. Eng. News., **1946**, 24,* 1375-1377.

17. Schowen, R. L., How an enzyme surmounts the activation energy barrier. *Proc. Natl. Acad. Sci. U.S.A., **2003**, 100,* 11931-11932.

18. Page, M. I.; Jencks, W. P., Entropic contributions to rate accelerations in enzymic and intramolecular reactions and the chelate effect. *Proc. Natl. Acad. Sci. U.S.A., **1971**, 68,* 1678-1683.

19. Warshel, A., Energetics of enzyme catalysis. *Proc. Natl. Acad. Sci. U.S.A., **1978**, 75,* 5250-5254.

20. Warshel, A.; Levitt, M., Theoretical studies of enzymic reactions: dielectric, electrostatic and steric stabilization of the carbonium ion in the reaction of lysozyme. *J. Mol. Biol., **1976**, 103,* 227-49.

21. Masgrau, L.; Roujeinikova, A.; Johannissen, L. O.; Hothi, P.; Basran, J.; Ranaghan, K. E.; Mulholland, A. J.; Sutcliffe, M. J.; Scrutton, N. S.; Leys, D., Atomic description of an enzyme reaction dominated by proton tunneling. *Science., **2006**, 312,* 237-41.

22. Nagel, Z. D.; Klinman, J. P., Tunneling and dynamics in enzymatic hydride transfer. *Chem. Rev., **2006**, 106,* 3095-118.

23. Johnson, D. S.; Weerapana, E.; Cravatt, B. F., Strategies for discovering and derisking covalent, irreversible enzyme inhibitors. *Future Med. Chem., **2010**, 2,* 949-64.

24. Singh, J.; Petter, R. C.; Baillie, T. A.; Whitty, A., The resurgence of covalent drugs. *Nat. Rev. Drug Discov., **2011**, 10,* 307-317.

25. Fischer, G.; Schmid, F. X., The mechanism of protein folding. Implications of in vitro refolding models for de novo protein folding and translocation in the cell. *Biochemistry., **1990**, 29,* 2205-12.

26. O'Byrne, P. M.; Israel, E.; Drazen, J. M., Antileukotrienes in the treatment of asthma. *Ann. Intern. Med., **1997**, 127,* 472-480.

27. Crooks, S. W.; Stockley, R. A., Leukotriene B4. *Int. J. Biochem. Cell Biol., **1998**, 30,* 173-178.

28. Khatami, M., *Inflammatory Diseases - Immunopathology, Clinical and Pharmacological Bases*. InTech: 2012.

29. Ago, H.; Kanaoka, Y.; Irikura, D.; Lam, B. K.; Shimamura, T.; Austen, K. F.; Miyano, M., Crystal structure of a human membrane protein involved in cysteinyl leukotriene biosynthesis. *Nature., **2007**, 448,* 609-12.

30. Molina, D. M.; Wetterholm, A.; Kohl, A.; McCarthy, A. A.; Niegowski, D.; Ohlson, E.; Hammarberg, T.; Eshaghi, S.; Haeggström, J. Z.; Nordlund, P., Structural basis for synthesis of inflammatory mediators by human leukotriene C4 synthase. *Nature., **2007**, 448,* 613-616.

31. Marron, A. O.; Akam, M.; Walker, G., Nitrile hydratase genes are present in multiple eukaryotic supergroups. *PLoS ONE., **2012**, 7,* e32867.

32. Hashimoto, K.; Suzuki, H.; Taniguchi, K.; Noguchi, T.; Yohda, M.; Odaka, M., Catalytic mechanism of nitrile hydratase proposed by time-resolved X-ray crystallography using a novel substrate, tert-butylisonitrile. *J. Biol. Chem., **2008**, 283,* 36617-23.

33. Martinez, S.; Wu, R.; Sanishvili, R.; Liu, D.; Holz, R., The active site sulfenic acid ligand in nitrile hydratases can function as a nucleophile. *J. Am. Chem. Soc., **2014**, 136,* 1186-1189.

34. Hopmann, K. H.; Guo, J. D.; Himo, F., Theoretical investigation of the first-shell mechanism of nitrile hydratase. *Inorg. Chem., **2007**, 46,* 4850-6.

35. Hopmann, K. H.; Himo, F., Theoretical investigation of the second-shell mechanism of nitrile hydratase. *Eur. J. Inorg. Chem., **2008**,* 1406-1412.

36. Jensen, F., *Introduction to Computational Chemistry*. John Wiley & Sons: New York, 1999.

37. Koch, W., Holthausen, M.C., *A Chemist's Guide to Density Functional Theory*. Second ed.; Wiley-VCH: New York, 2001.

38. Leach, A. R., *Molecular Modelling: Principles and Applications*. Second ed.; Pearson Education Limited: England, 2001.

39. Levine, I. N., *Quantum Chemistry*. Prentice Hall: New Jersey, 2013.

40. Gill, P. M. W., Molecular integrals over Gaussian basis functions. *Adv. Quantum Chem., **1994**, 25,* 141-205.

41. Pople, J. A.; Nesbet, R. K., Self- consistent orbitals for radicals. *J. Chem. Phys., **1954**, 22,* 571-572.

42. Ypma, T. J., Historical development of the newton–raphson method. *SIAM Rev., **1995**, 37,* 531-551.

43. Becke, A. D., Density-functional exchange-energy approximation with correct asymptotic behavior. *Phys. Rev. A., **1988**, 38,* 3098-3100.

44. Chai, J. D.; Head-Gordon, M., Long-range corrected hybrid density functionals with damped atom-atom dispersion corrections. *Phys. Chem. Chem. Phys. , **2008**, 10,* 6615-20.

45. D.A. Case, T. A. D., T.E. Cheatham, III, C.L. Simmerling, J. Wang, R.E. Duke, R. Luo, R.C. Walker, W. Zhang, K.M. Merz, B.P. Roberts, B. Wang, S. Hayik, A. Roitberg, G. Seabra, I. Kolossváry, K.F. Wong, F. Paesani, J. Vanicek, J. Liu, X. Wu, S.R. Brozell, T. Steinbrecher, H. Gohlke, Q. Cai, X. Ye, J. Wang, M.-J. Hsieh, G. Cui, D.R. Roe, D.H. Mathews, M.G. Seetin, C. Sagui, V. Babin, T. Luchko, S. Gusarov, A. Kovalenko, and P.A. Kollman. 2010, AMBER 11, University of California, San Francisco.

46. Bayly, C. I.; Cieplak, P.; Cornell, W. D.; Kollman, P. A., A well-behaved electrostatic potential based method using charge restraints for deriving atomic charges - the RESP model. *J. Phys. Chem., **1993**, 97,* 10269-10280.

47. Deslongchamps, G., In *Molecular Modeling – An Introduction to Molecular Mechanics.*; 2009.

48. Hawkins, P. C.; Skillman, A. G.; Warren, G. L.; Ellingson, B. A.; Stahl, M. T., Conformer generation with OMEGA: algorithm and validation using high quality structures from the Protein Databank and Cambridge Structural Database. *J. Chem. Inf. Model., **2010**, 50,* 572-84.

49. Perola, E.; Charifson, P. S., Conformational analysis of drug-like molecules bound to proteins: an extensive study of ligand reorganization upon binding. *J. Med. Chem., **2004**, 47,* 2499-510.

50. Knox, A. J.; Meegan, M. J.; Carta, G.; Lloyd, D. G., Considerations in compound database preparation--"hidden" impact on virtual screening results. *J. Chem. Inf. Model., **2005**, 45,* 1908-19.

51. McGann, M. R.; Almond, H. R.; Nicholls, A.; Grant, J. A.; Brown, F. K., Gaussian docking functions. *Biopolymers., **2003**, 68,* 76-90.

52. Peng, C. Y.; Schlegel, H. B., Combining synchronous transit and quasi-Newton methods to find transition-states. *Isr. J. Chem., **1993**, 33,* 449-454.

53. Peng, C. Y.; Ayala, P. Y.; Schlegel, H. B.; Frisch, M. J., Using redundant internal coordinates to optimize equilibrium geometries and transition states. *J. Comp. Chem., **1996**, 17,* 49-56.

54. Dapprich, S.; Komaromi, I.; Byun, K. S.; Morokuma, K.; Frisch, M. J., A new ONIOM implementation in Gaussian98. Part I. The calculation of energies, gradients, vibrational frequencies and electric field derivatives. *J. Mol. Struct. THEOCHEM., **1999**, 461,* 1-21.

55. Ranaghan, K. E.; Mulholland, A. J., Investigations of enzyme-catalysed reactions with combined quantum mechanics/molecular mechanics (qm/mm) methods. *Int. Rev. Phys. Chem.,* ***2010****, 29,* 65-133.

56. Senn, H. M.; Thiel, W., QM/MM methods for biomolecular systems. *Angew. Chem. Int. Ed.,* ***2009****, 48,* 1198-1229.

57. Vreven, T.; Morokuma, K., On the application of the IMOMO (integrated molecular orbital plus molecular orbital) method. *J. Comput. Chem.,* ***2000****, 21,* 1419-1432.

58. Morokuma, K.; Musaev, D. G.; Vreven, T.; Basch, H.; Torrent, M.; Khoroshun, D. V., Model studies of the structures, reactivities, and reaction mechanisms of metalloenzymes. *IBM J. Res. Dev.,* ***2001****, 45,* 367-395.

59. Vreven, T.; Byun, K. S.; Komáromi, I.; Dapprich, S.; Montgomery Jr, J. A.; Morokuma, K.; Frisch, M. J., Combining quantum mechanics methods with molecular mechanics methods in ONIOM. *J. Chem. Theory Comput.,* ***2006****, 2,* 815-826.

60. Vreven, T.; Morokuma, K., On the application of the IMOMO (integrated molecular orbital + molecular orbital) method. *J. Comput. Chem.,* ***2000****, 21,* 1419-1432.

61. Vreven, T.; Morokuma, K.; Farkas, O.; Schlegel, H. B.; Frisch, M. J., Geometry optimization with QM/MM, ONIOM, and other combined methods. I. Microiterations and constraints. *J. Comput. Chem.,* ***2003****, 24,* 760-769.

62. Investigating the Reactivity and Spectra of Large Molecules with ONIOM. http://www.gaussian.com/g_whitepap/oniom_technote.htm (June, 2014),

63. Rehwagen, C., WHO recommends DDT to control malaria. *Brit. Med. J.,* ***2006****, 333,* 622.

64. Rehwagen, C., WHO ultimatum on artemisinin monotherapy is showing results. *Brit. Med. J., **2006**, 332,* 1176.

65. Caraballo, H.; King, K., Emergency department management of mosquito-borne illness: malaria, dengue, and West Nile virus. *Emerg. Med. Pract., **2014**, 16,* 1-23; quiz 23-4.

66. MacDonald, C. A.; Boyd, R. J., Molecular docking study of macrocycles as Fk506-binding protein inhibitors. *J. Mol. Graphics Modell., **2015**, 59,* 117-122.

67. Mockenhaupt, F. P.; May, J.; Bergqvist, Y.; Meyer, C. G.; Falusi, A. G.; Bienzle, U., Evidence for a reduced effect of chloroquine against Plasmodium falciparum in alpha-thalassaemic children. *Trop. Med. Int. Health., **2001**, 6,* 102-7.

68. Plowe, C. V. Antimalarial Drug Resistance in Africa: Strategies for Monitoring and Deterrence. In *Malaria: Drugs, Disease and Post-genomic Biology*, Compans, R. W.; Cooper, M. D.; Honjo, T.; Koprowski, H.; Melchers, F.; Oldstone, M. B. A.; Olsnes, S.; Potter, M.; Vogt, P. K.; Wagner, H.; Sullivan, D.; Krishna, S., Eds.; Springer Berlin Heidelberg: 2005; Vol. 295, Chapter 3, pp 55-79.

69. Barber, M. A.; Rice, J. B.; Brown, J. Y., Malaria studies on the firestone rubber plantation in Liberia, West Africa. *Am. J. Hyg., **1932**, 15,* 601-633.

70. Zhang, V. M.; Chavchich, M.; Waters, N. C., Targeting protein kinases in the malaria parasite: update of an antimalarial drug target. *Curr. Top. Med. Chem., **2012**, 12,* 456-72.

71. Cheng, M., World's most advanced malaria vaccine is a disappointment but could still reduce cases. *Edmonton Journal, **2015***.

72. Ohnmar; Tun-Min; May-Aye-Than; San-Shwe; Wai-Wai-Myint; Chongsuvivatwong, V., Access to a blood test and antimalarials after introducing rapid diagnostic tests in rural Myanmar: initial experience in a malaria endemic area. *Int. Health., **2010**, 2,* 275-281.

73. Goodman, C.; Brieger, W.; Unwin, A.; Mills, A.; Meek, S.; Greer, G., Medicine sellers and malaria treatment in Sub-Saharan Africa: what do they do and how can their practice be improved? *Am. J. Trop. Med. Hyg., **2007**, 77,* 203-218.

74. Douglas, N. M.; Anstey, N. M.; Angus, B. J.; Nosten, F.; Price, R. N., Artemisinin combination therapy for vivax malaria. *Lancet Infect. Dis., **2010**, 10,* 405-16.

75. Wang, S. S., A Warning From the Heart of Malaria Research. *The Wall Street Journal* 2015.

76. Beausoleil, E.; Lubell, W. D., Steric effects on the amide isomer equilibrium of prolyl peptides. Synthesis and conformational analysis of N-acetyl-5-tert-butylproline N'-methylamides. *J. Am. Chem. Soc., **1996**, 118,* 12902-12908.

77. Byun, B. J.; Kang, Y. K., Conformational preferences and prolyl cis-trans isomerization of phosphorylated Ser/Thr-Pro motifs. *Biopolymers., **2010**, 93,* 330-9.

78. Cox, C.; Lectka, T., Solvent effects on the barrier to rotation in carbamates. *J. Org. Chem., **1998**, 63,* 2426-2427.

79. Bell, A.; Monaghan, P.; Page, A. P., Peptidyl-prolyl cis-trans isomerases (immunophilins) and their roles in parasite biochemistry, host-parasite interaction and antiparasitic drug action. *Int. J. Parasitol., **2006**, 36,* 261-276.

80. Fanghanel, J.; Fischer, G., Insights into the catalytic mechanism of peptidyl prolyl cis/trans isomerases. *Front. Biosci., **2004**, 9,* 3453-78.

81. Fischer, S.; Michnick, S.; Karplus, M., A mechanism for rotamase catalysis by the FK506 binding protein (FKBP). *Biochemistry.,* ***1993****, 32,* 13830-7.

82. Stein, R. L., Mechanism of enzymatic and nonenzymatic prolyl cis-trans isomerization. *Adv. Protein Chem.,* ***1993****, 44,* 1-24.

83. Alag, R.; Balakrishna, A. M.; Rajan, S.; Qureshi, I. A.; Shin, J.; Lescar, J.; Gruber, G.; Yoon, H. S., Structural insights into substrate binding by PvFKBP35, a peptidylprolyl cis-trans isomerase from the human malarial parasite Plasmodium vivax. *Eukaryot. Cell.,* ***2013****, 12,* 627-34.

84. Alag, R.; Qureshi, I. A.; Bharatham, N.; Shin, J.; Lescar, J.; Yoon, H. S., NMR and crystallographic structures of the FK506 binding domain of human malarial parasite Plasmodium vivax FKBP35. *Protein Sci.,* ***2010****, 19,* 1577-86.

85. Wilson, K. P.; Yamashita, M. M.; Sintchak, M. D.; Rotstein, S. H.; Murcko, M. A.; Boger, J.; Thomson, J. A.; Fitzgibbon, M. J.; Black, J. R.; Navia, M. A., Comparative X-ray structures of the major binding protein for the immunosuppressant FK506 (tacrolimus) in unliganded form and in complex with FK506 and rapamycin. *Acta Crystallogr. D. Biol. Crystallogr.,* ***1995****, 51,* 511-21.

86. Kotaka, M.; Ye, H.; Alag, R.; Hu, G.; Bozdech, Z.; Preiser, P. R.; Yoon, H. S.; Lescar, J., Crystal structure of the FK506 binding domain of Plasmodium falciparum FKBP35 in complex with FK506. *Biochemistry.,* ***2008****, 47,* 5951-61.

87. Choi, J.; Chen, J.; Schreiber, S. L.; Clardy, J., Structure of the FKBP12-rapamycin complex interacting with the binding domain of human FRAP. *Science.,* ***1996****, 273,* 239-42.

88. McGann, M., FRED and HYBRID docking performance on standardized datasets. *J. Comput. Aided Mol. Des., **2012**, 26,* 897-906.

89. Kellenberger, E.; Rodrigo, J.; Muller, P.; Rognan, D., Comparative evaluation of eight docking tools for docking and virtual screening accuracy. *Proteins., **2004**, 57,* 225-42.

90. Tuccinardi, T.; Botta, M.; Giordano, A.; Martinelli, A., Protein kinases: docking and homology modeling reliability. *J. Chem. Inf. Model., **2010**, 50,* 1432-1441.

91. Eldridge, M. D.; Murray, C. W.; Auton, T. R.; Paolini, G. V.; Mee, R. P., Empirical scoring functions: I. The development of a fast empirical scoring function to estimate the binding affinity of ligands in receptor complexes. *J. Comput. Aided Mol. Des., **1997**, 11,* 425-45.

92. Lape, M.; Elam, C.; Paula, S., Comparison of current docking tools for the simulation of inhibitor binding by the transmembrane domain of the sarco/endoplasmic reticulum calcium ATPase. *Biophys. Chem., **2010**, 150,* 88-97.

93. Hanwell, M. D.; Curtis, D. E.; Lonie, D. C.; Vandermeersch, T.; Zurek, E.; Hutchison, G. R., Avogadro: an advanced semantic chemical editor, visualization, and analysis platform. *J. Cheminform., **2012**, 4,* 17.

94. Quevedo, M. A.; Ribone, S. R.; Brinon, M. C.; Dehaen, W., Development of a receptor model for efficient in silico screening of HIV-1 integrase inhibitors. *J. Mol. Graph. Model., **2014**, 52,* 82-90.

95. Bharatham, N.; Chang, M. W.; Yoon, H. S., Targeting FK506 binding proteins to fight malarial and bacterial infections: current advances and future perspectives. *Curr. Med. Chem., **2011**, 18,* 1874-89.

96. Monaghan, P.; Bell, A., A Plasmodium falciparum FK506-binding protein (FKBP) with peptidyl-prolyl cis-trans isomerase and chaperone activities. *Mol. Biochem. Parasitol., **2005**, 139,* 185-95.

97. Rajan, S.; Austin, D.; Harikishore, A.; Nguyen, Q. T.; Baek, K.; Yoon, H. S., Crystal structure of Plasmodium vivax FK506-binding protein 25 reveals conformational changes responsible for its noncanonical activity. *Proteins., **2014**, 82,* 1235-44.

98. Smith, D. L.; Guerra, C. A.; Snow, R. W.; Hay, S. I., Standardizing estimates of the Plasmodium falciparum parasite rate. *Malaria journal, **2007**, 6,* 131.

99. Sinha, S.; Medhi, B.; Sehgal, R., Challenges of drug-resistant malaria. *Parasite., **2014**, 21,* 61.

100. White, N. J., Qinghaosu (artemisinin): the price of success. *Science., **2008**, 320,* 330-4.

101. Kino, T.; Hatanaka, H.; Hashimoto, M.; Nishiyama, M.; Goto, T.; Okuhara, M.; Kohsaka, M.; Aoki, H.; Imanaka, H., FK-506, a novel immunosuppressant isolated from a Streptomyces. I. Fermentation, isolation, and physico-chemical and biological characteristics. *J. Antibiot., **1987**, 40,* 1249-55.

102. Warren, J. T.; Rybczynski, R.; Gilbert, L. I., Stereospecific, mechanism-based, suicide inhibition of a cytochrome P450 involved in ecdysteroid biosynthesis in the prothoracic glands of Manduca sexta. *Insect Biochem. Mol. Biol., **1995**, 25,* 679-95.

103. Testa, S. M.; Gryaznov, S. M.; Turner, D. H., In vitro suicide inhibition of self-splicing of a group I intron from Pneumocystis carinii by an N3′ → P5′ phosphoramidate hexanucleotide. *Proc. Natl. Acad. Sci. USA., **1999**, 96,* 2734-2739.

104. Deussen, H. J.; Danielsen, S.; Breinholt, J.; Borchert, T. V., A novel biotinylated suicide inhibitor for directed molecular evolution of lipolytic enzymes. *Bioorg. Med. Chem., **2000**, 8,* 507-13.

105. Batke, J.; Gaal, J., Suicide inhibition of monoamine oxidases A and B by (-)-deprenyl. A computer-aided solution for determining inhibition specificity. *Biochem. Pharmacol., **1993**, 46,* 597-602.

106. Fry, D. W., Inhibition of the epidermal growth factor receptor family of tyrosine kinases as an approach to cancer chemotherapy: progression from reversible to irreversible inhibitors. *Pharmacol. Ther., **1999**, 82,* 207-18.

107. Grimme, S., Semiempirical GGA-type density functional constructed with a long-range dispersion correction. *J. Comput. Chem., **2006**, 27,* 1787-99.

108. Svensson, M.; Humbel, S.; Froese, R. D. J.; Matsubara, T.; Sieber, S.; Morokuma, K., ONIOM: a multilayered integrated MO + MM method for geometry optimizations and single point energy predictions. A test for Diels−Alder reactions and Pt(P(t-Bu)3)2 + H2 oxidative addition. *J. Phys. Chem., **1996**, 100,* 19357-19363.

109. Gold, B. G., FK506 and the role of immunophilins in nerve regeneration. *Mol. Neurobiol., **1997**, 15,* 285-306.

110. MOE *Molecular Operating Environment*, 2009.10; Chemical Computing Group Inc.: Montreal, Quebec, Canada, 2009.

111. Phillips, J. C.; Braun, R.; Wang, W.; Gumbart, J.; Tajkhorshid, E.; Villa, E.; Chipot, C.; Skeel, R. D.; Kale, L.; Schulten, K., Scalable molecular dynamics with NAMD. *J. Comput. Chem., **2005**, 26,* 1781-802.

112. Labute, P., Protonate3D: assignment of ionization states and hydrogen coordinates to macromolecular structures. *Proteins.,* ***2009****, 75,* 187-205.

113. Wang, J. M.; Cieplak, P.; Kollman, P. A., How well does a restrained electrostatic potential (RESP) model perform in calculating conformational energies of organic and biological molecules? *J. Comput. Chem.,* ***2000****, 21,* 1049-1074.

114. De Luna, P.; Bushnell, E. A.; Gauld, J. W., A molecular dynamics examination on mutation-induced catalase activity in coral allene oxide synthase. *J. Phys. Chem. B.,* ***2013****, 117,* 14635-41.

115. Bushnell, E. A.; Gherib, R.; Gauld, J. W., Insights into the catalytic mechanism of coral allene oxide synthase: a dispersion corrected density functional theory study. *J. Phys. Chem. B.,* ***2013****, 117,* 6701-10.

116. Frisch, M. J.; Trucks, G. W.; Schlegel, H. B.; Scuseria, G. E.; Robb, M. A.; Cheeseman, J. R.; Scalmani, G.; Barone, V.; Mennucci, B.; Petersson, G. A.; Nakatsuji, H.; Caricato, M.; Li, X.; Hratchian, H. P.; Izmaylov, A. F.; Bloino, J.; Zheng, G.; Sonnenberg, J. L.; Hada, M.; Ehara, M.; Toyota, K.; Fukuda, R.; Hasegawa, J.; Ishida, M.; Nakajima, T.; Honda, Y.; Kitao, O.; Nakai, H.; Vreven, T.; Montgomery, J., J.A.;; Peralta, J. E.; Ogliaro, F.; Bearpark, M.; Heyd, J. J.; Brothers, E.; Kudin, K. N.; Staroverov, V. N.; Keith, T.; Kobayashi, R.; Normand, J.; Raghavachar, K.; Rendell, A.; Burant, J. C.; Iyengar, S. S.; Tomasi, J.; Cossi, M.; Rega, N.; Millam, J. M.; Klene, M.; Knox, J. E.; Cross, J. B.; Bakken, V.; Adamo, C.; Jaramillo, J.; Gomperts, R.; Stratmann, R. E.; Yazyev, O.; Austin, A. J.; Cammi, R.; Pomelli, C.; Ochterski, J. W.; Martin, R. L.; Morokuma, K.; Zakrzewski, V. G.; Voth, G. A.; Salvador, P.; Dannenberg, J. J.;

Dapprich, S.; Daniels, A. D.; Farkas, O.; Foresman, J. B.; Ortiz, J. V.; Cioslowski, J.; Fox, D. J. *Gaussian 09, Revision C.01*, Gaussian, Inc.: Wallingford CT, 2010.

117. Bearpark, M. J.; Ogliaro, F.; Vreven, T.; Boggio-Pasqua, M.; Frisch, M. J.; Larkin, S. M.; Robb, M., A., *In Computation in Modern Science and Engineering, Vol.2, Parts A and B.* American Institute of Physics: Melville, 2007.

118. Humbel, S.; Sieber, S.; Morokuma, K., The IMOMO method: Integration of different levels of molecular orbital approximations for geometry optimization of large systems: Test for n-butane conformation and SN2 reaction: RCl+Cl. *J. Chem. Phys., **1996**, 105,* 1959.

119. Maseras, F.; Morokuma, K., IMOMM: A new integrated ab initio + molecular mechanics geometry optimization scheme of equilibrium structures and transition states. *J. Comput. Chem., **1995**, 16,* 1170-1179.

120. Himo, F., Quantum chemical modeling of enzyme active sites and reaction mechanisms. *Theor. Chem. Acc., **2006**, 116,* 232-240.

121. Cornell, W. D.; Cieplak, P.; Bayly, C. I.; Gould, I. R.; Merz, K. M.; Ferguson, D. M.; Spellmeyer, D. C.; Fox, T.; Caldwell, J. W.; Kollman, P. A., A second generation force field for the simulation of proteins, nucleic acids, and organic molecules. *J. Am. Chem. Soc., **1995**, 117,* 5179-5197.

122. Hu, L. H.; Soderhjelm, P.; Ryde, U., On the Convergence of QM/MM Energies. *J. Chem. Theory Comput., **2011**, 7,* 761-777.

123. *CRC handbook of chemistry and physics : a ready-reference book of chemical and physical data*. 85th ed. (2004-2005) ed.; Boca Raton, FL: CRC Press, 2004.

124. Choi, S.; Connelly, S.; Reixach, N.; Wilson, I. A.; Kelly, J. W., Chemoselective small molecules that covalently modify one lysine in a non-enzyme protein in plasma. *Nat. Chem. Biol., **2010**, 6,* 133-139.

125. Cohen, M. S.; Zhang, C.; Shokat, K. M.; Taunton, J., Structural bioinformatics-based design of selective, irreversible kinase inhibitors. *Science., **2005**, 308,* 1318-21.

126. Schirmer, A.; Kennedy, J.; Murli, S.; Reid, R.; Santi, D. V., Targeted covalent inactivation of protein kinases by resorcylic acid lactone polyketides. *Proc. Natl. Acad. Sci. U.S.A., **2006**, 103,* 4234-9.

127. Wissner, A.; Mansour, T. S., The development of HKI-272 and related compounds for the treatment of cancer. *Arch. Pharm. (Weinheim). **2008**, 341,* 465-477.

128. Zhou, W.; Hur, W.; McDermott, U.; Dutt, A.; Xian, W.; Ficarro, S. B.; Zhang, J.; Sharma, S. V.; Brugge, J.; Meyerson, M.; Settleman, J.; Gray, N. S., A structure-guided approach to creating covalent FGFR inhibitors. *Chem. Biol., **2010**, 17,* 285-95.

129. Mulliner, D.; Wondrousch, D.; Schuurmann, G., Predicting Michael-acceptor reactivity and toxicity through quantum chemical transition-state calculations. *Org. Biomol. Chem., **2011**, 9,* 8400-8412.

130. Dinkova-Kostova, A. T.; Massiah, M. A.; Bozak, R. E.; Hicks, R. J.; Talalay, P., Potency of Michael reaction acceptors as inducers of enzymes that protect against carcinogenesis depends on their reactivity with sulfhydryl groups. *Proc. Natl. Acad. Sci. U.S.A., **2001**, 98,* 3404-9.

131. Benigni, R.; Bossa, C., Mechanisms of chemical carcinogenicity and mutagenicity: a review with implications for predictive toxicology. *Chem. Revs., **2011**, 111,* 2507-2536.

132. Berger, A., What are leukotrienes and how do they work in asthma? *Brit. Med. J., **1999**, 319,* 90.

133. Dahlen, S. E.; Bjork, J.; Hedqvist, P.; Arfors, K. E.; Hammarstrom, S.; Lindgren, J. A.; Samuelsson, B., Leukotrienes promote plasma leakage and leukocyte adhesion in postcapillary venules: in vivo effects with relevance to the acute inflammatory response. *Proc. Natl. Acad. Sci. USA., **1981**, 78,* 3887-91.

134. Henderson, W. R., Jr., The role of leukotrienes in inflammation. *Ann. Intern. Med., **1994**, 121,* 684-97.

135. Ogawa, Y.; Calhoun, W. J., The role of leukotrienes in airway inflammation. *J. Allergy Clin. Immunol., **2006**, 118,* 789-98; quiz 799-800.

136. Okada, T.; Suzuki, H.; Wada, K.; Kumagai, H.; Fukuyama, K., Crystal structures of gamma-glutamyltranspeptidase from Escherichia coli, a key enzyme in glutathione metabolism, and its reaction intermediate. *Proc. Natl. Acad. Sci. USA., **2006**, 103,* 6471-6.

137. Salmon, J. A.; Higgs, G. A., Prostaglandins and leukotrienes as inflammatory mediators. *Br. Med. Bull., **1987**, 43,* 285-96.

138. Shi, Z. Z.; Han, B.; Habib, G. M.; Matzuk, M. M.; Lieberman, M. W., Disruption of gamma-glutamyl leukotrienase results in disruption of leukotriene D(4) synthesis in vivo and attenuation of the acute inflammatory response. *Molecular and cellular biology, **2001**, 21,* 5389-95.

139. MacDonald, C. A.; Bushnell, E. A. C.; Gauld, J. W.; Boyd, R. J., The catalytic formation of leukotriene C4: a critical step in inflammatory processes. *Phys. Chem. Chem. Phys., **2014**, 16,* 16284-16289.

140. Donnelly, A. L.; Glass, M.; Minkwitz, M. C.; Casale, T. B., The leukotriene D4-receptor antagonist, ICI 204,219, relieves symptoms of acute seasonal allergic rhinitis. *Am. J. Respir. Crit. Care Med.,* ***1995****, 151,* 1734-9.

141. Knapp, H. R., Reduced allergen-induced nasal congestion and leukotriene synthesis with an orally active 5-lipoxygenase inhibitor. *New Engl. J. Med.,* ***1990****, 323,* 1745-1748.

142. Pacor, M. L.; Di Lorenzo, G.; Corrocher, R., Efficacy of leukotriene receptor antagonist in chronic urticaria. A double-blind, placebo-controlled comparison of treatment with montelukast and cetirizine in patients with chronic urticaria with intolerance to food additive and/or acetylsalicylic acid. *Clin. Exp. Allergy.,* ***2001****, 31,* 1607-14.

143. Saino, H.; Ukita, Y.; Ago, H.; Irikura, D.; Nisawa, A.; Ueno, G.; Yamamoto, M.; Kanaoka, Y.; Lam, B. K.; Austen, K. F.; Miyano, M., The catalytic architecture of leukotriene C4 synthase with two arginine residues. *J. Biol. Chem.,* ***2011****, 286,* 16392-16401.

144. Beller, T. C.; Maekawa, A.; Friend, D. S.; Austen, K. F.; Kanaoka, Y., Targeted gene disruption reveals the role of the cysteinyl leukotriene 2 receptor in increased vascular permeability and in bleomycin-induced pulmonary fibrosis in mice. *J. Biol. Chem.,* ***2004****, 279,* 46129-34.

145. Kim, D. C.; Hsu, F. I.; Barrett, N. A.; Friend, D. S.; Grenningloh, R.; Ho, I. C.; Al-Garawi, A.; Lora, J. M.; Lam, B. K.; Austen, K. F.; Kanaoka, Y., Cysteinyl leukotrienes regulate Th2 cell-dependent pulmonary inflammation. *J. Immunol.,* ***2006****, 176,* 4440-8.

146. Rinaldo-Matthis, A.; Wetterholm, A.; Martinez Molina, D.; Holm, J.; Niegowski, D.; Ohlson, E.; Nordlund, P.; Morgenstern, R.; Haeggström, J. Z., Arginine 104 is a key catalytic residue in leukotriene C4 synthase. *J. Biol. Chem., **2010**, 285,* 40771-6.

147. Lam, B. K.; Penrose, J. F.; Freeman, G. J.; Austen, K. F., Expression cloning of a cDNA for human leukotriene C4 synthase, an integral membrane protein conjugating reduced glutathione to leukotriene A4. *Proc. Natl. Acad. Sci. USA., **1994**, 91,* 7663-7667.

148. Pompella, A.; Visvikis, A.; Paolicchi, A.; De Tata, V.; Casini, A. F., The changing faces of glutathione, a cellular protagonist. *Biochem. Pharmacol., **2003**, 66,* 1499-503.

149. Haeggström, J. Z.; Funk, C. D., Lipoxygenase and leukotriene pathways: biochemistry, biology, and roles in disease. *Chem. Rev., **2011**, 111,* 5866-98.

150. Corbeil, C. R.; Williams, C. I.; Labute, P., Variability in docking success rates due to dataset preparation. *J. Comput. Aided Mol. Des., **2012**, 26,* 775-86.

151. Bushnell, E. A. C.; Erdtman, E.; Llano, J.; Eriksson, L. A.; Gauld, J. W., The first branching point in porphyrin biosynthesis: a systematic docking, molecular dynamics and quantum mechanical/molecular mechanical study of substrate binding and mechanism of uroporphyrinogen-III decarboxylase. *J. Comput. Chem., **2011**, 32,* 822-834.

152. Maekawa, A.; Kanaoka, Y.; Xing, W.; Austen, K. F., Functional recognition of a distinct receptor preferential for leukotriene E4 in mice lacking the cysteinyl leukotriene 1 and 2 receptors. *Proc. Natl. Acad. Sci., **2008**, 105,* 16695-16700.

153. Paruchuri, S.; Tashimo, H.; Feng, C.; Maekawa, A.; Xing, W.; Jiang, Y.; Kanaoka, Y.; Conley, P.; Boyce, J. A., Leukotriene E(4)–induced pulmonary inflammation is mediated by the P2Y(12) receptor. *J. Exp. Med., **2009**, 206,* 2543-2555.

154. Davies, D. R.; Mamat, B.; Magnusson, O. T.; Christensen, J.; Haraldsson, M. H.; Mishra, R.; Pease, B.; Hansen, E.; Singh, J.; Zembower, D.; Kim, H.; Kiselyov, A. S.; Burgin, A. B.; Gurney, M. E.; Stewart, L. J., Discovery of leukotriene A4 hydrolase inhibitors using metabolomics biased fragment crystallography. *J. Med. Chem., **2009**, 52,* 4694-715.

155. Thunnissen, M. M.; Nordlund, P.; Haeggstrom, J. Z., Crystal structure of human leukotriene A(4) hydrolase, a bifunctional enzyme in inflammation. *Nat. Struct. Biol., **2001**, 8,* 131-5.

156. Rudberg, P. C.; Tholander, F.; Thunnissen, M. M.; Samuelsson, B.; Haeggström, J. Z., Leukotriene A4 hydrolase: selective abrogation of leukotriene B4 formation by mutation of aspartic acid 375. *Proc. Natl. Acad. Sci. USA., **2002**, 99,* 4215-20.

157. Rudberg, P. C.; Tholander, F.; Andberg, M.; Thunnissen, M. M.; Haeggström, J. Z., Leukotriene A4 hydrolase: identification of a common carboxylate recognition site for the epoxide hydrolase and aminopeptidase substrates. *J. Biol. Chem., **2004**, 279,* 27376-82.

158. Rudberg, P. C.; Tholander, F.; Thunnissen, M. M.; Haeggström, J. Z., Leukotriene A4 hydrolase/aminopeptidase. Glutamate 271 is a catalytic residue with specific roles in two distinct enzyme mechanisms. *J. Biol. Chem., **2002**, 277,* 1398-404.

159. Becke, A. D., A new mixing of Hartree-Fock and local density-functional theories. *J. Chem. Phys., **1993**, 98,* 1372-1377.

160. Lee, C.; Yang, W.; Parr, R. G., Development of the Colle-Salvetti correlation-energy formula into a functional of the electron density. *Phys. Rev. B., **1988**, 37,* 785-789.

161. Stephens, P. J.; Devlin, F. J.; Chabalowski, C. F.; Frisch, M. J., Ab-initio calculation of vibrational absorption and circular-dichroism spectra using density-functional force-fields. *J. Phys. Chem., **1994**, 98,* 11623-11627.

162. Vosko, S. H.; Wilk, L.; Nusair, M., Accurate spin-depdent electron liquid correlation energies for local spin-density calculations - a critical analysis. *Can. J. Phys., **1980**, 58,* 1200-1211.

163. Huang, W.; Jia, J.; Cummings, J.; Nelson, M.; Schneider, G.; Lindqvist, Y., Crystal structure of nitrile hydratase reveals a novel iron centre in a novel fold. *Structure., **1997**, 5,* 691-699.

164. Mascharak, P. K., Structural and functional models of nitrile hydratase. *Coord. Chem. Rev., **2002**, 225,* 201-214.

165. Brady, D.; Beeton, A.; Zeevaart, J.; Kgaje, C.; van Rantwijk, F.; Sheldon, R. A., Characterisation of nitrilase and nitrile hydratase biocatalytic systems. *Appl. Microbiol. Biotechnol., **2004**, 64,* 76-85.

166. Prasad, S.; Bhalla, T. C., Nitrile hydratases (NHases): At the interface of academia and industry. *Biotechnol. Adv., **2010**, 28,* 725-741.

167. Hopmann, K. H., Full reaction mechanism of nitrile hydratase: a cyclic intermediate and an unexpected disulfide switch. *Inorg. Chem., **2014**, 53,* 2760-2.

168. Hopmann, K. H.; Himo, F., On the role of tyrosine as catalytic base in nitrile hydratase. *Eur. J. Inorg. Chem., **2008**,* 3452-3459.

169. Miyanaga, A.; Fushinobu, S.; Ito, K.; Wakagi, T., Crystal structure of cobalt-containing nitrile hydratase. *Biochem. Biophys. Res. Commun., **2001**, 288,* 1169-1174.

170. Vreven, T.; Byun, K. S.; Komáromi, I.; Dapprich, S.; Montgomery, J. A.; Morokuma, K.; Frisch, M. J., Combining Quantum Mechanics Methods with Molecular Mechanics Methods in ONIOM. *J. Chem. Theory Comput., **2006**, 2,* 815-826.

171. Schmid, F. X.; Mayr, L. M.; Mucke, M.; Schonbrunner, E. R., Prolyl isomerases: role in protein folding. *Adv. Protein Chem., **1993**, 44,* 25-66.

172. Martin, R. B., Free energies and equilibria of peptide bond hydrolysis and formation. *Biopolymers., **1998**, 45,* 351-353.

APPENDIX: COPYRIGHT PERMISSIONS

The following is the copyright permission from the publishers of the journal articles included in this thesis.

- Chapter 3: Molecular docking study of macrocycles as Fk506-binding protein inhibitors by Corey A. MacDonald and Russell J. Boyd. *J. Mol. Graphics Modell.,* **2015**, 59, 117-122; **DOI:**10.1016/j.jmgm.2015.04.009 – Reproduced by permission of Elsevier and the Journal of Molecular Graphics and Modelling.

- Chapter 4: Computational insights into the suicide inhibition of *Plasmodium falciparum* fk506-binding protein 35 by Corey A. MacDonald and Russell J. Boyd. *Bioorg. Med. Chem. Lett.,* **2015**. Accepted. – Reproduced by permission of Elsevier and Bioorganic Medicinal Chemistry Letters.

- Chapter 5: The catalytic formation of leukotriene C_4: a critical step in inflammatory processes by Corey A. MacDonald, Eric A. C. Bushnell, James W. Gauld and Russell J. Boyd, *Phys. Chem. Chem. Phys.*, **2014**, 16, 16284-16289; **DOI:** 10.1039/C4CP01984A - Reproduced by permission of the PCCP Owner Societies.

- Chapter 7: Competing nitrile hydratase catalytic mechanisms: is cysteine-sulfenic acid acting as a nucleophile? By Corey A. MacDonald and Russell J. Boyd. *Comp. Theor. Chem.* **2015**, 1070, 48-54; **DOI:** 10.1016/j.comptc.2015.07.010 – Reproduced by permission of Elsevier and Computational and Theoretical Chemistry.

ELSEVIER LICENSE

TERMS AND CONDITIONS

Aug 19, 2015

This is a License Agreement between Corey A MacDonald ("You") and Elsevier ("Elsevier") provided by Copyright Clearance Center ("CCC"). The license consists of your order details, the terms and conditions provided by Elsevier, and the payment terms and conditions.

All payments must be made in full to CCC. For payment instructions, please see information listed at the bottom of this form.

Supplier	Elsevier Limited The Boulevard,Langford Lane Kidlington,Oxford,OX5 1GB,UK
Registered Company Number	1982084
Customer name	Corey A MacDonald
Customer address	Dalhousie University Halifax, NS B3S 0H2
License number	3692580859665
License date	Aug 19, 2015
Licensed content publisher	Elsevier
Licensed content publication	Journal of Molecular Graphics and Modelling

Licensed content title	Molecular docking study of macrocycles as Fk506-binding protein inhibitors
Licensed content author	None
Licensed content date	June 2015
Licensed content volume number	59
Licensed content issue number	n/a
Number of pages	6
Start Page	117
End Page	122
Type of Use	reuse in a thesis/dissertation
Portion	full article
Format	both print and electronic
Are you the author of this Elsevier article?	Yes
Will you be translating?	No
Title of your thesis/dissertation	Computational Investigation into Catalytic Mechanisms of Disease-Causing Enzymes and Biocatalysts
Expected completion date	Aug 2015
Estimated size (number of pages)	172
Elsevier VAT number	GB 494 6272 12

Permissions price	0.00 USD
VAT/Local Sales Tax	0.00 USD / 0.00 GBP
Total	0.00 USD

Terms and Conditions

INTRODUCTION

1. The publisher for this copyrighted material is Elsevier. By clicking "accept" in connection with completing this licensing transaction, you agree that the following terms and conditions apply to this transaction (along with the Billing and Payment terms and conditions established by Copyright Clearance Center, Inc. ("CCC"), at the time that you opened your Rightslink account and that are available at any time at http://myaccount.copyright.com).

GENERAL TERMS

2. Elsevier hereby grants you permission to reproduce the aforementioned material subject to the terms and conditions indicated.

3. Acknowledgement: If any part of the material to be used (for example, figures) has appeared in our publication with credit or acknowledgement to another source, permission must also be sought from that source. If such permission is not obtained then that material may not be included in your publication/copies. Suitable acknowledgement to the source must be made, either as a footnote or in a reference list at the end of your publication, as follows:

"Reprinted from Publication title, Vol /edition number, Author(s), Title of article / title of chapter, Pages No., Copyright (Year), with permission from Elsevier [OR APPLICABLE SOCIETY COPYRIGHT OWNER]." Also Lancet special credit - "Reprinted from The Lancet, Vol. number, Author(s), Title of article, Pages No., Copyright (Year), with permission from Elsevier."

4. Reproduction of this material is confined to the purpose and/or media for which permission is hereby

given.

5. Altering/Modifying Material: Not Permitted. However figures and illustrations may be altered/adapted minimally to serve your work. Any other abbreviations, additions, deletions and/or any other alterations shall be made only with prior written authorization of Elsevier Ltd. (Please contact Elsevier at permissions@elsevier.com)

6. If the permission fee for the requested use of our material is waived in this instance, please be advised that your future requests for Elsevier materials may attract a fee.

7. Reservation of Rights: Publisher reserves all rights not specifically granted in the combination of (i) the license details provided by you and accepted in the course of this licensing transaction, (ii) these terms and conditions and (iii) CCC's Billing and Payment terms and conditions.

8. License Contingent Upon Payment: While you may exercise the rights licensed immediately upon issuance of the license at the end of the licensing process for the transaction, provided that you have disclosed complete and accurate details of your proposed use, no license is finally effective unless and until full payment is received from you (either by publisher or by CCC) as provided in CCC's Billing and Payment terms and conditions. If full payment is not received on a timely basis, then any license preliminarily granted shall be deemed automatically revoked and shall be void as if never granted. Further, in the event that you breach any of these terms and conditions or any of CCC's Billing and Payment terms and conditions, the license is automatically revoked and shall be void as if never granted. Use of materials as described in a revoked license, as well as any use of the materials beyond the scope of an unrevoked license, may constitute copyright infringement and publisher reserves the right to take any and all action to protect its copyright in the materials.

9. Warranties: Publisher makes no representations or warranties with respect to the licensed material.

10. Indemnity: You hereby indemnify and agree to hold harmless publisher and CCC, and their respective officers, directors, employees and agents, from and against any and all claims arising out of

your use of the licensed material other than as specifically authorized pursuant to this license.

11. No Transfer of License: This license is personal to you and may not be sublicensed, assigned, or transferred by you to any other person without publisher's written permission.

12. No Amendment Except in Writing: This license may not be amended except in a writing signed by both parties (or, in the case of publisher, by CCC on publisher's behalf).

13. Objection to Contrary Terms: Publisher hereby objects to any terms contained in any purchase order, acknowledgment, check endorsement or other writing prepared by you, which terms are inconsistent with these terms and conditions or CCC's Billing and Payment terms and conditions. These terms and conditions, together with CCC's Billing and Payment terms and conditions (which are incorporated herein), comprise the entire agreement between you and publisher (and CCC) concerning this licensing transaction. In the event of any conflict between your obligations established by these terms and conditions and those established by CCC's Billing and Payment terms and conditions, these terms and conditions shall control.

14. Revocation: Elsevier or Copyright Clearance Center may deny the permissions described in this License at their sole discretion, for any reason or no reason, with a full refund payable to you. Notice of such denial will be made using the contact information provided by you. Failure to receive such notice will not alter or invalidate the denial. In no event will Elsevier or Copyright Clearance Center be responsible or liable for any costs, expenses or damage incurred by you as a result of a denial of your permission request, other than a refund of the amount(s) paid by you to Elsevier and/or Copyright Clearance Center for denied permissions.

LIMITED LICENSE

The following terms and conditions apply only to specific license types:

15. Translation: This permission is granted for non-exclusive world English rights only unless your

license was granted for translation rights. If you licensed translation rights you may only translate this content into the languages you requested. A professional translator must perform all translations and reproduce the content word for word preserving the integrity of the article. If this license is to re-use 1 or 2 figures then permission is granted for non-exclusive world rights in all languages.

16. Posting licensed content on any Website: The following terms and conditions apply as follows: Licensing material from an Elsevier journal: All content posted to the web site must maintain the copyright information line on the bottom of each image; A hyper-text must be included to the Homepage of the journal from which you are licensing at http://www.sciencedirect.com/science/journal/xxxxx or the Elsevier homepage for books at http://www.elsevier.com; Central Storage: This license does not include permission for a scanned version of the material to be stored in a central repository such as that provided by Heron/XanEdu.

Licensing material from an Elsevier book: A hyper-text link must be included to the Elsevier homepage at http://www.elsevier.com . All content posted to the web site must maintain the copyright information line on the bottom of each image.

Posting licensed content on Electronic reserve: In addition to the above the following clauses are applicable: The web site must be password-protected and made available only to bona fide students registered on a relevant course. This permission is granted for 1 year only. You may obtain a new license for future website posting.

17. For journal authors: the following clauses are applicable in addition to the above:

Preprints:

A preprint is an author's own write-up of research results and analysis, it has not been peer-reviewed, nor has it had any other value added to it by a publisher (such as formatting, copyright, technical

enhancement etc.).

Authors can share their preprints anywhere at any time. Preprints should not be added to or enhanced in any way in order to appear more like, or to substitute for, the final versions of articles however authors can update their preprints on arXiv or RePEc with their Accepted Author Manuscript (see below).

If accepted for publication, we encourage authors to link from the preprint to their formal publication via its DOI. Millions of researchers have access to the formal publications on ScienceDirect, and so links will help users to find, access, cite and use the best available version. Please note that Cell Press, The Lancet and some society-owned have different preprint policies. Information on these policies is available on the journal homepage.

Accepted Author Manuscripts: An accepted author manuscript is the manuscript of an article that has been accepted for publication and which typically includes author-incorporated changes suggested during submission, peer review and editor-author communications.

Authors can share their accepted author manuscript:

- – immediately
    - via their non-commercial person homepage or blog
    - by updating a preprint in arXiv or RePEc with the accepted manuscript
    - via their research institute or institutional repository for internal institutional uses or as part of an invitation-only research collaboration work-group
    - directly by providing copies to their students or to research collaborators for their personal use
    - for private scholarly sharing as part of an invitation-only work group on commercial sites with which Elsevier has an agreement
- – after the embargo period
    - via non-commercial hosting platforms such as their institutional repository
    - via commercial sites with which Elsevier has an agreement

In all cases accepted manuscripts should:

- – link to the formal publication via its DOI
- – bear a CC-BY-NC-ND license - this is easy to do
- – if aggregated with other manuscripts, for example in a repository or other site, be shared in alignment with our hosting policy not be added to or enhanced in any way to appear more like, or to substitute for, the published journal article.

Published journal article (JPA): A published journal article (PJA) is the definitive final record of published research that appears or will appear in the journal and embodies all value-adding publishing activities including peer review co-ordination, copy-editing, formatting, (if relevant) pagination and online enrichment.

Policies for sharing publishing journal articles differ for subscription and gold open access articles:

Subscription Articles: If you are an author, please share a link to your article rather than the full-text. Millions of researchers have access to the formal publications on ScienceDirect, and so links will help your users to find, access, cite, and use the best available version.

Theses and dissertations which contain embedded PJAs as part of the formal submission can be posted publicly by the awarding institution with DOI links back to the formal publications on ScienceDirect.

If you are affiliated with a library that subscribes to ScienceDirect you have additional private sharing rights for others' research accessed under that agreement. This includes use for classroom teaching and internal training at the institution (including use in course packs and courseware programs), and inclusion of the article for grant funding purposes.

Gold Open Access Articles: May be shared according to the author-selected end-user license and should contain a CrossMark logo, the end user license, and a DOI link to the formal publication on ScienceDirect.

Please refer to Elsevier's posting policy for further information.

18. For book authors the following clauses are applicable in addition to the above: Authors are permitted to place a brief summary of their work online only. You are not allowed to download and post the published electronic version of your chapter, nor may you scan the printed edition to create an electronic version. Posting to a repository: Authors are permitted to post a summary of their chapter only in their institution's repository.

19. Thesis/Dissertation: If your license is for use in a thesis/dissertation your thesis may be submitted to your institution in either print or electronic form. Should your thesis be published commercially, please reapply for permission. These requirements include permission for the Library and Archives of Canada to supply single copies, on demand, of the complete thesis and include permission for Proquest/UMI to supply single copies, on demand, of the complete thesis. Should your thesis be published commercially, please reapply for permission. Theses and dissertations which contain embedded PJAs as part of the formal submission can be posted publicly by the awarding institution with DOI links back to the formal publications on ScienceDirect.

Elsevier Open Access Terms and Conditions

You can publish open access with Elsevier in hundreds of open access journals or in nearly 2000 established subscription journals that support open access publishing. Permitted third party re-use of these open access articles is defined by the author's choice of Creative Commons user license. See our open access license policy for more information.

Terms & Conditions applicable to all Open Access articles published with Elsevier:

Any reuse of the article must not represent the author as endorsing the adaptation of the article nor should the article be modified in such a way as to damage the author's honour or reputation. If any changes have been made, such changes must be clearly indicated.

The author(s) must be appropriately credited and we ask that you include the end user license and a DOI link to the formal publication on ScienceDirect.

If any part of the material to be used (for example, figures) has appeared in our publication with credit or acknowledgement to another source it is the responsibility of the user to ensure their reuse complies with the terms and conditions determined by the rights holder.

Additional Terms & Conditions applicable to each Creative Commons user license:

CC BY: The CC-BY license allows users to copy, to create extracts, abstracts and new works from the Article, to alter and revise the Article and to make commercial use of the Article (including reuse and/or resale of the Article by commercial entities), provided the user gives appropriate credit (with a link to the formal publication through the relevant DOI), provides a link to the license, indicates if changes were made and the licensor is not represented as endorsing the use made of the work. The full details of the license are available at http://creativecommons.org/licenses/by/4.0.

CC BY NC SA: The CC BY-NC-SA license allows users to copy, to create extracts, abstracts and new works from the Article, to alter and revise the Article, provided this is not done for commercial purposes, and that the user gives appropriate credit (with a link to the formal publication through the relevant DOI), provides a link to the license, indicates if changes were made and the licensor is not represented as endorsing the use made of the work. Further, any new works must be made available on the same conditions. The full details of the license are available at http://creativecommons.org/licenses/by-nc-sa/4.0.

CC BY NC ND: The CC BY-NC-ND license allows users to copy and distribute the Article, provided this is not done for commercial purposes and further does not permit distribution of the Article if it is changed or edited in any way, and provided the user gives appropriate credit (with a link to the formal publication through the relevant DOI), provides a link to the license, and that the licensor is not represented as endorsing the use made of the work. The full details of the license are available at http://creativecommons.org/licenses/by-nc-nd/4.0. Any commercial reuse of Open Access articles published with a CC BY NC SA or CC BY NC ND license requires permission from Elsevier and will be subject to a fee.

Commercial reuse includes:

- – Associating advertising with the full text of the Article
- – Charging fees for document delivery or access
- – Article aggregation

- – Systematic distribution via e-mail lists or share buttons

Posting or linking by commercial companies for use by customers of those companies.

20. Other Conditions:

v1.7

Questions? customercare@copyright.com or +1-855-239-3415 (toll free in the US) or +1-978-646-2777.

ELSEVIER LICENSE

TERMS AND CONDITIONS

Aug 19, 2015

This is a License Agreement between Corey A MacDonald ("You") and Elsevier ("Elsevier") provided by Copyright Clearance Center ("CCC"). The license consists of your order details, the terms and conditions provided by Elsevier, and the payment terms and conditions.

All payments must be made in full to CCC. For payment instructions, please see information listed at the bottom of this form.

Supplier	Elsevier Limited The Boulevard,Langford Lane Kidlington,Oxford,OX5 1GB,UK
Registered Company Number	1982084
Customer name	Corey A MacDonald
Customer address	Dalhousie University Halifax, NS B3S 0H2
License number	3692581054804
License date	Aug 19, 2015
Licensed content publisher	Elsevier
Licensed content publication	Bioorganic & Medicinal Chemistry Letters

Licensed content title	Computational insights into the suicide inhibition of Plasmodium falciparum Fk506-binding protein 35
Licensed content author	Corey A. MacDonald,Russell J. Boyd
Licensed content date	15 August 2015
Licensed content volume number	25
Licensed content issue number	16
Number of pages	5
Start Page	3221
End Page	3225
Type of Use	reuse in a thesis/dissertation
Intended publisher of new work	other
Portion	full article
Format	both print and electronic
Are you the author of this Elsevier article?	Yes
Will you be translating?	No
Title of your thesis/dissertation	Computational Investigation into Catalytic Mechanisms of Disease-Causing Enzymes and Biocatalysts
Expected completion date	Aug 2015
Estimated size (number of pages)	172

Elsevier VAT number	GB 494 6272 12
Permissions price	0.00 USD
VAT/Local Sales Tax	0.00 USD / 0.00 GBP
Total	0.00 USD

Terms and Conditions

INTRODUCTION

1. The publisher for this copyrighted material is Elsevier. By clicking "accept" in connection with completing this licensing transaction, you agree that the following terms and conditions apply to this transaction (along with the Billing and Payment terms and conditions established by Copyright Clearance Center, Inc. ("CCC"), at the time that you opened your Rightslink account and that are available at any time at http://myaccount.copyright.com).

GENERAL TERMS

2. Elsevier hereby grants you permission to reproduce the aforementioned material subject to the terms and conditions indicated.

3. Acknowledgement: If any part of the material to be used (for example, figures) has appeared in our publication with credit or acknowledgement to another source, permission must also be sought from that source. If such permission is not obtained then that material may not be included in your publication/copies. Suitable acknowledgement to the source must be made, either as a footnote or in a reference list at the end of your publication, as follows:

"Reprinted from Publication title, Vol /edition number, Author(s), Title of article / title of chapter, Pages No., Copyright (Year), with permission from Elsevier [OR APPLICABLE SOCIETY COPYRIGHT OWNER]." Also Lancet special credit - "Reprinted from The Lancet, Vol. number, Author(s), Title of article, Pages No., Copyright (Year), with permission from Elsevier."

4. Reproduction of this material is confined to the purpose and/or media for which permission is hereby given.

5. Altering/Modifying Material: Not Permitted. However figures and illustrations may be altered/adapted minimally to serve your work. Any other abbreviations, additions, deletions and/or any other alterations shall be made only with prior written authorization of Elsevier Ltd. (Please contact Elsevier at permissions@elsevier.com)

6. If the permission fee for the requested use of our material is waived in this instance, please be advised that your future requests for Elsevier materials may attract a fee.

7. Reservation of Rights: Publisher reserves all rights not specifically granted in the combination of (i) the license details provided by you and accepted in the course of this licensing transaction, (ii) these terms and conditions and (iii) CCC's Billing and Payment terms and conditions.

8. License Contingent Upon Payment: While you may exercise the rights licensed immediately upon issuance of the license at the end of the licensing process for the transaction, provided that you have disclosed complete and accurate details of your proposed use, no license is finally effective unless and until full payment is received from you (either by publisher or by CCC) as provided in CCC's Billing and Payment terms and conditions. If full payment is not received on a timely basis, then any license preliminarily granted shall be deemed automatically revoked and shall be void as if never granted. Further, in the event that you breach any of these terms and conditions or any of CCC's Billing and Payment terms and conditions, the license is automatically revoked and shall be void as if never granted. Use of materials as described in a revoked license, as well as any use of the materials beyond the scope of an unrevoked license, may constitute copyright infringement and publisher reserves the right to take any and all action to protect its copyright in the materials.

9. Warranties: Publisher makes no representations or warranties with respect to the licensed material.

10. Indemnity: You hereby indemnify and agree to hold harmless publisher and CCC, and their respective

officers, directors, employees and agents, from and against any and all claims arising out of your use of the licensed material other than as specifically authorized pursuant to this license.

11. No Transfer of License: This license is personal to you and may not be sublicensed, assigned, or transferred by you to any other person without publisher's written permission.

12. No Amendment Except in Writing: This license may not be amended except in a writing signed by both parties (or, in the case of publisher, by CCC on publisher's behalf).

13. Objection to Contrary Terms: Publisher hereby objects to any terms contained in any purchase order, acknowledgment, check endorsement or other writing prepared by you, which terms are inconsistent with these terms and conditions or CCC's Billing and Payment terms and conditions. These terms and conditions, together with CCC's Billing and Payment terms and conditions (which are incorporated herein), comprise the entire agreement between you and publisher (and CCC) concerning this licensing transaction. In the event of any conflict between your obligations established by these terms and conditions and those established by CCC's Billing and Payment terms and conditions, these terms and conditions shall control.

14. Revocation: Elsevier or Copyright Clearance Center may deny the permissions described in this License at their sole discretion, for any reason or no reason, with a full refund payable to you. Notice of such denial will be made using the contact information provided by you. Failure to receive such notice will not alter or invalidate the denial. In no event will Elsevier or Copyright Clearance Center be responsible or liable for any costs, expenses or damage incurred by you as a result of a denial of your permission request, other than a refund of the amount(s) paid by you to Elsevier and/or Copyright Clearance Center for denied permissions.

LIMITED LICENSE

The following terms and conditions apply only to specific license types:

15. Translation: This permission is granted for non-exclusive world English rights only unless your license was granted for translation rights. If you licensed translation rights you may only translate this content into the languages you requested. A professional translator must perform all translations and reproduce the content word for word preserving the integrity of the article. If this license is to re-use 1 or 2 figures then permission is granted for non-exclusive world rights in all languages.

16. Posting licensed content on any Website: The following terms and conditions apply as follows: Licensing material from an Elsevier journal: All content posted to the web site must maintain the copyright information line on the bottom of each image; A hyper-text must be included to the Homepage of the journal from which you are licensing at http://www.sciencedirect.com/science/journal/xxxxx or the Elsevier homepage for books at http://www.elsevier.com; Central Storage: This license does not include permission for a scanned version of the material to be stored in a central repository such as that provided by Heron/XanEdu.

Licensing material from an Elsevier book: A hyper-text link must be included to the Elsevier homepage at http://www.elsevier.com . All content posted to the web site must maintain the copyright information line on the bottom of each image.

Posting licensed content on Electronic reserve: In addition to the above the following clauses are applicable: The web site must be password-protected and made available only to bona fide students registered on a relevant course. This permission is granted for 1 year only. You may obtain a new license for future website posting.

17. For journal authors: the following clauses are applicable in addition to the above:

Preprints:

A preprint is an author's own write-up of research results and analysis, it has not been peer-reviewed, nor has it had any other value added to it by a publisher (such as formatting, copyright, technical

enhancement etc.).

Authors can share their preprints anywhere at any time. Preprints should not be added to or enhanced in any way in order to appear more like, or to substitute for, the final versions of articles however authors can update their preprints on arXiv or RePEc with their Accepted Author Manuscript (see below).

If accepted for publication, we encourage authors to link from the preprint to their formal publication via its DOI. Millions of researchers have access to the formal publications on ScienceDirect, and so links will help users to find, access, cite and use the best available version. Please note that Cell Press, The Lancet and some society-owned have different preprint policies. Information on these policies is available on the journal homepage.

Accepted Author Manuscripts: An accepted author manuscript is the manuscript of an article that has been accepted for publication and which typically includes author-incorporated changes suggested during submission, peer review and editor-author communications.

Authors can share their accepted author manuscript:

- – immediately
    - via their non-commercial person homepage or blog
    - by updating a preprint in arXiv or RePEc with the accepted manuscript
    - via their research institute or institutional repository for internal institutional uses or as part of an invitation-only research collaboration work-group
    - directly by providing copies to their students or to research collaborators for their personal use
    - for private scholarly sharing as part of an invitation-only work group on commercial sites with which Elsevier has an agreement
- – after the embargo period
    - via non-commercial hosting platforms such as their institutional repository
    - via commercial sites with which Elsevier has an agreement

In all cases accepted manuscripts should:

- – link to the formal publication via its DOI
- – bear a CC-BY-NC-ND license - this is easy to do
- – if aggregated with other manuscripts, for example in a repository or other site, be shared in alignment with our hosting policy not be added to or enhanced in any way to appear more like, or to substitute for, the published journal article.

Published journal article (JPA): A published journal article (PJA) is the definitive final record of published research that appears or will appear in the journal and embodies all value-adding publishing activities including peer review co-ordination, copy-editing, formatting, (if relevant) pagination and online enrichment.

Policies for sharing publishing journal articles differ for subscription and gold open access articles:

Subscription Articles: If you are an author, please share a link to your article rather than the full-text. Millions of researchers have access to the formal publications on ScienceDirect, and so links will help your users to find, access, cite, and use the best available version.

Theses and dissertations which contain embedded PJAs as part of the formal submission can be posted publicly by the awarding institution with DOI links back to the formal publications on ScienceDirect.

If you are affiliated with a library that subscribes to ScienceDirect you have additional private sharing rights for others' research accessed under that agreement. This includes use for classroom teaching and internal training at the institution (including use in course packs and courseware programs), and inclusion of the article for grant funding purposes.

Gold Open Access Articles: May be shared according to the author-selected end-user license and should contain a CrossMark logo, the end user license, and a DOI link to the formal publication on ScienceDirect.

Please refer to Elsevier's posting policy for further information.

18. For book authors the following clauses are applicable in addition to the above: Authors are permitted to place a brief summary of their work online only. You are not allowed to download and post the published electronic version of your chapter, nor may you scan the printed edition to create an electronic version. Posting to a repository: Authors are permitted to post a summary of their chapter only in their institution's repository.

19. Thesis/Dissertation: If your license is for use in a thesis/dissertation your thesis may be submitted to your institution in either print or electronic form. Should your thesis be published commercially, please reapply for permission. These requirements include permission for the Library and Archives of Canada to supply single copies, on demand, of the complete thesis and include permission for Proquest/UMI to supply single copies, on demand, of the complete thesis. Should your thesis be published commercially, please reapply for permission. Theses and dissertations which contain embedded PJAs as part of the formal submission can be posted publicly by the awarding institution with DOI links back to the formal publications on ScienceDirect.

Elsevier Open Access Terms and Conditions

You can publish open access with Elsevier in hundreds of open access journals or in nearly 2000 established subscription journals that support open access publishing. Permitted third party re-use of these open access articles is defined by the author's choice of Creative Commons user license. See our open access license policy for more information.

Terms & Conditions applicable to all Open Access articles published with Elsevier:

Any reuse of the article must not represent the author as endorsing the adaptation of the article nor should the article be modified in such a way as to damage the author's honour or reputation. If any changes have been made, such changes must be clearly indicated.

The author(s) must be appropriately credited and we ask that you include the end user license and a DOI link to the formal publication on ScienceDirect.

If any part of the material to be used (for example, figures) has appeared in our publication with credit or acknowledgement to another source it is the responsibility of the user to ensure their reuse complies with the terms and conditions determined by the rights holder.

Additional Terms & Conditions applicable to each Creative Commons user license:

CC BY: The CC-BY license allows users to copy, to create extracts, abstracts and new works from the Article, to alter and revise the Article and to make commercial use of the Article (including reuse and/or resale of the Article by commercial entities), provided the user gives appropriate credit (with a link to the formal publication through the relevant DOI), provides a link to the license, indicates if changes were made and the licensor is not represented as endorsing the use made of the work. The full details of the license are available at http://creativecommons.org/licenses/by/4.0.

CC BY NC SA: The CC BY-NC-SA license allows users to copy, to create extracts, abstracts and new works from the Article, to alter and revise the Article, provided this is not done for commercial purposes, and that the user gives appropriate credit (with a link to the formal publication through the relevant DOI), provides a link to the license, indicates if changes were made and the licensor is not represented as endorsing the use made of the work. Further, any new works must be made available on the same conditions. The full details of the license are available at http://creativecommons.org/licenses/by-nc-sa/4.0.

CC BY NC ND: The CC BY-NC-ND license allows users to copy and distribute the Article, provided this is not done for commercial purposes and further does not permit distribution of the Article if it is changed or edited in any way, and provided the user gives appropriate credit (with a link to the formal publication through the relevant DOI), provides a link to the license, and that the licensor is not represented as endorsing the use made of the work. The full details of the license are available at http://creativecommons.org/licenses/by-nc-nd/4.0. Any commercial reuse of Open Access articles published with a CC BY NC SA or CC BY NC ND license requires permission from Elsevier and will be subject to a fee.

Commercial reuse includes:

- – Associating advertising with the full text of the Article
- – Charging fees for document delivery or access
- – Article aggregation

- – Systematic distribution via e-mail lists or share buttons

Posting or linking by commercial companies for use by customers of those companies.

20. Other Conditions:

v1.7

Questions? customercare@copyright.com or +1-855-239-3415 (toll free in the US) or +1-978-646-2777.

The catalytic formation of leukotriene c4: a critical step in inflammatory processes

C. A. MacDonald, E. A. C. Bushnell, J. W. Gauld and R. J. Boyd, *Phys. Chem. Chem. Phys.*, 2014, **16**, 16284
DOI: 10.1039/C4CP01984A

If you are not the author of this article and you wish to reproduce material from it in a third party non-RSC publication you must formally request permission using RightsLink. Go to our Instructions for using RightsLink page for details.

Authors contributing to RSC publications (journal articles, books or book chapters) do not need to formally request permission to reproduce material contained in this article provided that the correct acknowledgement is given with the reproduced material.

Reproduced material should be attributed as follows:

- For reproduction of material from NJC:
  Reproduced from Ref. XX with permission from the Centre National de la Recherche Scientifique (CNRS) and The Royal Society of Chemistry.
- For reproduction of material from PCCP:
  Reproduced from Ref. XX with permission from the PCCP Owner Societies.
- For reproduction of material from PPS:
  Reproduced from Ref. XX with permission from the European Society for Photobiology, the European Photochemistry Association, and The Royal Society of Chemistry.

ELSEVIER LICENSE

TERMS AND CONDITIONS

Aug 19, 2015

This is a License Agreement between Corey A MacDonald ("You") and Elsevier ("Elsevier") provided by Copyright Clearance Center ("CCC"). The license consists of your order details, the terms and conditions provided by Elsevier, and the payment terms and conditions.

All payments must be made in full to CCC. For payment instructions, please see information listed at the bottom of this form.

Supplier	Elsevier Limited The Boulevard,Langford Lane Kidlington,Oxford,OX5 1GB,UK
Registered Company Number	1982084
Customer name	Corey A MacDonald
Customer address	Dalhousie University Halifax, NS B3S 0H2
License number	3692581156739
License date	Aug 19, 2015
Licensed content publisher	Elsevier
Licensed content publication	Computational and Theoretical Chemistry

Licensed content title	Competing nitrile hydratase catalytic mechanisms: Is cysteine-sulfenic acid acting as a nucleophile?
Licensed content author	Corey A. MacDonald,Russell J. Boyd
Licensed content date	15 October 2015
Licensed content volume number	1070
Licensed content issue number	n/a
Number of pages	7
Start Page	48
End Page	54
Type of Use	reuse in a thesis/dissertation
Intended publisher of new work	other
Portion	full article
Format	both print and electronic
Are you the author of this Elsevier article?	Yes
Will you be translating?	No
Title of your thesis/dissertation	Computational Investigation into Catalytic Mechanisms of Disease-Causing Enzymes and Biocatalysts
Expected completion date	Aug 2015

Estimated size (number of pages)	172
Elsevier VAT number	GB 494 6272 12
Permissions price	0.00 USD
VAT/Local Sales Tax	0.00 USD / 0.00 GBP
Total	0.00 USD

Terms and Conditions

INTRODUCTION

1. The publisher for this copyrighted material is Elsevier. By clicking "accept" in connection with completing this licensing transaction, you agree that the following terms and conditions apply to this transaction (along with the Billing and Payment terms and conditions established by Copyright Clearance Center, Inc. ("CCC"), at the time that you opened your Rightslink account and that are available at any time at http://myaccount.copyright.com).

GENERAL TERMS

2. Elsevier hereby grants you permission to reproduce the aforementioned material subject to the terms and conditions indicated.

3. Acknowledgement: If any part of the material to be used (for example, figures) has appeared in our publication with credit or acknowledgement to another source, permission must also be sought from that source. If such permission is not obtained then that material may not be included in your publication/copies. Suitable acknowledgement to the source must be made, either as a footnote or in a reference list at the end of your publication, as follows:

"Reprinted from Publication title, Vol /edition number, Author(s), Title of article / title of chapter, Pages No., Copyright (Year), with permission from Elsevier [OR APPLICABLE SOCIETY COPYRIGHT

OWNER]." Also Lancet special credit - "Reprinted from The Lancet, Vol. number, Author(s), Title of article, Pages No., Copyright (Year), with permission from Elsevier."

4. Reproduction of this material is confined to the purpose and/or media for which permission is hereby given.

5. Altering/Modifying Material: Not Permitted. However figures and illustrations may be altered/adapted minimally to serve your work. Any other abbreviations, additions, deletions and/or any other alterations shall be made only with prior written authorization of Elsevier Ltd. (Please contact Elsevier at permissions@elsevier.com)

6. If the permission fee for the requested use of our material is waived in this instance, please be advised that your future requests for Elsevier materials may attract a fee.

7. Reservation of Rights: Publisher reserves all rights not specifically granted in the combination of (i) the license details provided by you and accepted in the course of this licensing transaction, (ii) these terms and conditions and (iii) CCC's Billing and Payment terms and conditions.

8. License Contingent Upon Payment: While you may exercise the rights licensed immediately upon issuance of the license at the end of the licensing process for the transaction, provided that you have disclosed complete and accurate details of your proposed use, no license is finally effective unless and until full payment is received from you (either by publisher or by CCC) as provided in CCC's Billing and Payment terms and conditions. If full payment is not received on a timely basis, then any license preliminarily granted shall be deemed automatically revoked and shall be void as if never granted. Further, in the event that you breach any of these terms and conditions or any of CCC's Billing and Payment terms and conditions, the license is automatically revoked and shall be void as if never granted. Use of materials as described in a revoked license, as well as any use of the materials beyond the scope of an unrevoked license, may constitute copyright infringement and publisher reserves the right to take any and all action to protect its copyright in the materials.

9. Warranties: Publisher makes no representations or warranties with respect to the licensed material.

10. Indemnity: You hereby indemnify and agree to hold harmless publisher and CCC, and their respective officers, directors, employees and agents, from and against any and all claims arising out of your use of the licensed material other than as specifically authorized pursuant to this license.

11. No Transfer of License: This license is personal to you and may not be sublicensed, assigned, or transferred by you to any other person without publisher's written permission.

12. No Amendment Except in Writing: This license may not be amended except in a writing signed by both parties (or, in the case of publisher, by CCC on publisher's behalf).

13. Objection to Contrary Terms: Publisher hereby objects to any terms contained in any purchase order, acknowledgment, check endorsement or other writing prepared by you, which terms are inconsistent with these terms and conditions or CCC's Billing and Payment terms and conditions. These terms and conditions, together with CCC's Billing and Payment terms and conditions (which are incorporated herein), comprise the entire agreement between you and publisher (and CCC) concerning this licensing transaction. In the event of any conflict between your obligations established by these terms and conditions and those established by CCC's Billing and Payment terms and conditions, these terms and conditions shall control.

14. Revocation: Elsevier or Copyright Clearance Center may deny the permissions described in this License at their sole discretion, for any reason or no reason, with a full refund payable to you. Notice of such denial will be made using the contact information provided by you. Failure to receive such notice will not alter or invalidate the denial. In no event will Elsevier or Copyright Clearance Center be responsible or liable for any costs, expenses or damage incurred by you as a result of a denial of your permission request, other than a refund of the amount(s) paid by you to Elsevier and/or Copyright Clearance Center for denied permissions.

LIMITED LICENSE

The following terms and conditions apply only to specific license types:

15. Translation: This permission is granted for non-exclusive world English rights only unless your license was granted for translation rights. If you licensed translation rights you may only translate this content into the languages you requested. A professional translator must perform all translations and reproduce the content word for word preserving the integrity of the article. If this license is to re-use 1 or 2 figures then permission is granted for non-exclusive world rights in all languages.

16. Posting licensed content on any Website: The following terms and conditions apply as follows: Licensing material from an Elsevier journal: All content posted to the web site must maintain the copyright information line on the bottom of each image; A hyper-text must be included to the Homepage of the journal from which you are licensing at http://www.sciencedirect.com/science/journal/xxxxx or the Elsevier homepage for books at http://www.elsevier.com; Central Storage: This license does not include permission for a scanned version of the material to be stored in a central repository such as that provided by Heron/XanEdu.

Licensing material from an Elsevier book: A hyper-text link must be included to the Elsevier homepage at http://www.elsevier.com . All content posted to the web site must maintain the copyright information line on the bottom of each image.

Posting licensed content on Electronic reserve: In addition to the above the following clauses are applicable: The web site must be password-protected and made available only to bona fide students registered on a relevant course. This permission is granted for 1 year only. You may obtain a new license for future website posting.

17. For journal authors: the following clauses are applicable in addition to the above:

Preprints:

A preprint is an author's own write-up of research results and analysis, it has not been peer-reviewed, nor has it had any other value added to it by a publisher (such as formatting, copyright, technical enhancement etc.).

Authors can share their preprints anywhere at any time. Preprints should not be added to or enhanced in any way in order to appear more like, or to substitute for, the final versions of articles however authors can update their preprints on arXiv or RePEc with their Accepted Author Manuscript (see below).

If accepted for publication, we encourage authors to link from the preprint to their formal publication via its DOI. Millions of researchers have access to the formal publications on ScienceDirect, and so links will help users to find, access, cite and use the best available version. Please note that Cell Press, The Lancet and some society-owned have different preprint policies. Information on these policies is available on the journal homepage.

Accepted Author Manuscripts: An accepted author manuscript is the manuscript of an article that has been accepted for publication and which typically includes author-incorporated changes suggested during submission, peer review and editor-author communications.

Authors can share their accepted author manuscript:

- – immediately
    - via their non-commercial person homepage or blog
    - by updating a preprint in arXiv or RePEc with the accepted manuscript
    - via their research institute or institutional repository for internal institutional uses or as part of an invitation-only research collaboration work-group
    - directly by providing copies to their students or to research collaborators for their personal use
    - for private scholarly sharing as part of an invitation-only work group on commercial sites with which Elsevier has an agreement
- – after the embargo period
    - via non-commercial hosting platforms such as their institutional repository
    - via commercial sites with which Elsevier has an agreement

In all cases accepted manuscripts should:

- – link to the formal publication via its DOI
- – bear a CC-BY-NC-ND license - this is easy to do
- – if aggregated with other manuscripts, for example in a repository or other site, be shared in alignment with our hosting policy not be added to or enhanced in any way to appear more like, or to substitute for, the published journal article.

Published journal article (JPA): A published journal article (PJA) is the definitive final record of published research that appears or will appear in the journal and embodies all value-adding publishing activities including peer review co-ordination, copy-editing, formatting, (if relevant) pagination and online enrichment.

Policies for sharing publishing journal articles differ for subscription and gold open access articles:

Subscription Articles: If you are an author, please share a link to your article rather than the full-text. Millions of researchers have access to the formal publications on ScienceDirect, and so links will help your users to find, access, cite, and use the best available version.

Theses and dissertations which contain embedded PJAs as part of the formal submission can be posted publicly by the awarding institution with DOI links back to the formal publications on ScienceDirect.

If you are affiliated with a library that subscribes to ScienceDirect you have additional private sharing rights for others' research accessed under that agreement. This includes use for classroom teaching and internal training at the institution (including use in course packs and courseware programs), and inclusion of the article for grant funding purposes.

Gold Open Access Articles: May be shared according to the author-selected end-user license and should contain a CrossMark logo, the end user license, and a DOI link to the formal publication on ScienceDirect.

Please refer to Elsevier's posting policy for further information.

18. For book authors the following clauses are applicable in addition to the above: Authors are permitted to place a brief summary of their work online only. You are not allowed to download and post

the published electronic version of your chapter, nor may you scan the printed edition to create an electronic version. Posting to a repository: Authors are permitted to post a summary of their chapter only in their institution's repository.

19. Thesis/Dissertation: If your license is for use in a thesis/dissertation your thesis may be submitted to your institution in either print or electronic form. Should your thesis be published commercially, please reapply for permission. These requirements include permission for the Library and Archives of Canada to supply single copies, on demand, of the complete thesis and include permission for Proquest/UMI to supply single copies, on demand, of the complete thesis. Should your thesis be published commercially, please reapply for permission. Theses and dissertations which contain embedded PJAs as part of the formal submission can be posted publicly by the awarding institution with DOI links back to the formal publications on ScienceDirect.

Elsevier Open Access Terms and Conditions

You can publish open access with Elsevier in hundreds of open access journals or in nearly 2000 established subscription journals that support open access publishing. Permitted third party re-use of these open access articles is defined by the author's choice of Creative Commons user license. See our open access license policy for more information.

Terms & Conditions applicable to all Open Access articles published with Elsevier:

Any reuse of the article must not represent the author as endorsing the adaptation of the article nor should the article be modified in such a way as to damage the author's honour or reputation. If any changes have been made, such changes must be clearly indicated.

The author(s) must be appropriately credited and we ask that you include the end user license and a DOI link to the formal publication on ScienceDirect.

If any part of the material to be used (for example, figures) has appeared in our publication with credit or acknowledgement to another source it is the responsibility of the user to ensure their reuse complies with the terms and conditions determined by the rights holder.

Additional Terms & Conditions applicable to each Creative Commons user license:

CC BY: The CC-BY license allows users to copy, to create extracts, abstracts and new works from the Article, to alter and revise the Article and to make commercial use of the Article (including reuse and/or resale of the Article by commercial entities), provided the user gives appropriate credit (with a link to the formal publication through the relevant DOI), provides a link to the license, indicates if changes were made and the licensor is not represented as endorsing the use made of the work. The full details of the license are available at http://creativecommons.org/licenses/by/4.0.

CC BY NC SA: The CC BY-NC-SA license allows users to copy, to create extracts, abstracts and new works from the Article, to alter and revise the Article, provided this is not done for commercial purposes, and that the user gives appropriate credit (with a link to the formal publication through the relevant DOI), provides a link to the license, indicates if changes were made and the licensor is not represented as endorsing the use made of the work. Further, any new works must be made available on the same conditions. The full details of the license are available at http://creativecommons.org/licenses/by-nc-sa/4.0.

CC BY NC ND: The CC BY-NC-ND license allows users to copy and distribute the Article, provided this is not done for commercial purposes and further does not permit distribution of the Article if it is changed or edited in any way, and provided the user gives appropriate credit (with a link to the formal publication through the relevant DOI), provides a link to the license, and that the licensor is not represented as endorsing the use made of the work. The full details of the license are available at http://creativecommons.org/licenses/by-nc-nd/4.0. Any commercial reuse of Open Access articles published with a CC BY NC SA or CC BY NC ND license requires permission from Elsevier and will be

subject to a fee.

Commercial reuse includes:

- – Associating advertising with the full text of the Article
- – Charging fees for document delivery or access
- – Article aggregation
- – Systematic distribution via e-mail lists or share buttons

Posting or linking by commercial companies for use by customers of those companies.

20. Other Conditions:

v1.7

Questions? customercare@copyright.com or +1-855-239-3415 (toll free in the US) or +1-978-646-2777.